

RECOVERY AND RECOVERABILITY IN THE CENTRAL NERVOUS SYSTEM
FOLLOWING
LONG-TERM ETHANOL CONSUMPTION

BY

MICHAEL A. KING

A DISSERTATION PRESENTED TO THE GRADUATE SCHOOL
OF THE UNIVERSITY OF FLORIDA IN
PARTIAL FULFILLMENT OF THE REQUIREMENTS
FOR THE DEGREE OF DOCTOR OF PHILOSOPHY

UNIVERSITY OF FLORIDA

1985

Copyright 1985

by

Michael A. King

ACKNOWLEDGEMENTS

We wish to thank Pat Burnett, Larry Ezell, Dot Robinson, and Regina Davis for technical assistance with these experiments. This work was supported in part by NIAAA predoctoral fellowship AA05175 to M.A.K.. Other sources of support include the Medical Research Service of the Veterans Administration and NIAAA grant AA00200 to D.W.W.. Data analyses were made using the Northeast Regional Data Center IBM 3081 computer with MVS/XA at the University of Florida, under release 82.4 of SAS (Statistical Analysis System, SAS Institute Inc., Cary, N.C.).

TABLE OF CONTENTS

	PAGE
ACKNOWLEDGEMENTS	iii
LIST OF TABLES	vii
LIST OF FIGURES	viii
ABSTRACT	xii
CHAPTER	
I. ETHANOL CONSUMPTION, BRAIN DAMAGE, AND PSYCHOLOGICAL DEFICITS	1
Brain Damage and Psychological Deficits Related to Ethanol Abuse	1
Alcoholism, Memory Deficits, and the Hippocampus	2
Recovery From Ethanol-Related Disorders	3
Tissue and Cellular Mechanisms Related to Memory Disorders	4
Dendrites and Dementia, Alcohol and Aging	6
Alcohol Abuse and Brain Injury of Non-alcoholic Origin	9
The Anatomy of the Rat Hippocampus	11
Major Features	11
Cell Types and Internal Features	13
Dentate Gyrus Afferent Connections	16
Entorhinal-Dentate Afferents	16
Septal-Dentate Afferents	18
Brainstem and Hypothalamic Dentate Afferents	20
Hilar Afferents to Dentate	20
Dentate Efferents	22
CA3 Afferents	24
CA3 Efferents	25
CA1 Afferents	26
CA1 Efferents	27
Reactive Synaptogenesis in the Dentate Gyrus	27
The Liquid Diet Chronic Ethanol Consumption Model	32

II. ALTERATIONS AND RECOVERY OF DENDRITIC MORPHOLOGY FOLLOWING LONG-TERM ETHANOL CONSUMPTION . . .	35
Design and Methods	35
Golgi Histology	36
Gross Brain Measurements	37
Dendritic Spine Counts	37
Results	41
Gross Measures	42
Spine Density Measures	44
CA1 Spine Density	44
Dentate Granule Cell Densities	45
Discussion	52
Experimental Considerations	52
Estimates of Total Neuron Alterations in Spine Number	59
Electrophysiological Consequences of Long- term Ethanol Exposure	61
Possible Mechanisms of Spine Density Alterations	63
Somatic proximity	63
Presynaptic influences	65
Systemic and molecular influences	67
Spine Density and Recovery in CT Scans	73
III. CNS RECOVERABILITY FOLLOWING LONG-TERM ETHANOL CONSUMPTION	74
Experimental Methods and Design	74
Entorhinal Cortex Lesions	74
Histological Preparation	75
Verification of Lesion Placement and Size	77
Measurements of Histological Sections	79
Measurement software for Timm's material	81
Measurement software for AChE material	83
Stain Intensity Normalization	84
Results	87
Alcohol Consumption	87
Alcohol Effects: Coronal Timm-stained Dentate	89
Timm's Band Widths in Unlesioned Animals	89
Timm's Stain Intensity in Unlesioned Animals	93
Alcohol Effects: The Contralateral Dentate	97
Contralateral Exposed Blade Widths in AChE Material	105
Contralateral Exposed Blade AChE Stain Intensity	109
Contralateral Buried Blade Widths in AChE Material	112
Contralateral Buried Blade AChE Stain Intensity	116
Entorhinal Lesions	120
Unlesioned vs. Contralateral AChE Patterns	132

Synaptic Reorganization Effects	139
Buried Blade Widths in AChE Material . .	139
Buried Blade AChE Intensity	140
Exposed Blade AChE Widths	150
Exposed Blade AChE Stain Intensity . . .	153
Discussion	161
Chronic Ethanol Consumption and Timm's	
Patterns in Dentate	165
AChE Patterns in the Contralateral Dentate	
Gyrus	166
Inhibited Reactive Synaptogenesis in Alcohol	
Animals	170
Lesion-induced AChE Intensity Changes . . .	172
Buried and Exposed Blade Differences Before	
and After Lesions	174
Possible Mechanisms of Long-term Ethanol	
Effects	176
Experimental Considerations	178
IV. GENERAL DISCUSSION	180
Spine Density Recovery, but Inhibited Reactive	
Synaptogenesis?	181
REFERENCES	186
BIOGRAPHICAL SKETCH	210

LIST OF TABLES

TABLE	PAGE
1. Gross Brain Measurements and Weights	43
2. CA1 Pyramidal Neuron Spine Densities	46
3. Dentate Granule Neuron Spine Densities	49
4. Timm's Stain Band Widths and Intensity Measures . . .	90
5. AChE Stain Band Widths	106
6. AChE Normalized Stain Intensity	107

LIST OF FIGURES

FIGURE	PAGE
1. The Hippocampus in Medial View	12
2. A Schematic Transverse Section Through the Hippocampus	14
3. Dentate Gyrus Timm's and AChE Staining Patterns . .	21
4. Schematic Summary of Dentate Reactive Synaptogenesis	30
5. Spine Density Variability as a Function of the Number of Segments Counted	38
6. Dendritic Spines on Golgi-stained Dendrite	44
7. CA1 Pyramidal Neuron Dendritic Spine Densities . . .	47
8. Dentate Granule Neuron Dendritic Spine Densities . .	50
9. Reconstruction of Entorhinal Cortex Lesions	78
10. Computer-assisted Timm's Width and Stain Intensity Measurement	82
11. Computer-assisted AChE Band Width and Stain Intensity Measurement	84
12. Linearity of EyeCom II Gray Levels	86
13. Alcohol Consumption Over the 20 Week Exposure Period	88
14. Buried Blade Coronal Unlesioned Timm's Band Widths .	91
15. Buried Blade Coronal Unlesioned Timm's Widths by A-P Level	92
16. Exposed Blade Coronal Unlesioned Timm's Band Widths	94
17. Exposed Blade Coronal Unlesioned Timm's Band Widths by A-P Level	95

18.	Exposed Blade Coronal Unlesioned Timm's Band Widths by M-L Level	96
19.	Coronal Buried Blade Unlesioned Timm's Band Raw Stain Intensity	98
20.	Coronal Buried Blade Unlesioned Timm's Band Normalized Stain Intensity	99
21.	Coronal Exposed Blade Unlesioned Timm's Band Raw Stain Intensity	100
22.	Timm's Intensity Means Along the Medial-lateral Axis	101
23.	Coronal Exposed Blade Unlesioned Timm's Band Stain Intensity	102
24.	Timm's Unlesioned Exposed Blade Normalized Stain Intensity by A-P Level	103
25.	Contralateral Exposed Blade Group Mean AChE Widths	108
26.	Contralateral Exposed Blade Group Mean AChE Band Widths by D-V Level	110
27.	Contralateral Exposed Blade Sucrose Group Mean Normalized AChE Stain Intensities by D-V Level	111
28.	Contralateral Exposed Blade Normalized C/A AChE Intensity by D-V Level	113
29.	Contralateral Exposed Blade Normalized OML AChE Intensity by D-V level	114
30.	Contralateral Exposed Blade Normalized OML AChE Intensity by D-V level	115
31.	Contralateral Buried Blade AChE Band Widths . . .	117
32.	Contralateral Buried Blade AChE Band Widths by D-V Level	118
33.	Contralateral Buried Blade Sucrose Group Mean Normalized AChE Stain Intensities by D-V Level	119
34.	Contralateral Buried Blade C/A AChE Band Intensity by D-V Level	121
35.	Contralateral Buried Blade OML AChE Band Intensity, by D-V Level	122

36.	Contralateral Buried Blade OML AChE Band Intensity, by D-V Level	123
37.	Contralateral Buried Blade OML AChE Band Intensity, by D-V Level	124
38.	Molecular Layer Shrinkage Following Entorhinal Lesion	125
39.	Molecular Layer Width Following Entorhinal Lesion	126
40.	AChE C/A Band Width Following Entorhinal Lesion .	127
41.	AChE C/A Band Expansion Following Entorhinal Lesion	128
42.	AChE Stain Patterns in Unlesioned and Lesioned Animals	130
43.	Timm's Stain Patterns in Unlesioned and Lesioned Animals	131
44.	Raw AChE Stain Intensity, Unlesioned vs. Contralateral Dentate	135
45.	Corrected AChE Stain Intensity, Unlesioned vs. Contralateral Dentate	136
46.	Normalized AChE Stain Intensity, Unlesioned vs. Contralateral Dentate	137
47.	Normalized and Corrected AChE Stain Intensity, Unlesioned vs. Contralateral Dentate	138
48.	Buried Blade AChE Stain Band Width Changes in Entorhinal Lesioned Animals	141
49.	Buried Blade Lesion-induced OML Shrinkage by D-V Level	142
50.	Buried Blade AChE C/A Band Widths, Ipsi- and Contralateral, by D-V Level	143
51.	Buried Blade AChE Band Stain Intensity Responses to Entorhinal Lesions	145
52.	Buried Blade AChE GCL and C/A Band Stain Intensity Responses to Entorhinal Lesion	146
53.	Buried Blade AChE GCL and C/A Band Stain Intensity Responses to Entorhinal Lesions by D-V Levels .	148
54.	Buried Blade AChE OML Band Stain Intensity Responses to Entorhinal Lesions by D-V Levels	150

55.	Buried Blade AChE OML Band Stain Intensity Responses to Entorhinal Lesions by D-V Levels	151
56.	Buried Blade AChE OML Band Stain Intensity Responses to Entorhinal Lesions by D-V Levels	152
57.	Exposed Blade AChE Band Width Responses to Entorhinal Lesions	154
58.	Exposed Blade OML Shrinkage in Response to Entorhinal Lesion, by D-V Level	155
59.	Exposed Blade AChE C/A Band Width Responses to Entorhinal Lesions, by D-V Levels	156
60.	Exposed Blade AChE Stain Intensity Responses to Entorhinal Lesions	158
61.	Exposed Blade AChE C/A Band Stain Intensity Responses to Entorhinal Lesions, by D-V Levels	159
62.	Exposed Blade AChE C/A Band Stain Intensity Responses	160
63.	Exposed Blade AChE OML Band Stain Intensity Responses to Entorhinal Lesions	162
64.	Exposed Blade AChE OML Band Stain Intensity Responses to Entorhinal Lesions	163
65.	Exposed Blade AChE OML Band Stain Intensity Responses to Entorhinal Lesions	164

Abstract of Dissertation Presented to the Graduate School
of the University of Florida in Partial Fulfillment of the
Requirements for the Degree of Doctor of Philosophy

RECOVERY AND RECOVERABILITY IN THE CENTRAL NERVOUS SYSTEM
FOLLOWING
LONG-TERM ETHANOL CONSUMPTION

By

Michael A. King

May 1985

Chairman: Don W. Walker
Major Department: Neuroscience

Recovery from central nervous system pathology consequent to chronic ethanol consumption was assessed by comparing the density of dendritic spines on two types of Golgi-stained neurons in the rat hippocampus, in animals with or without a post-consumption "abstinence" period. Spines are morphological postsynaptic specializations on some nerve cells and are theoretically related to intellectual competence. A nutrition-controlled liquid diet was used to expose male Long-Evans rats to ethanol. CA1 neurons initially showed a nonsignificant reduction in spine density, but significantly increased density after 20 weeks

abstinence. Dentate granule cells had significantly higher spine densities after 20 weeks of exposure, but a nonsignificant reduction during abstinence. Thus the changes in gross brain morphology observed in CT scans of human alcoholics before and after abstinence may be associated with neuronal recovery.

Recoverability, the capacity of the central nervous system to respond to acute invasive injury, was also examined for the effects of long-term ethanol consumption. Histochemical staining for hippocampal acetylcholinesterase, (AChE) an enzyme involved in synaptic neurotransmission, and the Timm's sulfide/silver stain for certain endogenous metals, describe distinct afferent axon terminal fields in the dentate gyrus; these form distinct bands in tissue sections. The width and stain intensity of these bands characteristically change following partial dentate deafferentation, reflecting synaptic reorganization within the dentate gyrus. Using an image analysis computer system, this remodelling was quantified to compare the responses of alcohol-exposed and control rats. Twenty weeks of alcohol exposure may produce a residual impairment in the ability of unlesioned axons to sprout new terminals in response to unilateral destruction of entorhinal afferents, even when an 8 week ethanol-free period precedes the lesion. In addition, evidence for pre-lesion damage was found in unlesioned alcohol controls, using measurements of Timm's

stain bands, and on the side opposite the unilateral lesion. Human alcoholics, predisposed to require neurological treatment, may thus require different therapeutic approaches than nonalcoholics.

CHAPTER I
ETHANOL CONSUMPTION, BRAIN DAMAGE, AND PSYCHOLOGICAL
DEFICITS

Brain Damage and Psychological Deficits Related to Ethanol Abuse

Residual cognitive impairment and brain damage have long been associated with chronic alcohol abuse. Recent reviews affirm that a consistent pattern of clinical symptoms may be exhibited by alcoholic patients (Begleiter et al., '80, Goodwin and Hill, '75; Parsons, '77; Ron, '77; Ryan, '80; Tarter, '75). The presence of physical brain damage in human alcoholics has been inferred from electroencephalographic (Coker et al., '79) and evoked potential (Salamy et al., '80) abnormalities, and pneumoencephalographs (Brewer and Perrett, '71; Haug, '68; Tumarkin, '55). It has been confirmed directly in postmortem examinations (Alling and Bostrom, '80; Courville, '66; Lynch, '60; Miyakawa et al., '77; Victor et al., '71), and over 1000 cases of computed tomographic (CT) evidence of damage in vivo have now been reported in the clinical literature (Cala and Mastaglia, '81). Neurological examination of chronic alcoholics commonly reveals motor performance loss, and cerebral atrophy, if a CT scan is obtained, as well as the evoked potential and EEG

abnormalities. Upon psychological testing, deficient perception, subnormal conceptual and problem solving abilities, and decremented learning and recent memory capacity are commonly found. Additional complications often include autonomic and endocrine imbalances, sleep disorders, and emotional problems (Kissin, '79; Wagman and Allen, '77). Because it is estimated that there are currently between ten and twenty million "problem" drinkers in the United States (Clark and Midanic, '82; Malin et al., '82), the clinical neurobiological effects of chronic ethanol abuse constitute an increasingly important health issue.

Alcoholism, Memory Deficits, and the Hippocampus

Human alcoholics, when neuropsychologically tested, often exhibit disabilities of memory, especially recent, or short term memory (Ryan, '80). Their performance is typically sensitive to any interference or distraction they encounter during testing (Butters et al., '77; Ryan, 80). In humans who have undergone neurosurgery resulting in damage to the hippocampal formation in the inferior temporal lobe, a very similar memory disorder has been described (Butters and Cermak, '75, Milner et al., '68, Sidman et al., '68). A similar effect is also found in rodents after long term consumption of ethanol (Freund and Walker, '71; Walker and Hunter, '74, '78; Bond and DiGuisto, '76; MacDonnall and Marcucella, '78; Denoble and Begleiter, '79; Smith et al.,

'79; Irle and Markowitsch, '83), or damage to the hippocampal formation (Walker and Means, '73; Winocur, '79). The consistent findings of hippocampal formation damage in the brains of human alcoholics at autopsy (Brion '69; Victor et al., '71; McLardy, '73a; Miyakawa et al., '77), and in laboratory rodents (Riley and Walker, '78; McMullen et al., '84; Irle and Markowitsche, '83; Phillips and Cragg, '83) and non-human primates (Montgomery et al., '79) exposed repeatedly to ethanol have led to a working hypothesis that alcoholic neuropathology in this structure is intimately related to the functional deficits that are so consistently observed (cf. Walker et al., '81; Irle and Markowitsch, '83). Thus the hippocampus serves as the anatomical focus in the experiments described below.

Recovery From Ethanol-Related Disorders

A recent issue in the study of central nervous system (CNS) effects of human chronic alcoholism concerns the propensity for recovery from the pronounced intellectual and neurobiological consequences that are commonly observed (Carlen and Wilkinson, '80; Ryan, '80). Evidence for the operation of some form of recovery comes from both neuropsychological improvement on diagnostic tests during abstinence (Guthrie and Elliot, '80; Hester et al., '80; Schau et al., '80; Sharp et al., '77; Cermak and Ryback, '76; Templer et al., '75; Clark and Houghton, '75; Farmer,

'73; Long and McLachlan, '74; Page and Linden, '74) and indices of the morphological and physiological state of the brain. The latter consist primarily of a tendency for cerebral atrophy, as defined by the apparent enlargement of extrabrain spaces, to spontaneously decrease in severity during abstinence (Carlen et al., '78; Hill and Mikhael, '79). In addition, measures of cerebral cortical blood flow, and its regional activation during specific cognitive activities, have been reported to improve (Berglund and Risberg, '80), while abnormalities in stimulus-evoked electrical waveform components recorded from the scalp have been found to return toward normal (Salamy et al., '80;). Sleep disorders may also abate during abstinence (Wagman and Allen, '77). It appears likely, therefore, that functional recovery from some of the deleterious effects of chronic alcoholism may occur.

Tissue and Cellular Mechanisms Related to Memory Disorders

How could neuropathological changes subsequent to chronic ethanol result in cognitive disabilities in mammals? The tissue effects, in humans, are commonly demyelination (Alling and Bostrom, '80), and various degrees of focal encephalopathy (Lynch, '60; Victor et al., '71; Miyakawa et al., '77; Ron, '77; Nakada and Knight, '84); cell loss is reported although little quantitative data exist to substantiate this observation. Cell loss is also indicated

by shrinkage of cortical folds, and findings that chronic ethanol treatment in rats results in hippocampal cell loss in both of its main component substructures (Walker et al., '80) corroborate this view. Cell loss in other brain regions, specifically the cerebellum, has also been documented in animals exposed to alcohol for long periods (Tavares and Paula-Barbosa, 82; Walker et al., '81; Irle and Markowitsch, '83). A decrease in the number of neurons in the CNS, however, is virtually permanent since there is almost no cell division in neurons in the adult central nervous system. If the apparent recovery of cerebral atrophy and cognitive dysfunction really does occur, then some other mechanism than replacement of lost neurons must underlie this recovery. Several possible general mechanisms for recovery from brain damage have been proposed (Finger and Stein, '82), such as the takeover of functional abilities by undamaged areas, or development of alternative behavioral strategies for solving some task, using different anatomical circuitry. One possible mechanism that is experimentally related to relative intellectual capacity in humans and animals, and consistent with current cellular neurobiological evidence, is that the degree of differentiation of the dendritic tree of neurons is flexible (Morest, '69), and determinant of the number and perhaps quality of synaptic contacts received from incoming axons. If some condition results in a decrease in the number of

contacts a neuron maintains, then that cell cannot integrate as much information (Freund, '82). From this it follows that the information processing capabilities of neuronal ensembles, and the nervous system as a whole, would be compromised by any agent that reduced the number of connections made by individual neurons.

Dendrites and Dementia, Alcohol and Aging

In several neurological conditions having the quality of dementia (the decreased ability to think, remember, and perceive), dendritic de-differentiation is common (Purpura, '75, Buell and Coleman, '79), and takes two main forms. The first is a decrease in the length of the treelike dendritic branches, the second, a decrease in the density, or morphological integrity, of dendritic spines. These are small protrusions first described by Ramon y Cajal in 1891 that often cover the majority of dendrites, and contain attachment sites for incoming axon terminals. Both changes often occur together, resulting in substantial losses in the number of connections a neuron can make. This net degeneration of dendritic integrity is in contrast with what appears to be the normal situation throughout most of life, where both degeneration and synthesis occur, with some net dendritic growth (Buell and Coleman, '79). Both forms of dendritic disintegration have been reported to occur in senile and Alzheimer's dementias (Mehraein et al., '75;

Buell and Coleman, '79), temporal lobe epilepsy (Scheibel et al., '76), and mental retardation (Purpura, '74), in humans, and in senescence (Bondareff and Genisman, '76; Bondareff et al., '78; Machado-Salas and Scheibel, '79; Cupp and Uemura, '80; Uemura, '81; Mervis, '81) and experimental chronic alcoholism in animals (Riley and Walker, '78, Tavares et al., '83a,b; McMullen et al., '84; Phillips and Cragg, '83). Following long term ethanol exposure in animals, dendrites in the hippocampal formation and elsewhere have been reported to become vacuolated and contain various vesicular organelles (Goldstein et al., '83;), and display anomalous spine morphology (Tavares et al., '83a,b; Phillips and Cragg, '83; Popova, '83), in addition to outright decreases in spine numbers (Tavares et al., '83b; Popova, '83; Riley and Walker, '78) and dendritic extent (Tavares et al., '83a; McMullen et al., '84).

If numerical decreases in connections manifest in intellectual disabilities, could increases in dendritic complexity take place that might be associated with recovery of such abilities? According to basic principles in the cell biology of toxic substances, recovery of cell processes, both chemical and physical, is often observed unless a cell has been exposed to some critical, lethal amount of the offending substance (Bridges et al., '83). Such a restoration by the cellular elements of the CNS has been proposed as a mechanism by which the ameliorization of

the cerebral atrophy diagnosed in CT scans might be possible (Carlen et al., '78; Hill and Mikhael, '79), but experimental discrimination among several possible hypotheses is not yet possible in humans. Such a mechanism could also account for the lack of cognitive recovery in alcoholics with extreme consumption histories (Guthrie, '80). Recently, a translation of a report from the Soviet Union describes qualitative recovery of dendritic branching and spines damaged by long term ethanol exposure (Popova, '83), and what must be considered a preliminary quantitative study of hippocampal dendritic branching recovery has also recently appeared (McMullen et al., '84). It has also been reported that, following an experimental partial deafferentation of dentate granule cells, both dendrites and spines can be observed to undergo phases of de- and regeneration (Steward and Vinsant, '83; Steward and Caceres, '83), which consists of both replacement by new structures and reconstruction by some of those dendrites and spines actually having exhibited internal pathology. Presynaptic axonal sprouting is known to accompany these changes (Cotman et al., '81). According to the neuronal deafferentation hypothesis of the Toronto researchers (Carlen et al., '78), cerebral atrophy is at least partly a reflection of a degenerative disconnection of neuronal circuitry due to ethanol neurotoxicity. Recovery from this condition would necessitate reconnection, which would require elaboration of both pre- and postsynaptic structures.

The first experiment was designed to quantitatively investigate one particular form of dendritic pathology in neurons of the hippocampal formation of rats following long term ethanol exposure, and the possibility that some recovery from those effects might occur. To expose animals to ethanol, a nutrition-controlled liquid diet model of chronic ethanol consumption was used. This model of chronic dietary ethanol consumption has been refined over the past decade to address experimentally questions that are unresolvable using clinical approaches. The effects of ethanol on dendritic spine density were measured in two types of hippocampal neurons, comparing animals with and without postethanol abstinence periods. To determine whether dendritic recovery might account for a restoration of cerebral volume such as appears to occur in CT scans of some abstinent human alcoholics, gross brain morphometrics were also collected.

Alcohol Abuse and Brain Injury of Non-alcoholic Origin

It has recently come to be appreciated that alcoholics, especially young alcoholics, are as much as three times as likely to suffer strokes and other cerebrovascular disorders compared to nonalcoholics (cf. Nakada and Knight, '84; Koval', 78). Alcohol abuse can also be causally related to accidental falls (Honkanen et al., '83), automobile accidents, and other forms of violent injury. In one study,

in almost 40% of emergency medical cases involving 30-59 year old patients, chronic and/or acute alcohol abuse was found (Kristensson-Aas et al., '81). A significant percentage of these patients will require neurological treatment at some time in their lives. Very little is known, however, about the effects of long term alcohol intake on recovery from nervous system damage. Two factors complicate attempts to investigate this problem systematically in humans. First, alcoholics can often be shown to have CNS (central nervous system) pathology directly (neurotoxicity) or indirectly (poor nutrition, peripheral organ dysfunction, etc.) related to alcoholism. Since these variables vary considerably within the human population, experimental control is extremely difficult to obtain. Second, the CNS of adult mammals is often notoriously intractable to recovery from pathological insults. Together with the high degree of variation in natural and accidental injuries to the CNS, and the lack of technical means by which to assess human brain damage and recovery noninvasively, the current problems in analyzing neurobiological recovery in the clinic make it difficult if not impossible to sort out the effects of another variable such as alcohol use. It cannot presently be determined, for example, how much of an observed functional recovery from CNS injury represents a regeneration of damaged connections, circuitry replacement by other brain systems, or simple but

subtle substitutions of behavioral strategies. Furthermore, such hypothetical mechanisms are neither necessarily mutually exclusive nor generalizable to all forms of injury (Finger and Stein, '82).

To circumvent some of these difficulties, we have used an animal model of chronic alcohol consumption and a well-studied animal model system of adult mammalian CNS tissue response to extrinsic damage to investigate the effect of prior long-term ethanol exposure on CNS recovery. This is part of a series of experiments to isolate effects of ethanol prior to, following, or both before and after an experimental brain lesion.

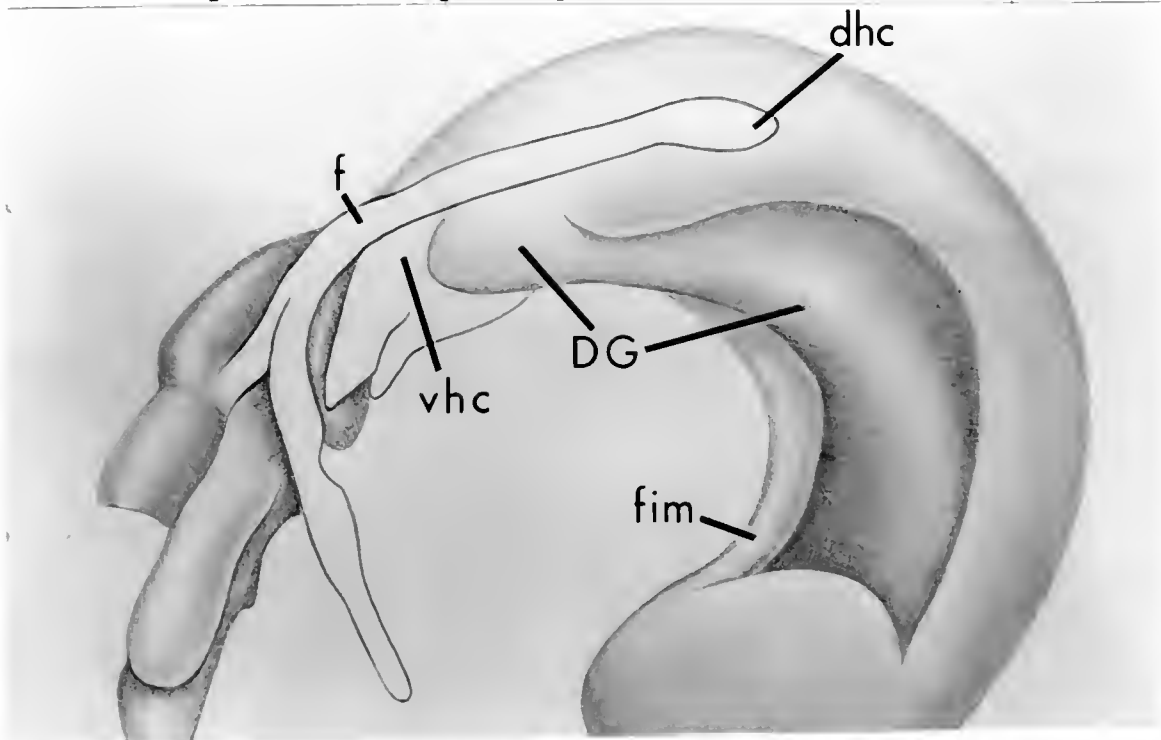
Before describing either the "recovery" or the "recoverability" experiment in more detail, the anatomy of the hippocampus and the experimental model of brain injury will be reviewed, and the methods common to both experiments (the liquid diet procedure) will be presented.

The Anatomy of the Rat Hippocampus

Major Features

The hippocampal formation is a unique cortical structure that consists of two sheets of neurons folded into one another. In any transverse section these appear as interlocked, forward and backward 'C's (figure 2). In the rat, it lies curved over the top of the thalamus, and forms the internal wall of much of the lateral cerebral ventricles

(Cajal, '68; Lorente de No, '34). Gross dissection of the hippocampus (an excellent example is found in Fjerdingstad et al., '74a) reveals some basic principles of hippocampal anatomy. Looking like a pair of bananas (figure 1), with the stem ends joined at the midline dorsally and anteriorly, the hippocampi diverge, descend, and finally turn forward before blending in to other temporal lobe cortical structures. The "stem" end is the septal pole, while the ventral tip is the temporal pole.



Legend: DG, dentate gyrus; f, fornix; fim, fimbria; dhc, dorsal hippocampal commissure; vhc, ventral hippocampal commissure. Anteriorly, the septal complex is observed.

Figure 1: The Hippocampus in Medial View

At the septal poles, narrow bundles of white matter, the fornices, consist of axons travelling to and from each hippocampus and the septal complex, the hypothalamus, and midbrain nuclei. Between each fornix at about the point where hippocampal gray matter causes the enlargement of the "banana", dorsal and ventral hippocampal commissures carry axons from each hippocampus to the other. As the hippocampus gray matter begins, the fornices spread out over it like the peel of the banana. This covering of white matter on the dorsal surface of the hippocampus is called the alveus, and where it forms a lateral ridge along the lesser curvature, it forms the fimbria.

Cell Types and Internal Features

The elegant internal structure of the hippocampus attracted the attention of many of the nineteenth and early twentieth century neuroanatomists, who devised the descriptive terminology still in use today (Lorente de No, '34). As the most evolutionarily primitive form of cerebral cortex, it has a relative structural simplicity that underlies its use as an anatomical and physiological model for investigating the neurobiology of cerebral cortex (cf. Swanson et al., '82). In cross section, the two main component structures of the hippocampal formation can be easily discerned (figure 2). The ventral and medial portion, the dentate gyrus, assumes approximately the shape

neuronal type, the granule cell, may be 10 neurons or more in thickness. The crest of the V-shaped granule cell layer defines the transition between buried blade, where the neurons abut the fissure, and the exposed blade, facing the extraventricular cistern. The dentate gyrus is formed by about 2,170,000 granule neurons, in the rat (West and Anderson '80), that each extend a conical arborization of dendrites exclusively to the outside surface of the dentate. Between the granule cell body layer and the pia mater at these external dentate borders, granule cell dendrites extend into a somata-poor zone called the molecular layer (ML). Here, incoming (afferent) axons to granule cells form synaptic contacts on their dendrites, which form conical arborizations with many branches. The dendrites of granule neurons are extensively covered with spines in normal animals.

In the space enclosed by the granule cell layer, the hilus of the dentate, over 21 morphological types of neurons (Amaral, '78) form the most complex anatomical region in the hippocampal formation. For this reason they are commonly referred to collectively as comprising the polymorph zone, where the transition from dentate to hippocampus occurs. Granule cell axons descend into the hilus, making contacts with many hilar neurons (Blackstad and Kjaerheim, 61; Blackstad et al., '70). They then enter the Ammon's horn, the ventral portion of which is known as regio inferior

(Lorente de No', '34). Regio inferior is populated by large pyramidal neurons. These extend a thick, tree-like apical dendritic arborization toward the fissure; a broad region of the proximal dendritic tree courses through the stratum radiatum, while the distal fifth extends into stratum lacunosum/moleculare. Regio inferior pyramidal cells also elaborate a basal dendritic tree, into stratum oriens. This extends all the way from the cell body layer to the alveus. About halfway along the cell body layer, a rapid and dramatic transition to a smaller pyramidal cell occurs. This defines the beginning of regio superior. In other terminology, regio superior is called CA1 (for Cornu Ammonis), the narrow transition zone is CA2, the regio inferior neurons in a layer form CA3, and the scattered hilar neurons constitute CA4.

Dentate Gyrus Afferent Connections

The pattern of connections between the hippocampal formation and its inputs and outputs is astonishingly simply ordered, compared to more recently evolved cortex. Not only are the major cell types arranged in compact layers, but many of the inputs terminate in distinct layers along particular portions of hippocampal neurons.

Entorhinal-Dentate Afferents.

One major source of input to the hippocampus is the entorhinal neocortical region. Layer II pyramidal neurons

from medial and lateral entorhinal areas send axons into the medial and lateral perforant paths, respectively (Hjorth-Simonsen, '73). These "perforate" the dentate molecular layer after crossing through regio superior, then the axons course orthogonally to granule cell dendrites, making en passage, asymmetrical Type I synapses (Nafstad, '67; Laatch and Cowan, '66) on at least 85% (Matthews et al., '76a) of the dendritic spines of the granule cells. Terminals from lateral entorhinal afferents stratify exclusively in the outer third of the molecular layer, while medial entorhinal input restricts itself to the middle third (Steward, '76). The projection is bilateral, although only about 5% of the entorhinal output is believed to innervate the contralateral hippocampal formation (Steward and Scoville, '76). The crossed lateral entorhinal projection has been observed to terminate more heavily in exposed than the buried blade, especially along the most distal region of the granule cell dendritic tree (Wyss '81; Hjorth-Simonsen, '72). In contrast, the ipsilateral projection terminates more heavily in the buried blade. The crossed medial entorhinal projection apparently terminates equally in both the buried and exposed blade. With the Timm's metal-sulfide stain, the separation of the termination zones of the lateral and medial entorhinal afferents to the dentate is revealed by the presence of distinct dark (lateral) and light (medial) bands that appear to correspond exactly to the afferent

terminal labelling pattern observed with tracing techniques such as autoradiography or HRP (Wyss, '81; Hjorth-Simonsen and Jeune, '72). The underlying difference in these two afferents is not known; few electrophysiological differences have been confirmed (McNaughton, '80; Abraham and McNaughton, '84). The restriction of immunohistochemical staining for enkephalins in the lateral entorhinal axon terminal zone (Gall et al., '84), and for cholecystekinin in the medial entorhinal termination area (Stengaard-Pedersen et al., '83) indicates that some specializations exist.

Both entorhinal inputs are of particular interest to neurobiologists because they exhibit a form of physiological plasticity known as long term potentiation. In brief, it appears that the proper pattern of electrical stimulation of these afferents can result in a lasting increase in synaptic efficiency in this pathway (Swanson et al., '82). Even more exciting is the observation that some rapid change in the shape of the dendritic spines of the granule cells is associated with LTP (Desmond and Levy, '81; Fifkova and Anderson, '82; Fifkova and Van Harreveld, '77). The implications of such processes for learning and memory research are enhanced by the long history of behavioral learning and memory research focused on the hippocampus (O'Keefe and Nadel, '78).

Septal-Dentate Afferents.

A more diffuse input to the dentate comes from the medial septal nucleus and the nucleus of the diagonal band (of Broca). These axons travel through the fornix, alveus, and fimbria and synapse sparsely throughout the molecular layer (Milner et al., '83; Swanson and Cowan, '79); in a narrow, dense band along the margin of the granule cell layer and the inner molecular layer (Raisman, '66a); and densely throughout the hilus. Because destruction of the cell bodies of origin of the septal projection results in greatly reduced hippocampal concentrations of acetylcholinesterase, the degradative enzyme for the putative neurotransmitter molecule acetylcholine, the septohippocampal projection is believed to employ ACh as its transmitter (Storm-Mathisen, '74). Histochemical staining for AChE has been thought to be coextant with the location of cholinergic septal afferent terminals as localized with degeneration (Storm-Mathisen, '64) and autoradiographic tracing methods (Swanson and Cowan, '79; Rose et al., '76), but this correspondance may be less than has commonly been assumed (Milner et al., '84). In general, however, AChE stains heaviest where neuroanatomical tracing methods indicate the heaviest septal-dentate termination: the supragranular band in the proximal molecular layer. Evidence is also beginning to indicate that some and maybe most of the septal afferents do not use acetylcholine (Baisden et al., '84) and may use the peptide substance P (Vincent and McGeer, '81).

Brainstem and Hypothalamic Dentate Afferents.

Less dense inputs to the dentate gyrus originate in hypothalamic and brainstem nuclei. Many of these appear to use catecholamines as neurotransmitters. A diffuse serotonergic plexus arises from the dorsal raphe (Moore and Halaris, '75), while a sparse noradrenergic input is sent from locus coeruleus and less so from other brainstem noradrenergic cell groups (Swanson and Hartman, '75; Pickel et al., '74; Koda and Bloom, '77). A dopaminergic projection may arise in the midbrain raphe as well (Reyman et al., '83). The catecholaminergic afferents terminate most densely in the hilus, followed by the granule cell layer; only scattered fibers and terminals are observable in the molecular layer. The most obvious hypothalamic projection appears to come from the supramammillary nucleus (Dent et al., '83; Segal '79; Wyss et al., '79), and terminates primarily along the most proximal portion of the granule cell dendrites. Lateral hypothalamic and zona incerta neurons demonstrating immunoreactivity for α -MSH, dynorphin, and angiotensin II have been reported to project to both the hippocampus and spinal cord (Kohler et al., '84).

Hilar Afferents to Dentate.

The polymorph cells in the hilus are of special interest as much for their morphological variety (Amaral, '78; Cajal, '68; Lorente de No, '34) as for the fact that they send associational projections to ipsilateral granule cells

anterior and posterior to their own location, and commissural projections to the contralateral dentate, in a similar pattern (Swanson et al., '81). They form asymmetrical synapses on granule cell dendrites and dendritic spines in the proximal one-third of the molecular layer (Laatch and Cowan, '66; Kiishi et al., '80; Gottlieb and Cowan, '73; Amaral et al., '80), in a band apparently defined by dark Timm's metal-sulfide staining (Amaral et al., '80), and a conspicuous lack of staining in AChE histochemical preparations (figure 3). Thus the commissural/associational projection constitutes a major afferent source to the granule cells. A band of positive staining for the peptide cholecystekinin, distinctly separated from the one marking medial entorhinal input, has also been described in this inner zone (Stengaard-Pedersen et al., '83).

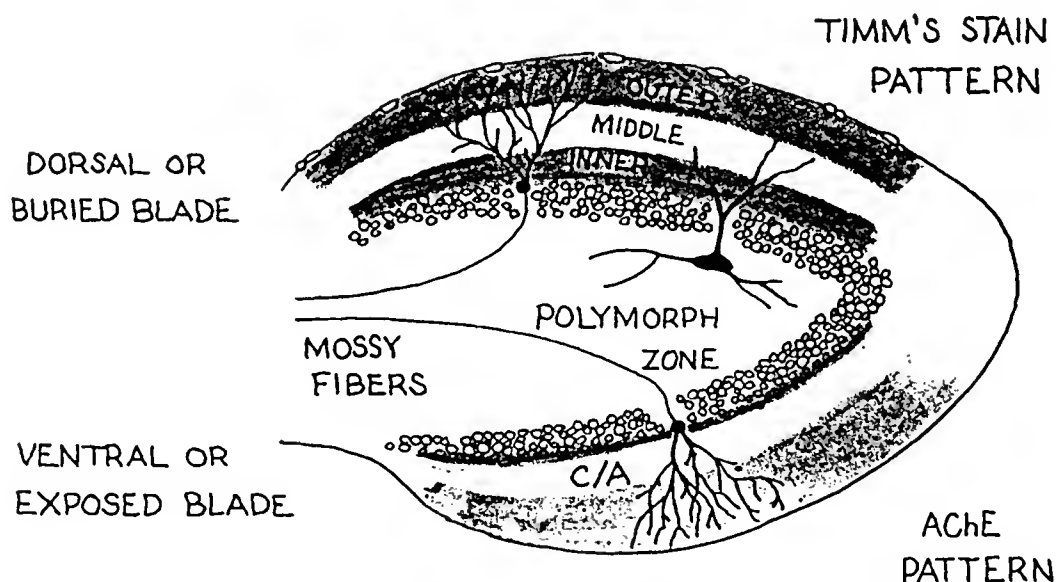


Figure 3: Dentate Gyrus Timm's and AChE Staining Patterns

The C/A projection diverges with an interesting topography. Associational (ipsilateral) axons tend to spread toward the ventral exposed blade in the temporal hippocampus, and toward the septal buried blade in the septal half (Zimmer, '71; Hjorth-Simonsen and Laurberg, '77; Fricke and Cowan, '78; West et al., 79). The ipsilateral projection is greater than the contralateral, and some of the hilar neurons may give rise to both ipsilateral and crossing collaterals (Laurberg and Sorensen, '81). Electrophysiologically, the C/A projection appears to be excitatory to granule cells ipsilaterally, but the commissural fibers evoke inhibitory responses that appear to dominate any excitatory effects (Douglas et al., '83). In addition to excitatory input from the ipsilateral hilus, putative GABAergic inhibitory basket cells distribute synaptic terminals in the granule cell and molecular layers (Cajal, '68; Amaral, '78; Ribak, '83); these may also send commissural afferents to the contralateral dentate.

Dentate Efferents

As for the output of the dentate, the granule cells emit one or few axons that descend into the hilus. Once in the hilus, they may send rare collaterals back into the molecular layer (Frotscher and Zimmer '83), but most characteristically begin to exhibit 4-8 micrometer enlargements that have been shown with the electron

microscope to be huge synaptic terminals (Blackstad, '61). At light microscopic magnifications, these give the mossy fibers their name. The thin, unmyelinated mossy fibers (Laatch and Cowan, '66) project to and synapse en passage with spines on the proximal dendrites of CA3 pyramidal neurons, and also non-pyramidal hilar neurons. The translucent quality of these bundled axons in the light microscope has led to the naming of the stratum lucidum along the proximal apical CA3 dendrites. They do, however, send terminals into the basal dendritic tree of regio inferior pyramids, especially along the more hilar region. This infrapyramidal mossy fiber terminal band exhibits considerable genetic variation and appears particularly sensitive to toxins during development (West et al., '83). Behavioral correlates related to perseveration have been observed following experimental manipulation of the infrapyramidal terminal band (Schwegler and Lipp, '83).

The synaptic terminals of the mossy fibers are of special interest for the high concentrations of the element zinc they contain (Crawford and Conner, '72). Its purpose there is currently a matter for investigation, but it is known that zinc is a cofactor for the enzyme glutamic acid dehydrogenase (Storm-Mathisen '74), which would be consistent with evidence that mossy fiber terminals employ an amino acid, either glutamate or its relative aspartate, as their neurotransmitter molecule. Zinc is present

throughout the hippocampus, at levels about three times those of the rest of the brain (Fjerdingsstad et al., '74a); this in part accounts for the relatively dense Timm's staining in the hippocampus (Haug, '74; Danscher, '81). Fjerdingsstad et al., ('74b) also report that lead is present at tenfold the concentration of the rest of the brain, but its role is unknown as well.

CA3 Afferents

The large CA3 pyramidal neurons are notable for their thick, branching dendrites covered with spines. Their proximal portions exhibit larger protruberances, called excrescences. Like spines, these are specialized postsynaptic structures onto which mossy fibers synapse (Blackstad and Kjaerheim, '61). In fact, they often perforate completely mossy fiber terminals, creating toroidal synaptic contacts. More distally, the apical dendrites narrow and spread, and are contacted by axons from entorhinal areas, hilar neurons, and other CA3 neurons, both ipsilateral and contralateral. Layer III entorhinal neurons project to stratum lacunosum-moleculare (Steward and Scoville, '76), while the extensive associational and commissural projections terminate in oriens and radiatum (Gottlieb and Cowan, '72, '73). Septal, hypothalamic, and brainstem input is diffuse and probably varies in exact pattern depending upon the anterior-posterior hippocampal

level. In general, medial septum projects most strongly to strata pyramidale and oriens, and much less so to radiatum (Raisman, '66a). Locus coeruleus sends its most dense input to strata lucidum and lacunosum-moleculare, but diffusely to the other layers as well (Swanson and Hartman, '75; Loy et al., '80). The raphe innervates predominantly stratum lacunosum-moleculare (Moore and Halaris, '75; Wyss et al., '79a).

CA3 Efferents

CA3 axons, in addition to making commissural and associational connections within regio inferior, reach several other target areas. In fact, individual CA3 pyramids may project to five or more areas (Swanson et al., '81). As the axons descend through stratum oriens into the fimbria, they branch into several collaterals. These then travel separately to the lateral septum and subiculum, perhaps bilaterally, in addition to the bilateral CA3 collaterals (Swanson et al., '80, '81). Axons to intrahippocampal sites form the Schaffer collateral system, passing via stratum radiatum to form asymmetrical spine synapses in that layer and stratum oriens of CA1 (Gottlieb and Cowan, '72, '73). Those that travel to contralateral destinations exit the fimbria to cross via the hippocampal commissures located toward the septal pole. It has been suggested that the Schaffer system projects in a lamellar

fashion, that is, from a narrow transverse slice of CA3 the axons will remain oriented in a narrow plane with little anterior-posterior dispersion. While the electrophysiological evidence for this organization is persuasive, the difficulty in differentiating the longitudinally oriented associational system from the transversely oriented associational system has precluded anatomical resolution of this question (O'Keefe and Nadel, '78).

CA1 Afferents

The last subregion of the hippocampus is the regio superior (Cajal, '68), or CA1 (Lorente de No, '34). These neurons are smaller and have finer dendrites than the CA3 pyramids, but are similar in the tree-like shape of their dendritic elaborations. In CA1 pyramidal cells, afferents from ipsilateral CA3 form the Schaffer collateral system. Ipsilateral regio inferior terminals innervate both strata oriens and radiatum, but appear to be more dense in the latter (Swanson et al., '78; Laurberg, '79). Contralateral CA3 sends a similar input to CA1, but synapses more densely in oriens (Swanson et al., '78; Laurberg, '79). Other inputs originate from entorhinal cortex, septum, and brainstem loci that parallel those of CA3. Entorhinal afferents stratify in stratum lacunosum-moleculare (Steward and Scoville, '76). In addition, an input from thalamic

nucleus reuniens to stratum lacunosum-moleculare has been described (Herkenham, '78; Riley and Moore, '81).

CA1 Efferents

These neurons project, via the alveus, to the lateral septum, to the subiculum, and to medial and lateral entorhinal areas (Hjorth-Simonsen, '73; Swanson and Cowan, '77; Meiback and Siegel, '77; Raisman, '66b), completing circuits that originate and end there. Thus the basic anatomy of the hippocampus is two loops. One can be thought of as originating in entorhinal cortex, relaying to dentate granule cell, then to CA3, to CA1, and back to entorhinal cortex. The other begins and ends in the septum and has the same interposed hippocampal neurons. Of course, the actual anatomical organization is considerably more complicated, but this model serves as a useful conceptual simplification that is entirely adequate for the purposes of the experiments described here.

Reactive Synaptogenesis in the Dentate Gyrus

The dentate gyrus is a useful structure for studying CNS synaptic reorganization because when any of the major afferent sources is removed, a compensatory restoration of synaptic density can be observed to occur following degeneration of the damaged axons and terminals. Because the elimination of entorhinal afferents is technically

simplest, dentate reactive synaptogenesis has been best described using this paradigm. The literature on dentate reactive synaptogenesis will be considered only where germane to the present experiment.

When the entorhinal cortex on one side of the brain is destroyed by aspiration, electrolysis, or mechanical separation, granule cells ipsilateral to the lesion lose about 60% of their molecular layer synapses (85% of outer ML synapses, Matthews et al., '76a). Among the early effects that are observed are a decreased glucose utilization (Steward and Smith, '80), which is noticeable by 1 day and lasts about 5 days before returning rapidly to normal between days 6 and 12. During this period, several pre- and postsynaptic changes occur. The presynaptic terminals degenerate and the debris is rapidly phagocytosed by nonneuronal cells, probably microglia, which increase in number by about 3 days postlesion (Matthews et al., '76a; Rose et al., '76; Cotman and Nadler, '78). Astroglia hypertrophy and migrate to the deafferented zone by 3 days postlesion (Matthews et al., '76a; Rose et al., '76; Cotman and Nadler, '78). These reactive glia are evident until about 15 days postlesion (Matthews et al., '80; Storm-Mathisen, '74), but prevention of their proliferation does not appear to be detrimental to the synaptic reorganization that occurs (Avendano '83). Postsynaptically, granule cell dendrites undergo a rapid change in shape during the first

few days (Steward and Caceres, '83). From the margin of the deafferented zone outward, they appear to wilt and sag, as if they were normally provided with structural support by their afferents. Protein precursor incorporation increases during the time reactive synaptogenesis is taking place (Pass and Steward, '83). A reorganization of the microvasculature appears to occur such that the preferred orientation of capillaries parallels the granule cell layer rather than the perpendicular dendritic axis (Scheff et al., '78); the significance of this is unknown. Degeneration products are cleared by about 10 days postlesion, but synaptic density does not reach normal levels until about 30 days after the lesion (Matthews et al., '76b).

New presynaptic terminals form from axons originating in the contralateral entorhinal cortex (Cotman et al., '77; Steward et al., '74, '76; Zimmer and Hjorth-Simonsen, '75); these arise from neurons undistinguishable in type from those that provide the ipsilateral afferents (Steward, '76; Steward et al., '74; Steward and Scoville, '76; Steward and Vinsant, '78). The contralateral entorhinal cortex normally contributes about 5% of the synapses in the unlesioned animal, so the proliferation of replacement synapses by the intact crossed pathway represents what is known as homotypic (same type) reinnervation (Cotman et al., '81). New presynaptic endings also arise from the associational and commissural afferents from the hilar polymorph neurons,

which expand the AChE C/A stain zone in both an absolute and relative fashion (Lynch et al., '76) and from septal afferents (Stanfield and Cowan, '82). The latter withdraw from the inner molecular layer C/A zone, and form a compact terminal band in the outer molecular layer. The overall result of this reorganization, as schematically summarized in figure 4, is an overall shrinkage of the molecular layer, an expansion and lightening of the AChE C/A zone, a contraction and darkening of the cholinesterase-positive outer molecular layer terminal zone, and possibly an expansion of the Timm's C/A band (Amaral et al., '80). Photographs of these effects are presented in Chapter 3 (figures 39, 40).

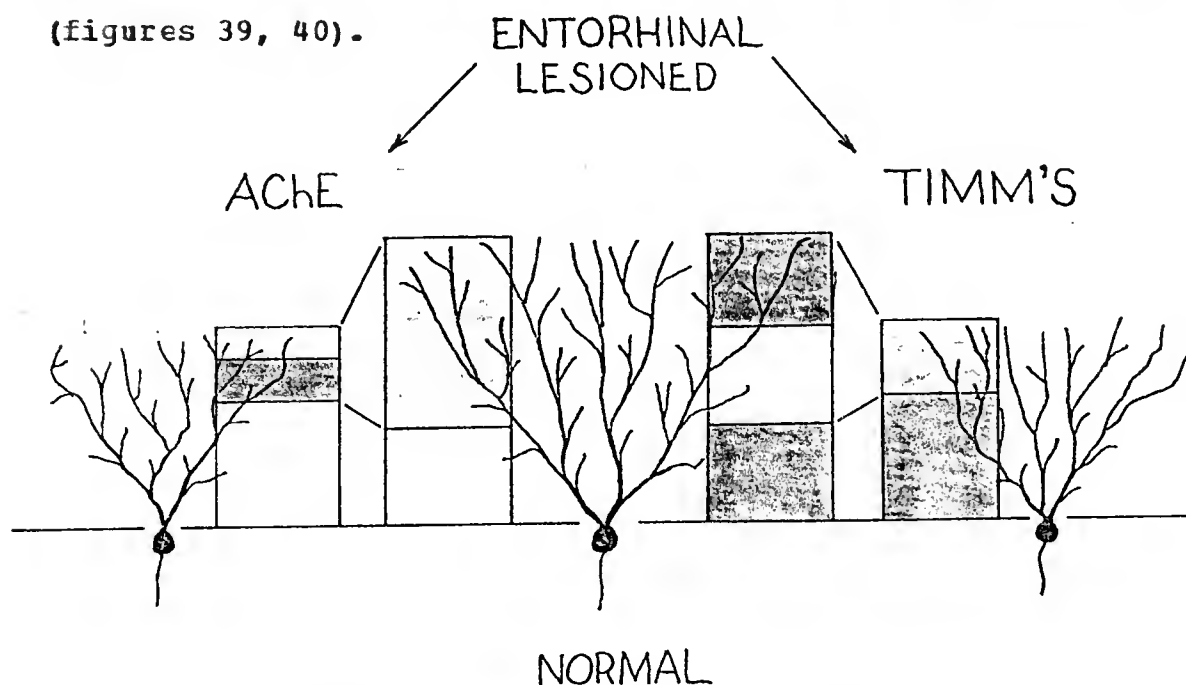


Figure 4: Schematic Summary of Dentate Reactive Synaptogenesis

The new presynaptic terminals attach to both new and old postsynaptic sites (Steward and Vinsant, '83), and show normal morphology (Matthews et al., '76b). They are also able to support electrogenic neurotransmission (Steward et al., '73, '74, '76), and exhibit at least some of the electrophysiological properties of the normal input (Harris et al., '78; Steward et al., '76; Wilson et al., '79). There is also evidence the a behavior lost after entorhinal lesion recovers with a time course similar to that of the synaptic reorganization (Loesche and Steward, '77), although it is not yet known to what extent dentate reactive synaptogenesis mediates this recovery. In any case, there is a growing body of evidence that this synaptic reorganization is in some sense functional.

It is also known that the number of spines, and the geometric branching characteristics, of these neurons are affected adversely in mental retardation in humans, chronic ethanol treatment in rats and mice, behavioral impairment in an animal model of mental retardation related to prenatal alcohol exposure, and age-related demented states (vide supra). Degeneration, and later regrowth, of spines and dendritic branches, have been found to occur after a partial deafferenting of these cells (Parnevelas et al., '74, Goldowitz et al., '79; McWilliams and Lynch, '78; Matthews et al., '76a,b; Steward and Vinsant, '83; Steward and Caceres, '83), like some, but not all, CNS neurons

(Protscher, '83). Change in granule cell spine shape has been associated with electrophysiological synaptic efficiency increases that occur with certain stimulation procedures, and which may be related to the formation and/or maintenance of memories (Desmond and Levy, '81; Fifkova and Van Harreveld, '77; Fifkova and Anderson, '82). Thus these cells exhibit some natural morphological plasticity that may serve some normal functional purpose, in addition to being provokable via deafferenting lesions.

The Liquid Diet Chronic Ethanol Consumption Model

Over the past decade, an animal model of chronic alcohol consumption has been developed in the University of Florida laboratory of Drs. Don Walker and Bruce Hunter to specifically address issues not currently amenable to experimental analysis in human alcoholic patients. Age, nutritional intake, duration and amount of consumption, and to some extent, genetic heterogeneity, can be more tightly controlled and/or monitored than is possible with human beings. Experimental evidence obtained through the use of this model, and others like it in use in other laboratories, demonstrates its relevance to the study of the biology of alcohol. Perhaps the single most important result of employing this animal model of chronic alcohol consumption is the finding that CNS pathology following long-term dietary alcohol intake is neither caused by concomitant

malnutrition nor preventable by proper nutrition (Walker et al., '81; Freund, '82). This has helped to begin to put to rest a longstanding dogma that has hindered research progress in treating alcohol related disabilities. While nutrition can evidently play an interactive role, data from animals demonstrate that ethanol itself or its immediate metabolites possess neurotoxic qualities. Both behavioral and neuroanatomical findings obtained with this model closely resemble those observed in human alcoholics (Walker et al., '81).

Male Long-Evans rats were obtained at approximately 30 days of age and housed individually in stainless steel cages in a colony room until they reached 60 days of age. During this acclimation animals received ad libitum Purina Lab Chow and tap water. Animals were paired by weight and pairs were divided to form two diet treatment groups at the end of acclimation. The alcohol diet consisted of the nutritional formula Sustacal (Mead Johnson Co.), containing progressively 8.1-9.8 % v/v ethanol over the 20 weeks animals were exposed. These ethanol concentrations provide 35-39% ethanol-derived calories in the diet, in increments of 1% per month to compensate for the development of tolerance. To this formula were added several times the recommended daily requirements of vitamins and minerals (3.0 g/l Vitamin Diet Fortification Mixture, 5.0 g/l Salt Mixture XIV, Nutritional Biochemicals, Cleveland), as described

previously (Walker and Freund, '71). A control diet was prepared by substituting sucrose isocalorically for ethanol. Alcohol-receiving animals were given 120 ml of the freshly prepared diet each day; their weight-matched control animals were given as much as their counterparts drank the previous day. Thus, for 20 weeks, alcohol and sucrose animal pairs had equivalent vitamin, mineral, protein, fat, carbohydrate, and total caloric intake; the only difference in diet being the presence or absence of ethanol. Individual daily consumption data were collected throughout the diet treatment to calculate average daily ethanol consumption, and animals were weighed and inspected for general health weekly. Prior to sacrifice of the animals, neutral code numbers were assigned by an otherwise uninvolved third party to assure the unbiased collection of all measurements.

CHAPTER II
ALTERATIONS AND RECOVERY OF DENDRITIC MORPHOLOGY FOLLOWING
LONG-TERM ETHANOL CONSUMPTION

Design and Methods

Previous studies in our laboratory have reported electrophysiological evidence that a rearrangement of some of the synaptic input to both the CA1 and dentate neurons may occur consequent to chronic ethanol treatment (Abraham et al., '84; Abraham and Hunter, '82; Abraham et al., '81). In brief, commissural afferents to CA1 radiatum, and lateral entorhinal afferents to dentate, appeared to be reduced in spatial distribution, number, and/or synaptic efficiency. In addition, spine loss has been reported to occur after chronic ethanol exposure in these neuronal types. Thus, we chose to measure the linear density of dendritic spines within several discrete regions of CA1 and granule cell dendritic trees, and compare the spine densities measured in animals sacrificed immediately after a 20 week ethanol exposure with densities from animals allowed 20 weeks post-exposure for any natural recovery to occur.

One ethanol and one sucrose control group were sacrificed immediately following the 20 week exposure period, and one ethanol and sucrose group were maintained for 20 weeks more

on ad libitum lab chow and water in individual cages before being sacrificed. The two by two factorial design of this experiment thus provides the means to test for initial ethanol effects, residual effects, and any recovery that might occur during abstinence. The use of two sucrose diet control groups allows any effect of aging to be factored into the analysis.

Golgi Histology

The rapid Golgi method of Scheibel and Scheibel ('78) was modified to produce reliable staining in the hippocampal formation. In brief, pentobarbital-overdosed animals were transcardially perfused first with isotonic phosphate-buffered saline, followed by 1%:1.25% glutaraldehyde: formaldehyde in phosphate buffered saline, followed by a stronger 4%: 5% aldehyde solution. The brains were removed, trimmed square at the frontal poles and behind the cerebellum, weighed, and photographed on graph paper for later measurements. The extracted whole brains were then refrigerated in the second fix overnight, cut into coronal 2 mm slabs the following day, and fixed until 48 hours from sacrifice. They were then placed in aqueous 0.33% osmium tetroxide, 2.7% potassium dichromate solution for 48 hours, during which they were turned over once. Slabs were then rinsed in 0.75% silver nitrate, and placed in fresh silver nitrate for 24 hours in light-tight boxes. Dehydration and

celloidin embedding were carried out as quickly as possible. Mounted blocks were cut on a sliding microtome at 80 to 120 microns and mounted on glass slides with Eukitt synthetic medium (Calibrated Instruments, Ardsley, NY).

Gross Brain Measurements

Photographs of the freshly extracted, trimmed, coded brains were measured with the aid of a Numonics 1224 digitizer. The scaled length, width, and area of each cerebral hemisphere and the cerebellum was collected. These measures correspond roughly to the type of measurements that are made on CT scans to diagnose cerebral atrophy (Cala and Mastaglia, '81; Ishii, '83).

Dendritic Spine Counts

Using oil immersion optics and a final magnification of 2250X, representative dendritic segments and the position of spines thereon were traced using a drawing tube attached to an Olympus BH-2 microscope. Dividing the number of spines per segment by the scaled segment lengths, obtained using the digitizer, yielded spine density estimates. The number of samples necessary to produce per-animal estimates with sufficiently low variability was calculated by plotting the population standard error estimate by number of samples (figure 5). Standard error estimates from our animal samples averaged less than 6% of the mean density estimates.

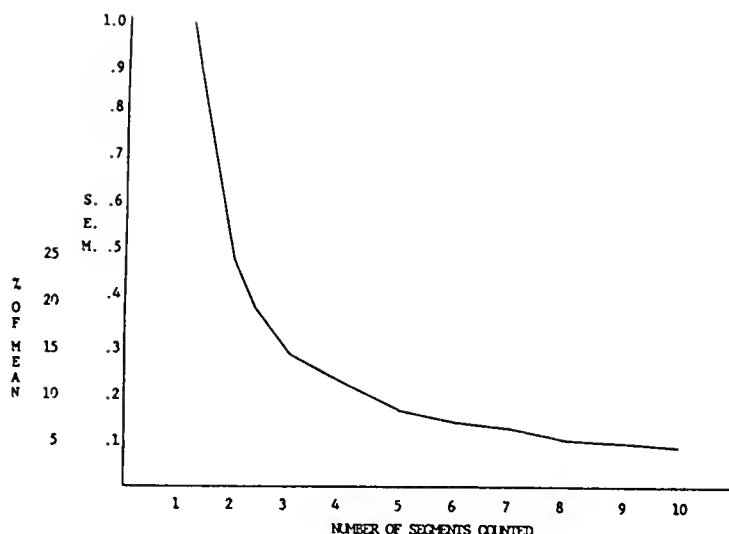


Figure 5: Spine Density Variability as a Function of the Number of Segments Counted

With further error checking it was found that the critical measure for estimating linear density, i.e., segment length, varied less than 1% on two measurement replications made for one animal. Across counting days, spine density estimates varied by an average of less than 5%. Six animals were selected at random for measurement of area, width, and height of the face of both tissue pieces, from photographs taken at each stage in the histological procedure. Because a high degree of variability in tissue shrinkage was attributable to initial dehydration after the staining steps, it was not possible to normalize each slab by amount of shrinkage and some error in segment length can be expected from this. Little or no distortion of the tissue size was detected before the dehydration steps. As a

result, the gross brain size measurements are not likely to contain this error. Mean tissue shrinkage in the slide-mounted tissue was found to be about 15% relative to the initial size of the fixed brains.

Dendritic segments selected for drawing were without obvious distortion, cut or broken surfaces, and uneven or overimpregnation. In general, the first n segments encountered that were subjectively judged to be representative for the section under observation were used, with n being the number of samples to be collected for a particular area. For all areas, not more than three samples were obtained from the same neuron, and one sample per neuron was considered desirable when enough cells were stained to criterion. Optimal segments were stained red to rust in color, with some transparency, and had 25-50 micrometers of dendritic branch in a relatively flat orientation to and situated near the top of the tissue section. This insured a narrow depth of field difference and maximum resolution of individual spines. Spines were counted wherever a discrete bulge from the dendritic surface was observed, but only where connection to the dendrite could be ascertained. In this respect, we may have missed counting some of the spines with a "lollipop" shape and a spine neck at or beyond the resolving power of the light microscope. Spine localization onto segment tracings was made once with the microscope condenser adjusted to the

numerical aperture of the principle objective, and once with the condenser adjusted to decrease the depth of field and increase image contrast, in order to check the decision to identify the spines. Segments selected did not branch within the distance measured, did not cross other impregnated dendrites, glial processes, blood vessels, or histological artifacts, and were chosen with an eye to avoiding possible overlap with adjacent sampling regions. Samples were also not taken on dendrites exhibiting any grossly visible aberrations of shape or size, and were thus conservatively chosen as representative of the populations under study.

For the CA1 pyramidal neuron, five samples were sought in each of four regions of the dendritic tree (figure 2): strata oriens, radiatum 1 (proximal 1/2), radiatum 2 (distal 1/2), and lacunosum-moleculare. This last region was defined by a conspicuous change in the density of spines and the size and orientation of the dendrites. A marked decrease in spine density and a turn to orient parallel to the hippocampal fissure were observed. In the dentate gyrus molecular layer, three regions were sampled, and 10 segments per region per animal were sought: inner, middle, and outer third, which correspond to the stratification of afferent axons from three major sources of input to granule cell dendrites (commissural/associational, medial, and lateral entorhinal cortex) (Amaral et al., '80). Division between

sampling regions was made subjectively, but conservatively, such that it would be very unlikely for a spine density estimate to be attributed to the improper sampling region. Within a sampling region, dendritic segments were selected to form a sample corresponding subjectively to the average size of dendrites in that area, e.g. in the stratum radiatum region, the main shafts of CA1 pyramids were avoided in favor of the more numerous smaller caliber branches. Sections to be used were taken at random through the dorsal hippocampal formation, since the initial cutting of the brain into slabs influenced the location of the best-impregnated sections in the final product.

All data were analyzed with a two way analysis of variance, for diet treatment, recovery time, and their interaction. Additionally, means within diet or recovery groups were tested using the student's t tests and one-way analyses of variance. Analyses were performed using SAS (Statistical Analysis Systems, SAS Institute Inc., Cary, NC).

Results

For clarity and convenience, the following shorthand will be used to designate the individual treatment groups: A0, alcohol/no recovery period; A20, alcohol/20 week recovery; S0, sucrose/no recovery; S20, sucrose/20 week recovery.

Gross Measures

The gross measures data and statistical results are summarized in Table 1. Body weight was not significantly different between diet groups at either recovery time. However, mean body weight for the A0 group was slightly lower than for the S0 group, and body weight for the A20 group was slightly higher than that of S20 animals. Thus it is possible that some rebound and overshoot of body weight occurs in alcohol animals, although sample size may merely have precluded the statistical significance of other group differences. Both diet groups significantly increased mean body weight during the recovery interval.

Brain weight was higher in both alcohol groups than their respective sucrose control groups (n.s.). Both alcohol and sucrose groups had significantly higher brain weights at 20 weeks than at 0 weeks. A significant 7% difference in the brain weight of 0 and 20 week alcohol animals was found, while 0 and 20 week sucrose group brain weights differed by only 3% (n.s.).

Similarly, animals exposed to either diet treatment showed significant increases in total cerebral hemisphere area after 20 weeks. The means for the 0 week groups are nearly identical, while the A20 group was slightly higher than the S20 group (n.s.). The A20 animals were found to have almost 9% more hemisphere area than A0 animals, while S0 group hemisphere area differed from S20 group hemisphere

area by only 5%. Left hemisphere area patterns are virtually identical to the combined hemisphere results; the right cerebral hemisphere follows the same pattern but the interaction between diet and recovery was significant.

Cerebellar area, which was only slightly lower in A0 animals than S0 controls (1%), also increased more (13%) over the 20 week recovery period in alcohol animals than in sucrose controls (11%), although this interaction did not reach significance. Although many of these effects failed to reach the .05 significance level, their uniformity supports the possibility that some grossly observable recovery is occurring during abstinence.

TABLE 1

Gross Brain Measurements and Weights

	SUCROSE		ALCOHOL		EFFECTS:
	0 WEEKS S0 v. S20	20 WEEKS S0 v. A0	0 WEEKS A0 v. A20	20 WEEKS S20 v. A20	
TOTAL HEMISPHERE AREA (sq. cm)	N=15 1.868 (.034) n.s. .5769	N=8 1.962 (.032) n.s. .7722	N=20 1.867 (.024)	N=13 2.005 (.101) * n.s. .1517	Diet: P<.9708 Recovery: P<.003 D*R: P<.1007 * P<.0007
LEFT HEM. AREA	N=15 .927 (.018) n.s. .1455	N=8 .994 (.015) n.s. .4326	N=20 .926 (.015)	N=13 1.003 (.013) * n.s. .1017	Diet: P<.8623 Recovery: P<.0027 D*R: P<.6985 * P<.0073
RIGHT HEM. AREA	N=15 .94 (.023) n.s. .5398	N=8 .968 (.025) n.s. .6146	N=20 .941 (.018)	N=13 1.002 (.018) * n.s. .4739	Diet: P<.9938 Recovery: P<.1057 D*R: P<.0434 * P<.0182
CEREBELLAR AREA	N=15 .592 (.011) *	N=8 .662 (.014) n.s. .9606	N=20 .583 (.010)	N=13 .657 (.019) ** n.s. .3588	Diet: P<.5542 Recovery: P<.0001 D*R: P<.3250 * P<.0096 ** P<.0006
BRAIN WT. (grams)	N=9 1.604 (.042) n.s. .4197	N=9 1.647 (.056) n.s. .2357	N=11 1.622 (.027)	N=12 1.709 (.051) n.s. .0503	Diet: P<.1861 Recovery: P<.0428 D*R: P<.4879
BODY WT. (grams)	N=17 608 (9) n.s. .1145	N=9 651 (20) n.s. .3549	N=20 576 (17)	N=13 672 (22) * n.s. .2211	Diet: P<.6914 Recovery: P<.0008 D*R: P<.0852 * P<.0038

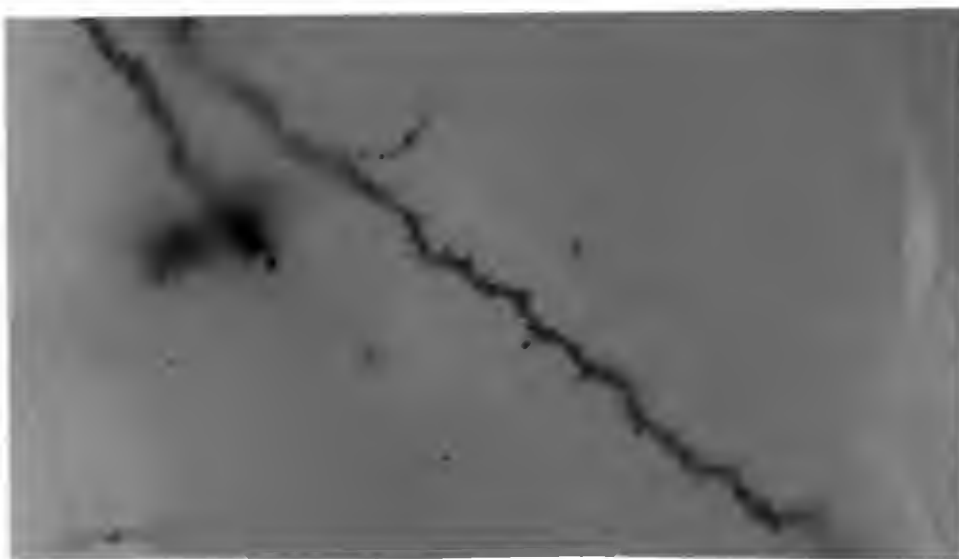


Figure 6: Dendritic Spines on Golgi-stained Dendrite

Spine Density Measures

As Figure 6 shows, the rapid Golgi method demonstrates the prominent spines along all levels of hippocampal neuron dendrites. A total of 1790 dendritic segments were sampled from 40 animals. The results of the spine density comparisons complement the gross measures data.

CA1 Spine Density.

Ethanol did not result in a significant lowering of spine density in any of the CA1 zones, although a consistent reduction was observed for the mean spine density in each (table 2). In CA1 pyramids, the basal dendritic spine density, in stratum oriens, was slightly lower in the A0 animals than S0 controls (6%). This pattern held in the apical dendritic tree; proximal stratum radiatum density was 3% and distal radiatum 10% lower than the same regions in

sucrose control animals, and a 6% reduction was observed in stratum lacunosum-moleculare. Significant recovery period (20 week) effects were observed only in proximal radiatum, according to the analysis of variance for all 4 groups. However, t-tests revealed that while no significant differences in mean spine density were found between the S0 and S20 groups, in alcohol-treated animals the density means in all CA1 areas (except lacunosum-moleculare, $P < .0749$) were significantly higher in 20 week than in 0 week animals. In stratum oriens, A20 week group density was 13% higher than in A0 animals. Proximal radiatum density was 14%, and distal radiatum 19% higher in 20 week than in 0 week alcohol subjects, and a 19% greater density also was found in stratum lacunosum-moleculare. In fact, with the exception of this last region, A20 CA1 linear spine densities were higher in all regions than either of the sucrose control groups! Conservative comparisons of the A20 densities with the higher of the two obtained control values indicate at least a 7% greater density in oriens, proximal, and distal radiatum than in controls. Interactions between diet and recovery time were significant, however, only in distal radiatum. These results are presented in graphic form in Figure 7.

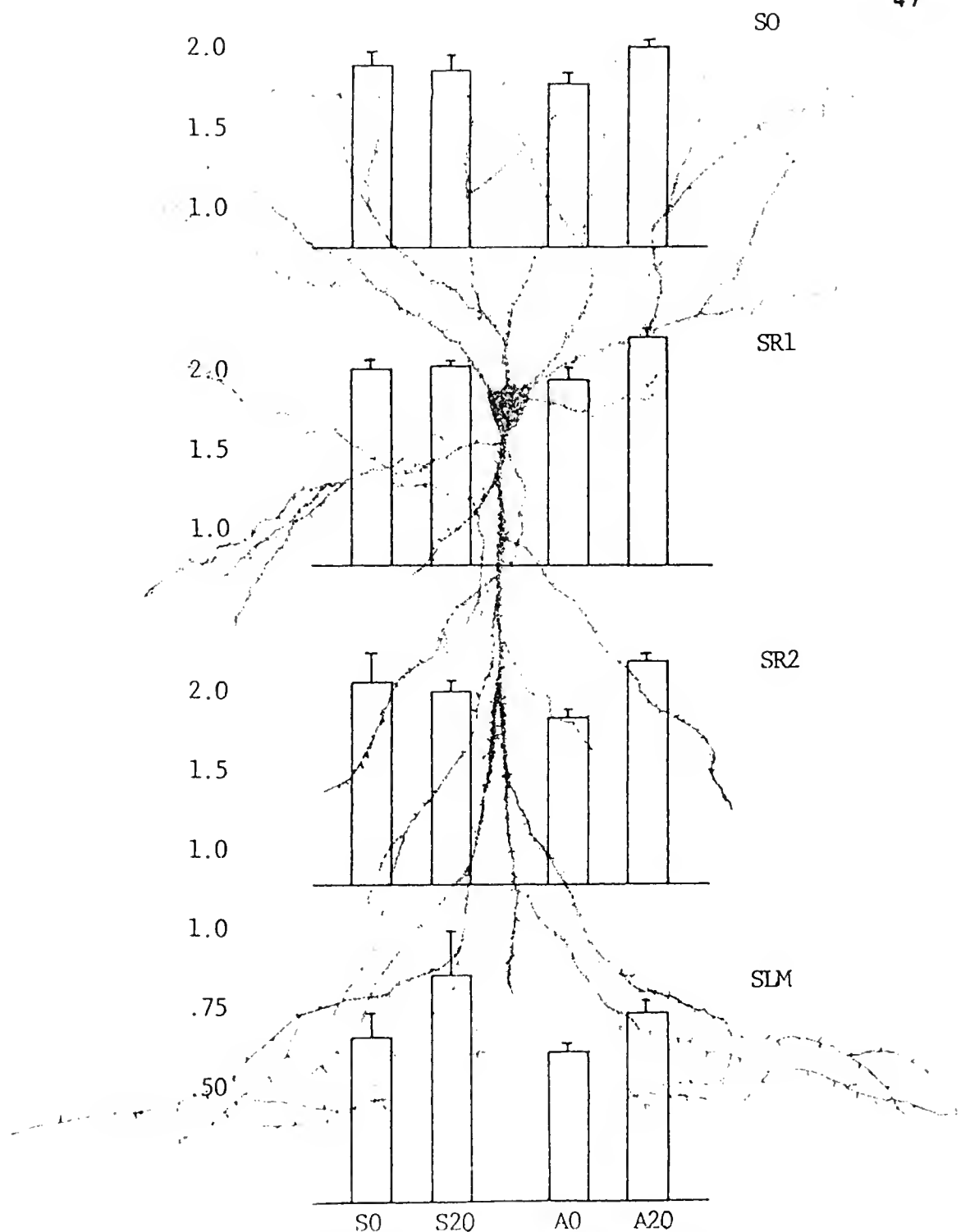
Dentate Granule Cell Densities.

The dentate granule cells were found to be much differently affected by CET (Chronic Ethanol Treatment) than

TABLE 2

CA1 Pyramidal Neuron Spine Densities

	SUCROSE		ALCOHOL		EFFECTS:
	0 WEEKS S0 v. S20	20 WEEKS A0 v. S0	0 WEEKS A0 v. A20	20 WEEKS A20 v. S20	
STRATUM ORIENS	N=6 1.892 (.079) n.s. .9016	N=8 1.873 (.115) n.s. .3687	N=11 1.779 (.079) *	N=8 2.010 (.045) n.s. .2861	Diet: P<.9532 Recovery: P<.1568 D*R: P<.1604 * P<.0345
PROXIMAL RADIATUM	N=6 1.984 (.075) n.s. .5789	N=8 2.049 (.080) n.s. .5941	N=11 1.928 (.064) *	N=9 2.192 (.061) n.s. .1722	Diet: P<.7199 Recovery: P<.0148 D*R: P<.1751 * P<.0088
DISTAL RADIATUM	N=5 2.019 (.198) n.s. .8068	N=8 1.975 (.070) n.s. .2207	N=11 1.814 (.064) *	N=8 2.164 (.040) **	Diet: P<.8106 Recovery: P<.0244 D*R: P<.0294 *P<.0004 ** P<.0305
LACUNOSUM- MOLECULARE	N=5 .638 (.081) n.s. .3371	N=8 .838 (.146) n.s. .6463	N=11 .602 (.038) n.s. .0749	N=9 .718 (.050) n.s. .4318	Diet: P<.2226 Recovery: P<.0911 D*R: P<.6377
COLLAPSED RADIATUM	N=6 2.001 (.113) n.s. .9381	N=9 2.011 (.074) n.s. .2529	N=11 1.868 (.056) *	N=8 2.181 (.046) n.s. .0647	Diet: P<.6952 Recovery: P<.0844 D*R: P<.1377 * P<.0005
ALL CA1	N=5 1.695 (.093) n.s. .9811	N=8 1.692 (.090) n.s. .3407	N=11 1.574 (.058) *	N=8 1.780 (.026) n.s. .2641	Diet: P<.6952 Recovery: P<.0844 D*R: P<.1377 * P<.0079



Abscissae, linear spine density per micrometer, \pm S.E.M..
 S0, stratum oriens; SR1, proximal stratum radiatum; SR2,
 distal radiatum; SLM, stratum lacunosum-moleculare. S0,
 S20, A0, A20 as in text.

Figure 7: CA1 Pyramidal Neuron Dendritic Spine Densities

the CA1 pyramids (table 3, figure 8). While significant diet effects were detected only for the inner and middle thirds of the dentate molecular layer, the mean linear spine density along granule cell dendrites was uniformly highest in the A0 animals, lowest in the sucrose groups, and intermediate in the A20 group. This increase in spine density in granule cells was an unexpected finding. Significantly more spines per micron were found in the A0 group than the S0 group, in the commissural and medial entorhinal terminal regions, and this difference disappeared when the 20 week groups were compared.

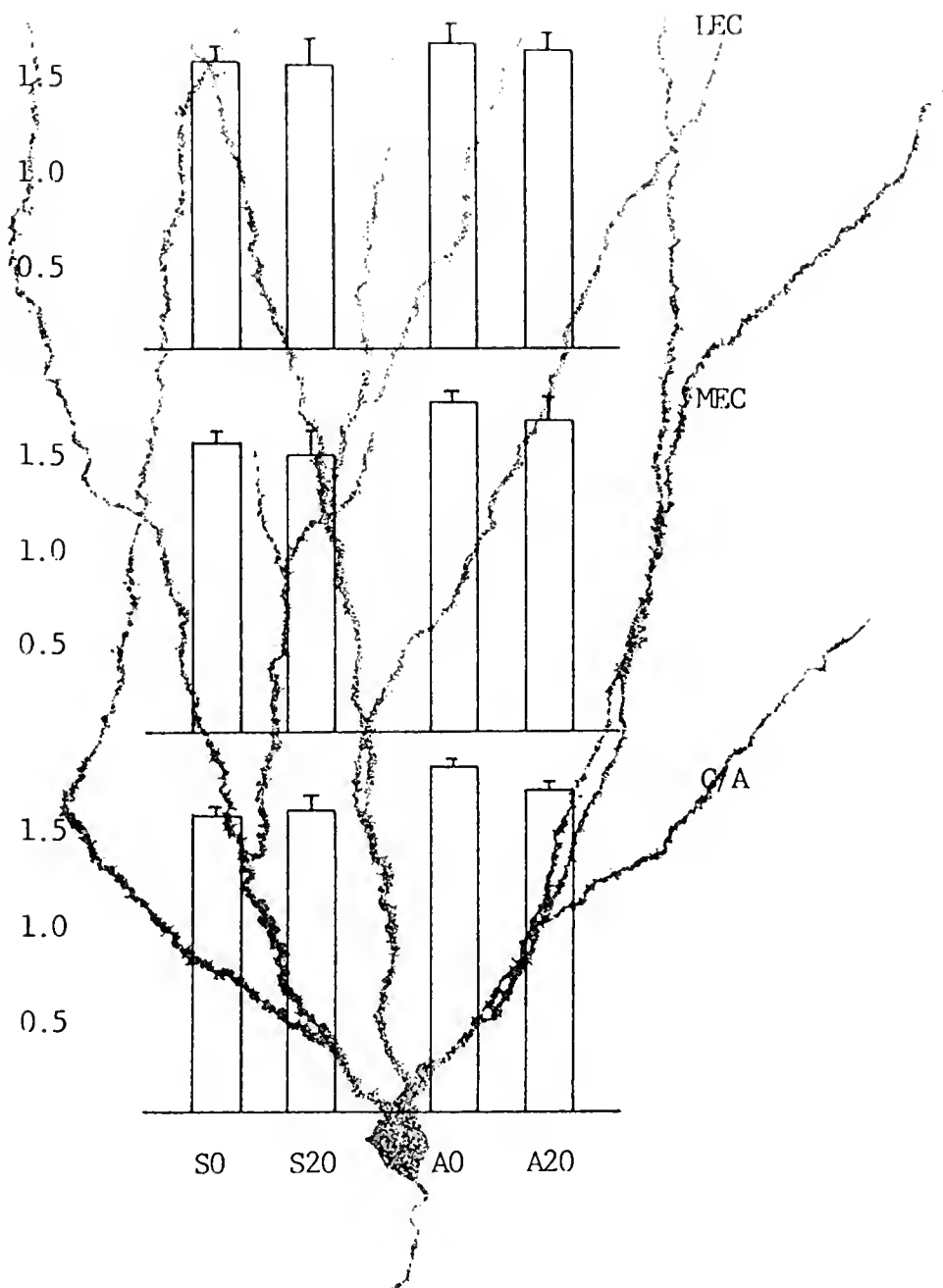
Each of the three molecular layer regions sampled showed increased density in A0 animals: 6% in the outer molecular zone, 14% in the middle, and 17% in the inner third, when compared against S0 values. A 6% increase in granule cell soma area was found as well. Analysis of variance revealed a significant diet effect in the C/A zone and the medial entorhinal zone but not in the outer molecular layer. Recovery effects and interactions failed to reach significance. After 20 weeks, alcohol values returned toward the sucrose levels. Although not statistically different, the A20 mean spine densities were still slightly higher than those of the S20 group. Dendritic spine density in the outer third decreased 2%, the middle zone 6%, and the inner region 7%, compared to 0 week alcohol animals. Thus they all remained higher than either of the control groups

TABLE 3

Dentate Granule Neuron Spine Densities

	SUCROSE		ALCOHOL		EFFECTS:
	0 WEEKS	20 WEEKS	0 WEEKS	20 WEEKS	
	S0 v. S20	A0 v. S0	A0 v. A20	A20 v. S20	
SOMA AREA (sq. μ m)	N=3 106.3 (8.9)	N=2 94.5 (10.0)	N=8 112.56 (4.1)	N=2 112.35 (10.2)	Diet: P<.1764 Recovery: P<.5843 D*R: P<.5487
	n.e. .5267	n.e. .4765	n.e. .9825	n.e. .3827	
COMM./ASSOC (inner third)	N=6 1.570 (.047)	N=6 1.596 (.156)	N=13 1.835 (.069)	N=7 1.713 (.081)	Diet P<.0333 Recovery: P<.5039 D*R: P<.4419 * P<.0254
	n.e. .0751	*	n.s. 2906	n.s. .5045	
MEDIAL EC (middle third)	N=6 1.541 (.061)	N=6 1.470 (.158)	N=13 1.750 (.057)	N=7 1.653 (.130)	Diet: P<.0436 Recovery: P<.3926 D*R: P<.6972 * P<.0413
	n.e. .6871	*	n.e. 4388	n.e. .3859	
LATERAL EC (outer third)	N=7 1.544 (.083)	N=6 1.543 (.141)	N=13 1.640 (.088)	N=7 1.612 (.072)	Diet: P<.3963 Recovery: P<.8709 D*R: P<.8947
	n.e. 9973	n.e. 4065	n.e. 0348	n.e. 6563	
COLLAPSED MOLECULAR LAYER	N=7 1.571 (.058)	N=6 1.538 (.145)	N=13 1.753 (.053)	N=7 1.659 (.088)	Diet: P<.0533 Recovery: P<.4087 D*R: P<.7174 * P<.0425
	n.s. 8258	*	n.e. .3382	n.s. 4750	

Hippocampal dendritic spine density results: group means \pm S.E.M. by sampling region. The rightmost column displays the results of two-way ANOVAs for diet treatment, recovery time and their interaction. The four columns interposed between the group means show the results of one-way ANOVAs and T-tests performed within diet groups or recovery times. Asterisks mark effects significant above the .05 level, but note that several other differences approach this level.



Abscissae, linear spine density per micrometer, \pm S.E.M..
 C/A, commissural/associational; MEC, LEC, medial and lateral
 entorhinal terminal zones. S0, S20, A0, A20 as in text.

Figure 8: Dentate Granule Neuron Dendritic Spine Densities

at both recovery times. No change in granule cell soma area was detected across the recovery interval. Thus, although the initial effect of CET was opposite in these neurons from CA1, at the end of a 20 week abstinence interval dendritic spine densities for both neuronal types were more like those of normal animals than they were immediately after the exposure period.

When the counting regions were collapsed by cell type, the only significant finding in CA1 pyramids was the difference between spine densities of A0 and A20 groups. In granule cells, spine density was significantly higher in the A0 than the S0 group, but this difference disappeared over the 20 week recovery interval.

After these results were analyzed, qualitative observations on the appearance of dendritic architecture were followed up in the decoded tissue. While no valid quantitative data support these observations, it can be noted that elongated dendritic spines, dendritic varicosities, increased tortuosity of dendritic paths, and an increase in the size of stained astrocytes may be associated with the consumption of ethanol for 20 weeks. However, gross pathology was not often detected in the alcohol animals, and noticeably abnormal dendrites were only occasionally seen.

Discussion

Experimental Considerations

Abberant dendritic changes following chronic ethanol exposure have been reported before. In one of the earliest reports, Riley and Walker found substantially greater spine loss in both CA1 and granule cells, in female mice exposed for 4 months. Since the same liquid diet paradigm was used in that study as in the present one, our failure to replicate their results can only be explained as a function of the use of a different Golgi method, a different species, the use of different measurement techniques, or some difference in the maintenance of the experimental animals. It is widely known that the different Golgi variations can produce very different pictures of the dendritic architecture of neurons, especially in the representation of spines. Although the Golgi-Kopsch variant used by Riley and Walker does impregnate spines well, it was decided during pilot studies that the rapid Golgi variant yielded better and more consistent spine impregnation and definition in our hands. (It is not recommended for use where the branching or lengths of dendrites are required, as unobstructed views of completely impregnated neurons occur only infrequently.) This raises the issue of whether Golgi stains accurately reflect the number of spines in the tissue, one of several methodological considerations discussed in detail by Mervis ('81). If some deafferentation of hippocampal neurons

occurs with chronic ethanol treatment, and deafferented spines are less amenable to Golgi impregnation (Powell, '67), then spines might be present but not become stained. We consider that a change in stainability reflects some change in physical or chemical properties of the spine that is indicative in its own right (Riley and Walker, '78). It is possible, then, that the methods used by Riley and Walker ('78) led to an overestimation of spine loss, if their Golgi picture reflected not a loss but a difference in stainability or visibility of spines in the alcohol animals. Phillips and Cragg ('83) present some data that supports this possibility; spine head area is significantly decreased 13% in the alcohol treated C57 black mouse, even after 4 months for recovery, to a size less than the wavelength of blue visible light. In alcohol treated mice, therefore, spines may simply not be resolvable using light microscopy. Spine head area, estimated at $.149 \pm .003 \text{ } \mu\text{m}^2$ in mouse basilar CA1 dendrites (Phillips and Cragg, '83), has been estimated to be $.72 \pm .02 \text{ } \mu\text{m}^2$ in the guinea pig, (Turner and Schwartzkroin, '83) which is probably closer to the size in the rat, and greater than the wavelength of visible light.

Other differences between rats and mice could also account for some of the differences in results. Mice have a shorter life expectancy than rats, and a 4 month exposure period in mice might be considerably more detrimental than a

longer duration in rats. Perhaps more significant is that the mice in the previous study consumed an average of almost 25 g/kg ETOH/day, in contrast to less than 15 g/kg/d in the rats. Although mice have a higher capacity for metabolizing ethanol (Wallgren, '70), it is not understood how the doses correspond between the species. If the relative exposure or exposure duration was greater in mice in the Riley and Walker study, the present results might not seem inconsistent. Such a possibility is supported by data from Kunz et al., ('76) who found an increase in rat CA1 spine density (.94/ μ m v. 0.71, apical; 0.94 v. 0.65/ μ m, basal), using a chronic ethanol consumption model with a shorter exposure period (52 days) and different dosing procedure (6.7 g/kg/d intubation, once per day) than that used in the present study. It is possible that dendritic degeneration and recovery might be sensitive to ethanol exposure parameters, considering that variables as apparently subtle as the quality of the sensory environment (Connor et al., '80; Juraska, '84) may affect dendritic morphology.

Another possible factor might be the sex of the experimental animals. In humans, sex differences in psychometric performance by alcoholics have been described (Fabian et al., '84; Ellenberg et al., '80), and sex differences in dendritic spine changes consequent to experimental environmental conditions have been observed (Juraska, '84). Female mice were used by Riley and Walker

('78), while the present study used male rats. The last major difference between our rats and Riley and Walker's mice is that the rats were individually caged, while the mice were housed in groups. Housing, in combination with other environmental conditions, has been shown to affect dendritic spine density in mice (Connor et al., '80).

With the small and statistically non-significant differences we find in many of our across-group means, it is necessary to consider the significance of these effects. Two points should ease the reader's mind. First, the statistical analyses were made using animals within groups rather than spine counts within groups. Good arguments can be made for either approach; it was decided that the more conservative method of averaging spine counts within animals would be used. This may have sacrificed some of the statistical weight of the results, since more degrees of freedom would have been used in the analyses of variance if spine counts per group were evaluated. Second, in other studies of the effects of chronic ethanol treatment on dendritic spine and branching parameters in cerebellar Purkinje cells, it has been found that a non-significant 15% decrease in the number of branches, and a significant 22% loss of spines, after 3 months exposure (Tavares et al., '83a,b). Greater losses were consistently observed at 6 months exposure, with both measures reaching statistical significance. In several other studies, alcohol treated

animals exhibit apparently detrimental although nonsignificant differences in quantitative dendritic parameters (Pentney, '82; Phillips and Cragg, '83; McMullen et al., '84), suggesting that initially nonsignificant changes tend to become progressively more pronounced with longer exposures, and may be considered to be real effects even though failing to reach acceptable levels of significance at early time points. The uniformity in the direction of the differences, and the fact that many of our hypothesis testing probabilities approach the .05 level, argue that this sort of continuum may exist for the neurons we measured. In addition, most of our nonsignificant results still have a better than even chance of being real effects. Although strict statistical interpretation of the individual tests does not allow us to claim either an initial ethanol effect in CA1 or a recovery effect in granule cells, neither does post-hoc consideration of all the results conclusively negate these possibilities. While future experiments may have better statistical success by using other durations of both diet and recovery, the present results are supportive, if not unequivocally, of the hypothesis that dendritic spine damage and recovery can partly underlie CNS pathomorphology and its amelioration.

Our selection of 20 weeks as the sole diet duration was made on the basis of earlier studies in our laboratory indicating that a significant 15-20% loss of granule cells, and a significant 10% loss of CA1 pyramids, was present

following this exposure in rats (Walker et al., '80), and that a 50-60% spine loss occurred in dentate granule cells and CA1 basilar dendrites in mice exposed for 16 weeks (Riley and Walker, '78). Since it is a general principle of toxicology that, with chronic sublethal exposures, cells eventually reach a point of no return from which recovery is impossible (Bridges et al., '83), we wanted to insure that we used a diet period sufficiently long to result in detectable dendritic pathology, but not so long that recovery might be impaired. In contrast to the Riley and Walker spine loss data, 18 weeks of ethanol consumption has been reported by two groups not to affect spine density in the rodent hippocampus at all, when electron microscopy is used to estimate spine density (Phillips and Cragg, '83; Lee et al., '81), although the average daily consumption of ethanol by animals in the study that used rats may have been less than our rats received (Lee et al., '81). Furthermore, Lee et al. made their measurements in proximal radiatum, where we find the smallest spine density changes.

A second possible source of apparent discrepancy between spine estimates of different researchers is the finding that spine density decreases on cerebral cortical pyramidal cells by almost 50% between 90 and 414 days of age in normal rats (Globus et al., '73), and then increases again by 630 days to the levels of young animals. Similarly, primates undergo an initial postnatal overproduction of spines (Duffy and

Rakic, '83), peaking at about 6 months of age, and then spine density returns to neonatal levels by adulthood. Thus the age of the animal at the time of sacrifice may be especially important, and in a species (and possibly strain) specific manner, to comparisons of spine density across experiments. The last major possible cause is a difference in the type of Golgi method used. Wide differences in spine representation exist across the many Golgi procedures available, and some variability can occur even within individual stained blocks of tissue.

Other sources of error in estimating morphometric parameters in populations from relatively small groups of animals include the normal genetic heterogeneity of a particular strain of animal. We consider that the variability between our sucrose control groups is in part indicative of the degree of heterogeneity encountered across batches of Long-Evans rats obtained at different times. Although all of our animals were obtained from the same source, because of the labor-intensive nature of our liquid diet consumption model it was necessary to use three sets of animals obtained at different times. We can only explain the intergroup variability by speculating that some genetic, seasonal, or other unknowable source for this variability exists apart from our own experimental error. Thus we maintain that we in fact do see two small yet consistent experimental effects that would be better statistically

validated if larger groups of animals were used. First, the chronic dietary consumption of ethanol, in the face of adequate nutrition, results in a decrease in dendritic spine density in CA1 pyramidal cells and an increase in density in dentate granule cells, in the male Long-Evans rat. Second, these changes at least partially revert during a post-ethanol recovery period.

Estimates of Total Neuron Alterations in Spine Number

Using published data for the total length of the dendritic trees of the two neuronal types measured in this report, and the effects of chronic ethanol treatment thereon, estimates can be derived of the degree of change in connectivity that results from density alterations as found here. For granule cells, probably the best estimates for total dendritic length are those of Desmond and Levy ('82) (rat) and Turner and Schwartzkroin ('83) (guinea pig), who arrive at figures of $3,662 \pm 88$ and $3,700 \pm 300$ μm , respectively. Using our estimated average (control animal) spine density for granule cells of $1.56/\mu\text{m}$, and a total length estimate of $3,662$ μm , about $5,700$ spine synapses are probably observable in Golgi material per granule cell. This is lower than estimates of $10,000$ molecular layer synapses per granule cell in the adult Wistar rat (West and Anderson, '80) derived from electron microscopic observations. Using a figure reported by Matthews et al.

('76b) that 85% of synapses in the molecular layer occur on spines, assuming 1 synapse per spine, and accepting that only about .3 to .4 of the spines can be counted (Feldman and Peters, '79, figure 6, $S_d = .5$, dendritic diameter $\leq 4 \mu m$, spine length = $1 \mu m$), then a derived estimate of the true number of spines per granule cell comes to about 16,000 and the total number of molecular layer synapses per granule cell may be as high as 19,000.

For CA1 pyramids in the rat, total dendritic branch length has been calculated to be about 4,885 μm at 90 days of age (Pokorny and Yamamoto, '81), (but 8,400 μm in guinea pigs (Turner and Schwartzkroin, '83)). Using their regional total branch lengths with our regional spine count estimates, we calculate that about 10,000 countable spines occur along a normal CA1 pyramid of the control rats used here. (Because of the greater range of dendritic diameter in these neurons we do not attempt a corrected estimate of the total number of spines per cell.) If a 10% decrease in the branch length occurs after this duration of ethanol treatment (McMullen et al., '84), and only a 10% decrease in spine density on the remaining dendrites accompanies this loss, then the CA1 pyramids would similarly support about 2,000 fewer countable spines per cell, at the end of 20 weeks of ethanol consumption. With the magnitude of recovery of synaptic density that is reported here, CA1 pyramids in alcohol animals may gain 4-5,000 synapses during

the 20 weeks post-exposure, while sucrose animals may not change significantly. Individual granule cells, in contrast, might form about 3,000 more spine synapses with their afferents, by the end of a 20 week ethanol exposure, but lose about 2,000 of these during the post-ethanol period.

Electrophysiological Consequences of Long-term Ethanol Exposure

It might be expected that changes of this magnitude, without even considering cell deaths, would noticeably alter the electrophysiological synaptic transmission characteristics recorded in response to a controlled stimulation of afferent pathways; paradoxically, however, significant effects have been difficult to detect for EPSPs (excitatory postsynaptic potentials), or nearly any other measure of synaptic efficiency that has been obtained (Abraham et al., '81; Lee et al., 81; but see Durand et al., '80 (impaired long-term synaptic potentiation)). However, the degree to which an extracellularly recorded CA1 population action potential spike is increased in response to a test stimulus applied to ipsilateral regio inferior afferents shortly after a conditioning pulse (paired pulse synaptic potentiation) has been found to be enhanced after chronic ethanol treatment in previous studies in this laboratory (in vivo, Abraham et al., '81; in vitro, Rogers et al., unpublished data). The EPSP potentiation is

unchanged by the ethanol treatment. This indicates that some adaptation of individual surviving synapses occurs in the face of chronic ethanol treatment and withdrawal. Since these animals were tested at least 8 weeks after exposure to ethanol, this adaptation may include recovery of synaptic structures. In support of the idea that spine density recovery might be reflected in electrophysiological recovery, Durand et al., ('84) described impaired long-term potentiation in CA1 pyramidal neurons in chronic ethanol animals before, but not after 2 month withdrawal periods. In contrast to CA1, and possibly related to differences in spine density effects, paired pulse potentiation of the granule cell population action potential in response to stimulation of the entorhinal-dentate pathway is diminished in alcohol animals (Abraham et al., '84). Since the postsynaptic potentials are unchanged in alcohol animals in either neuronal type, the significance of the differential spine density effects for understanding the differential effects on the action potential is unclear. This electrical event does not directly reflect synaptic (spine) properties but the integration of synaptic potentials and their conversion into action potentials. These contrasting physiological findings could be an indication of specific alcohol effects on interneurons. CA1 appears to have both a greater population and variety of non-pyramidal neurons than the dentate gyrus.

Possible Mechanisms of Spine Density Alterations

Somatic proximity.

The proximodistal pattern of spine density effects in granule cells deserves some comment. Both the greatest initial increases and the greatest subsequent "recovery" occur proximally, and decrease progressively at more distal levels of the dendritic tree. Two possible explanations for this pattern can be entertained. First, if the manufacture and maintenance of spines requires a significant investment of raw materials and energy by the soma, then those dendritic regions close to the soma will be best able to respond to metabolic influences on the soma: first served, first cleared. Alternatively, the presynaptic axons providing input to the granule cell dendritic tree, some of which are known to sprout in response to deafferentation of the outer dendritic tree (Cotman et al., '81), may exert some control over the number of postsynaptic sites available as the turnover of the terminals is affected by CET. Factors as simple as the proximity of afferent somata may explain a more robust effect in the terminal region of hilar associational afferents than in the termination zone of the more distant entorhinal cortex projection neurons. A slightly different explanation is that entorhinal neurons are just more susceptible to the neurotoxic effects of chronic ethanol exposure. In this context the findings of Abraham et al. ('82a,b) are of particular interest.

Current source density analysis indicates that, in the dentate molecular layer, some reorganization of afferents occurs following chronic ethanol treatment, such that the current sink representative of the entorhinal input shrinks in relation to the height of the granule cell dendritic tree. In CA1, a similar shrinkage occurs in the current sink putatively attributed to afferent terminals arising in the contralateral CA3 region. Since these are myelinated, but their ipsilateral counterparts are not, (and neither are they as affected in CSD measures) it must be considered likely that alcohol may preferentially disrupt input carried long distances, relayed mostly by myelinated axons. This is consistent with the human clinical literature, and may be related to our finding that both the initial decrease and later increase in spine density are more pronounced in distal than in proximal radiatum: It might be expected that commissural fibers damaged by CET would be replaced by collaterals from the same side, simply because of the proximity of the new terminals to their perikarya. This appears to be the reaction seen following neurotoxic deafferentation of CA1 with kainic acid, which kills regio inferior neurons preferentially (Nadler, '80). Since dendritic spines density does not reveal the source of the afferent fibers (the same number of spines may obtain even if afferent reorganization occurs), quantitative autoradiographic tracing experiments are currently being

conducted in our laboratory in order to bring more resolution to this question.

Presynaptic influences.

It has been hypothesised that presynaptic terminals play an inductive role in spine formation (Hamori, '73; Frotscher et al., '77; but see Hirano, '83), and that the anomalous long spines observed following ethanol treatment may represent "seeking" of presynaptic terminals by deafferented dendrites (Tavares et al., '83). A lower density of presynaptic terminals in the vicinity of the dendrite may lead to such spine elongation. There are several reports that dendrites and spines become altered following deafferentation (Jones and Thomas, '62; White and Westrum, '64; Chen and Hillman, '82; Steward and Caceres, '83). If spines are in fact extended in an effort to form synapses, and CET produces preterminal degeneration of afferents to the granule cell dendrites, then spine number would increase. This would be especially advantageous if granule cells not killed off were to attempt to compensate for the loss of whole cells and portions of the dendritic trees of the remaining neurons, and in fact appears to exist as a compensatory mechanism for aging-related neuronal loss (Cotman and Scheff, '79). To maintain the total number of synapses within the structure, more spines would have to be formed on the survivors. Such a response might also be more likely to occur in the absence of a cytotoxin, i.e., during

the postethanol period, and to itself abate as the health of damaged surviving neurons returned, allowing them to support more synapses. This may also relate to the overproduction of CA1 spines in the 20 week alcohol group; different initial and late responses to chronic ethanol by pyramidal and granule cells may reflect differences in the time course of toxic effects. If pyramidal cells die more slowly, and continue to die after ethanol exposure, and granule cells die early and rapidly but survivors exhibit greater compensatory spine growth both during and post-exposure, then a delayed increase in the number of spines per surviving CA1 neuron may still result from the effect of decreases in the number of cells. In support of the hypothesis that surviving neurons increase spine density in response to neuron loss, Phillips and Cragg ('83) observed no loss of CA1 pyramidal cells in animals sacrificed immediately after ethanol exposure, but a 9% loss in animals allowed to survive 4 months. Also, Kunz et al. ('76) have described increased CA1 spine density in tissue where electron microscopy reveals neuronal degeneration. Since various neurotoxic agents and treatments are known to affect these cell types differently (Nadler, '80; Walker et al., '80; Irle and Markowitsch, '83; Kirino and Sano, '84 a,b) the parsimony and probability of such an hypothesis merits its further investigation. Our finding that spine density remains higher in both neuronal types after 20 weeks of

recovery may then reflect the fact that both areas do suffer permanent neuronal loss, with survivors maintaining a compensatory increase in spine density.

Systemic and molecular influences.

Several factors known to affect neurons might be of physiological importance for spine density changes resulting from chronic ethanol consumption. In addition to any direct effect upon neurons, such as the reported increase in cholesterol content in alcohol-adapted neuronal membranes (Crews et al., '83), alcoholism is known to produce many peripheral organ effects (Cohen and Gallant, '81), many of which may underlie pathological processes in the CNS. For example, in human alcoholics, macrocythemia is very common, and may result in the slowing of blood flow through capillaries (Larkin and Watson-Williams, '84). Since the hippocampus is especially susceptible among CNS regions to the adverse effects of anoxia, hypoxia, and ischemia (Johansen et al., '84; Kirino and Sano, '84a), and acute ethanol exposure results in ischemia specifically in hippocampus and cerebellum (Goldman et al., '73), (two of the most susceptible regions to alcohol-related neuropathology), the role of hematological changes in alcoholic hippocampal pathology may be very important. The cytopathology of all four situations is very similar, with degenerative processes that especially affect dendrites (Johansen et al., '84; Kirino and Sano, '84b). Furthermore,

it has been observed that in humans, dentate gyrus alcoholic neuropathology has been noted to be most severe in proximity to blood vessels (McLardy, '74). Another line of evidence that supports the role of altered blood supply in alcoholic neuropathology is that patients with alcoholic organic brain syndrome improve better on psychometric tests and EEG diagnostics when treated with antihypoxidotic/nootropic drugs, which allow nervous tissue metabolism rates to remain normal while requiring less oxygen (Saletu et al., 83).

A second common finding in human alcoholics is elevated circulating corticosteroid concentrations, and abnormal regulation of steroid release (Bertello et al., '82; de La Fuente et al., '83; Abou-Saleh et al., '84; Khan et al., '84). Abnormalities in the hypothalamic-pituitary-adrenal axis, as reflected in dexamethasone suppression tests, appear to rectify in the early weeks of abstinence (Abou-Saleh et al., '84; Khan et al., '84), and may thus account for some of the synaptic structural changes seen in chronic alcohol consumption that recover with abstinence. Physiological doses of corticosteroids, or disrupting the normal circadian rhythm of release, have been shown to adversely affect the magnitude of reactive synaptogenesis in the rat dentate gyrus (DeKosky et al., '84), and have thereby been implicated in the relative failure of old animals to exhibit the same synaptic regenerative capacity as young animals. Since chronic alcohol treatment also

reduces the amount of reactive synaptogenesis that rats can produce in response to damage (West et al., '82; Walker et al., '84), corticosteroid elevations might be a common deleterious symptom of alcohol consumption and aging. Corticosteroids have also been shown to play a role in the regulation of synapse formation in developing retina (Puro, '83). If there is natural turnover of hippocampal synapses, then elevated steroid levels, or normal levels but disordered circadian patterns might significantly reduce at least the replacement component of turnover.

Another reported effect of chronic ethanol exposure is a decrease in protein synthesis (Noble and Tewari, '74; Earvin et al., '80; Lieber, '84). Since spines appear to contain a specialized cytoskeletal network (Cohen et al., '83; Landis and Reese, '83), composed of several protein species (Fifkova and Delay, '82; Caceres et al., '83; see also Cohen et al., '83), and have been reported to be spatially associated with most of the protein synthetic apparatus, polyribosomes, in the dendrites of hippocampal neurons (Steward and Levy, '82), ethanol may affect the metabolic and structural integrity of spines directly. It has been shown that the organization of spine-associated polyribosomes is responsive to experimental deafferentation (Steward, '83); if CET produces a partial denervation, and the normal polyribosome response is altered, then some change in the morphology of dendritic spines might be

expected. As spines are currently under intense investigation because of the possibility that they may undergo morphological and enzymatic changes in response to synaptic activation that may reflect functional modulations in the synaptic efficiency of connections (vide supra), this possibility deserves more attention. However, the increased spine density found on granule cells confounds such a simple explanation. It may be important that, even though synaptic connections are changed in number, population neurotransmission characteristics are little changed from normal. Can individual surviving synapses be modified in their efficiency, so that normal I/O relationships hold even in alcoholized animals? The evidence to date suggests that EPSP generation and action potential thresholds are unchanged, indicating that the answer may be "yes". In this regard, membrane fluidity and composition changes may be highly adaptive (Harris, '84; Crews et al., '83).

The primary metabolite of ethanol, acetaldehyde, is itself reported to decrease the activity of microtubules and protein synthesis, and also to cause cells to retain proteins internally (Lieber, '84). These effects would be detrimental to the cytoskeleton, and decrease a neuron's ability to elaborate healthy dendrites and spines. In some neurons, chronic ethanol treatment has been found to increase intranucleolar bodies, aggregates of ribonucleoproteins and RNA that are believed to represent

'stored' protein synthetic components (Dunmire and LaVelle, '83). Others have observed increased somatic rough endoplasmic reticulum and multivesicular bodies, while dendrites showed marked vacuolization and degeneration (Goldstein et al., '83; Irle and Markowitsch, '83), suggesting that distal protein synthetic material may become sequestered in the soma at the expense of the peripheral processes. Thus ethanol may produce disruption in the extranuclear protein synthetic machinery while at the same time lead to intranuclear sequestration of replacement molecules. Such a process might facilitate cytological recovery once alcohol is no longer present, since stored elements could be recruited more rapidly and with less energy than required by the induction and execution of translation processes. It may also represent an attempt by the cell to limit its losses to the peripheral processes, in order to save the soma, or be, simply, an aberrant pathological condition.

Other molecules related to cytoskeletal dynamics that are affected by chronic ethanol include cyclic AMP and calmodulin. The former has been shown to regulate synaptogenesis in culture, by influencing calcium channel expression, glycoprotein modifications, and the levels of certain proteins in the cell (Nirenberg et al., '83). In mice, chronic ethanol treatment has been reported to decrease the ability of neurotransmitter molecules to

increase adenylate cyclase activity (Tabakoff and Hoffman, '79), and chronic ethanol treatment may reduce CNS calmodulin levels (Towle et al., '81; but see Luthin and Tabakoff, '84). Since calmodulin regulates adenylate cyclase by associating with calcium ions, which enter the spine upon the reception of neurotransmitter molecules, a decrease in this enzyme could reduce the amount of cAMP produced by activating a synapse. This might produce a disruption in molecular communication between pre- and postsynaptic structures necessary for maintaining the functional properties of the connection, and would have important implications for the hypothesized processes by which synaptic potentiation might occur (Baudry and Lynch, '80). Possibly related to the cAMP/calmodulin phenomena is the finding that catecholamine metabolism is often abnormal in chronic alcoholics. Norepinephrine, in particular, has been linked to normally occurring synaptic plasticity (cf. Cotman et al., '81), and found to be affected by alcohol (Eisenhofer et al., '83).

Finally, many disorders of vitamin, mineral, and nutrient metabolism, some of nutritional and some of pathophysiological origin, are common in alcoholics (Lieber, '84, Sherlock, '84). Thus differences in amino acid availability, carbohydrate energy sources, electrolytes, or biocatalysts may have important consequences for neurons with spines.

Spine Density and Recovery in CT Scans

Since in living human alcoholics only gross morphology can be quantified, the present results speak to those who are interested in the mechanisms underlying the reversal of cerebral atrophy diagnosed in CT scans. Although several non-exclusive hypotheses have been proposed to explain the neurobiology of this phenomenon, experimental evidence for any one is minimal or nonexistent. We consider it interesting, in light of the tissue dehydration/rehydration hypothesis of alcoholic CNS damage (Carlen and Wilkinson, '80), that we find an apparent difference in tissue density between our groups, judging from the brain weight/area data. This indicates that perhaps more than one symptom is responsible for CT cerebral atrophy. The loss and regrowth of dendritic spines on CNS neurons, although it may not be extraordinarily large in magnitude, may be sufficient to explain the occurrence and reversal of a change in tissue volume, but other effects, such as hydration, may be partly responsible for the effects of chronic ethanol consumption on intellectual abilities.

CHAPTER III CNS RECOVERABILITY FOLLOWING LONG-TERM ETHANOL CONSUMPTION

Experimental Methods and Design

To study recoverability, or the relative capacity of CNS tissue to respond to an extrinsic injury, the amount of sprouting of spared afferent axons to the dentate gyrus was quantified in alcohol and control animals following a partially deafferentating lesion. The dependent variables are the widths and stain intensity of afferent-specific stain bands in tissue prepared using AChE histochemistry, and the amount of intra-animal difference in these bands following unilateral entorhinal cortex lesions. Intra-animal differences were calculated by comparing the lesioned with the unlesioned sides. Baseline alcohol effects were determined in unlesioned alcohol-treated animals and by comparing the unlesioned side of alcohol and control animals.

Entorhinal Cortex Lesions

Eight weeks after the end of the liquid diet treatment, the entorhinal cortex of the left cerebral hemisphere was destroyed by passing a 1 milliamp current through the central carrier of a 75 micron insulated concentric bipolar

electrode (Frederick Haer) for 45 seconds at each of six stereotaxically defined locations. With the skull mounted level, lesions were made 2.5, 4.0, and 5.5 mm below the surface of the brain at 8.5 mm posterior to the bregma skull landmark and 3.7 mm lateral to the midline. At 8.7 mm posterior and 4.6 mm lateral, lesions were made 3.0, 4.5, and 6.0 mm beneath the surface. Current passage through the electrode, which was introduced at an angle of 11 degrees from vertical, was sufficient to produce a discrete destruction of medial and lateral entorhinal cortex without infringing upon the nearby dentate gyrus or other cortical regions. Lesions were performed on animals anesthetized with pentobarbital (50 mg/kg, 0.1 cc atropine and 0.2 cc bicillin for postsurgical prophylaxis).

Histological Preparation

During the post-liquid diet period and continuing during the postlesion survival, animals were fed ad lib with ordinary lab chow and tap water. Forty days after being lesioned, they were sacrificed with intraperitoneal pentobarbital overdose and perfused with gravity-fed solutions delivered into the left cardiac ventricle through 18 gauge hypodermic tips. To process these brains for both Timm's and AChE histochemical reactions, animals were first perfused with phosphate buffered physiological saline (approx. 300 ml, 30 degrees C.), followed by 500 ml of a

solution made from 11.7 g sodium sulfide, 11.9 g sodium phosphate, and 1.0 g sodium diphosphate in 1000 ml distilled water. This causes CNS cations like Zn^{+2} , Pb^{+2} , and Cu^{+2} to form visible, insoluble sulfides. The brain was immediately removed from the skull and placed for 1-2 hours in a 20% sucrose fixative (975 ml Sorensen's buffer (.066 M potassium dihydrogen phosphate, 19.6%; .066 M disodium phosphate, 80.4%), 10 g paraformaldehyde, and 25 ml 50% glutaraldehyde). The fixed brains were embedded in gelatin albumin and cut at 40 microns on a freezing stage micrctome. Alternate sections were collected separately for subsequent Timm's or AChE processing.

Sections for the Timm's stain were mounted on alum dipped glass slides and developed in a photographic darkroom for 55-100 minutes in a mixture of 120 ml gum arabic, 20 ml citrate buffer (25.5 g citric acid, 23.5 g sodium citrate, 100 ml triple distilled water), 60 ml 5.67% hydroquinone, and 1.0 ml 17% aqueous silver nitrate. Following this intensification step, slides were dehydrated and coverslipped with Eukitt medium (Calibrated Instruments, Ardsley, NY).

Sections for AChE staining were collected into saturated sodium sulfate over ice, then incubated at 21 degrees C. for 75 minutes in a solution of 7.2 ml ethopropazine HCl, 115.6 mg acetylthiocholine iodide, 75.0 mg glycine, 50.0 mg copper sulfate, 885 mg sodium acetate, and 100 ml distilled water

(cf. Geneser-Jensen and Blackstad, '73). This reduces nonspecific cholinesterase staining while forming a chromogenic complex between the enzyme and its artificial substrate. The sections are mounted on glass slides after being rinsed 6-7 times with distilled water and immersion for 1 minute in 1.25% sodium sulfide in .1 N HCl (8.08 ml HCl in 1000 ml water) in a fume hood, followed by 6-7 more distilled water rinses. The last rinse was 30% ethanol, and began dehydration prior to clearing in xylene and coverslipping with Fukitt.

Verification of Lesion Placement and Size

The location and extent of the entorhinal cortex lesions were evaluated on tracings made using a microprojector. Four dorsal-ventral levels (1, 4, 7, and 10) were compared for evidence of complete entorhinal deafferentation via either entorhinal cortex or perforant path/angular bundle destruction. Animals were not included if lesions encroached upon the dentate itself. Figure 9 shows the lesion reconstruction of one representative animal. Ten animals from each diet group were ultimately selected for measurements. Measurements of the the extent and location of the lesions are presented in the Results section.

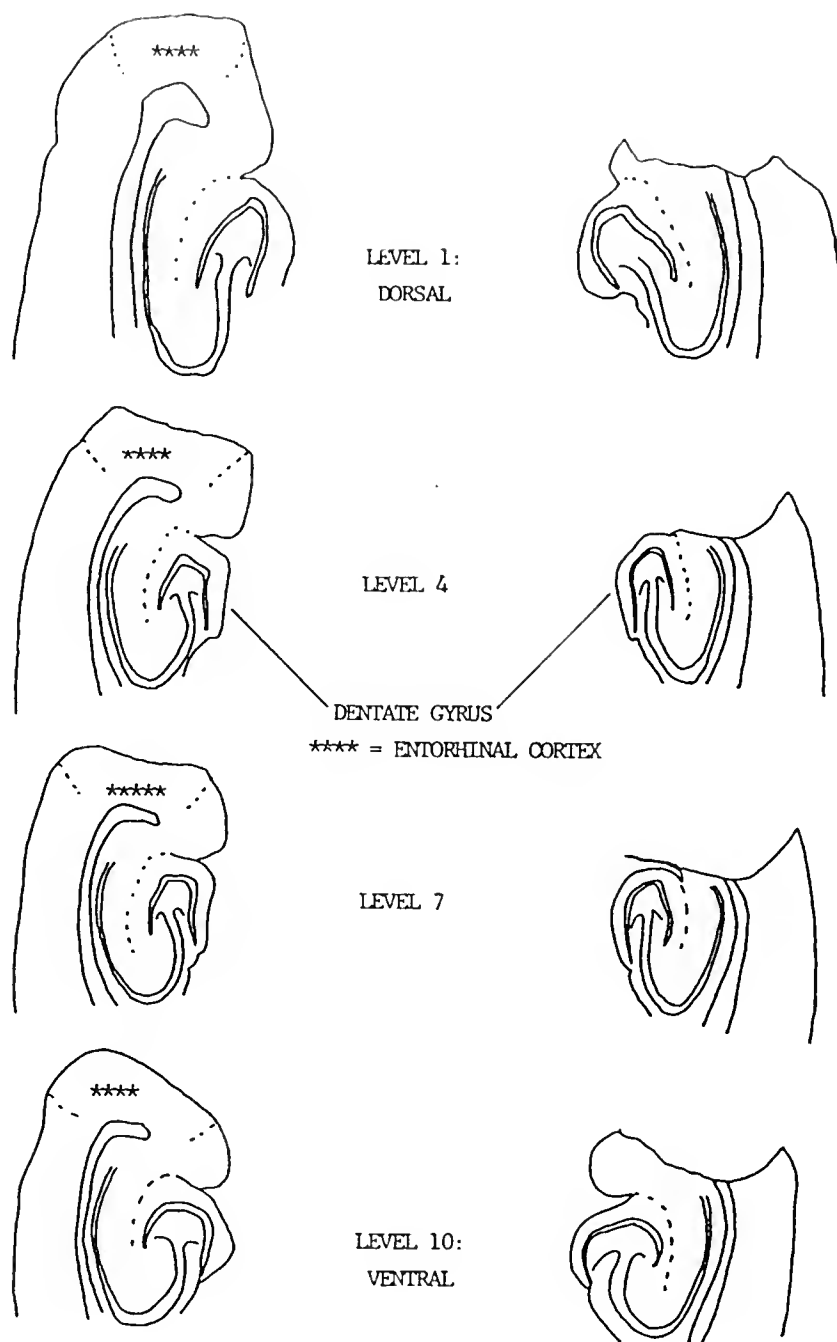


Figure 9: Reconstruction of Entorhinal Cortex Lesions

Measurements of Histological Sections

Reactive synaptogenesis following unilateral entorhinal lesion was evaluated by measuring the width and stain intensity of the bands in the AChE-stained histological sections. The band of principle interest was that corresponding to the associational/commissural afferent terminal field, in the inner third of the dentate molecular layer. Measurements of other stain bands provided 1) data corroborating the lesion reconstruction drawings, since shrinkage should reflect the extent of molecular layer deafferentation at the point the band measurements are obtained, 2) evaluation of reactive synaptogenesis by contralateral entorhinal and septal afferents, and 3) data revealing lesion effects previously unobserved or unreported.

Ten stained sections, spaced at approximately equal intervals, were selected for measurement for each animal. These were found between anatomical landmarks that were common to all animals, defined an optimum sampling range of the hippocampal formation for each plane of sectioning, and could easily be replicated by other researchers. For coronal sections, these landmarks were selected after empirical evaluation of several possible features revealed the two with the lowest interanimal variation in interlandmark distance (King et al., in press). Anteriorly, the first coronal section to exhibit the joining of the

buried and exposed blades of the dentate gyrus, and posteriorly, the first section to show fibers of the posterior commissure crossing the midline of the brain, these landmarks defined a region of dorsal hippocampal formation $1.56 \pm .8$ mm thick. For horizontally sectioned material, sections for measurement were selected from between, dorsally, the section first demonstrating a clear separation of CA3 pyramidal cell somata from the dentate gyrus, forming a separated anterior and posterior hippocampus, and ventally, the loss of a V-shaped dentate granule cell layer, and the occurrence of a grossly distorted molecular layer, near the temporal pole of the hippocampus. These correspond to Plates 63 and 58, respectively, in the rat brain atlas of Paxinos and Watson ('82). This yielded a sampling region about 2.2 mm in animals whose brains were sectioned horizontally.

Measurements were obtained by projecting black and white video images of histological sections from the microscope (10X1.25X2.5X) to the terminal screen of a Spatial Data Systems EyeCom II image analysis terminal, then converting the online images into arrays of digital values encoding position (X,Y) and gray level (Z). Gray levels between 0 (black) and 255 (white) were then sampled at the desired locations in the image to obtain indices of the optical density of stain bands, with the use of Fortran programs specifically designed for the patterns of staining in Timm's or AChE histologies (figures 10 and 11).

Measurement software for Timm's material.

For the Timm's material, where the molecular layer exhibits three bands, and particularly sharp borders between bands, the program required the operator to first trace along the granule cell layer/molecular layer border (figure 10). This measured the blade length, and this measurement was used to calculate where to place markers on the screen (but not in the measured image) at 10% intervals when the operator retraced the blade. Next the operator moved the cursor to a point at the distal border of the molecular layer (pia mater for the exposed, and hippocampal fissure for the buried blade) where a traverse from the first marker to the point would be as perpendicular as possible to the stain bands at that location. The computer generated this line, and used it as a guide to sample a swath, 9 pixels wide, at every pixel along the traverse (without "seeing" the traverse line itself). From the average of the 9 pixel samples at each point along the line, an optical density profile along the traverse was collected. Using a half-height algorithm to recognize the sharp Timm's band borders, i.e. the positions in the profiles where the gray level changes were greatest, the widths of each band were automatically calculated. A scaling factor was included to produce corrected terminal field widths for commissural/associational, medial entorhinal, and lateral entorhinal afferents to the dentate. Summing these resulted

in an estimate of total molecular layer width. This process was then repeated at each subsequent marker until 10 profiles were collected for the blade, then the program stored the information. Both blades on both sides of the brain were measured in the 10 sections for each animal, resulting in the generation of a measurement sample 10 sections by 10 measurement locations for each blade of each dentate.

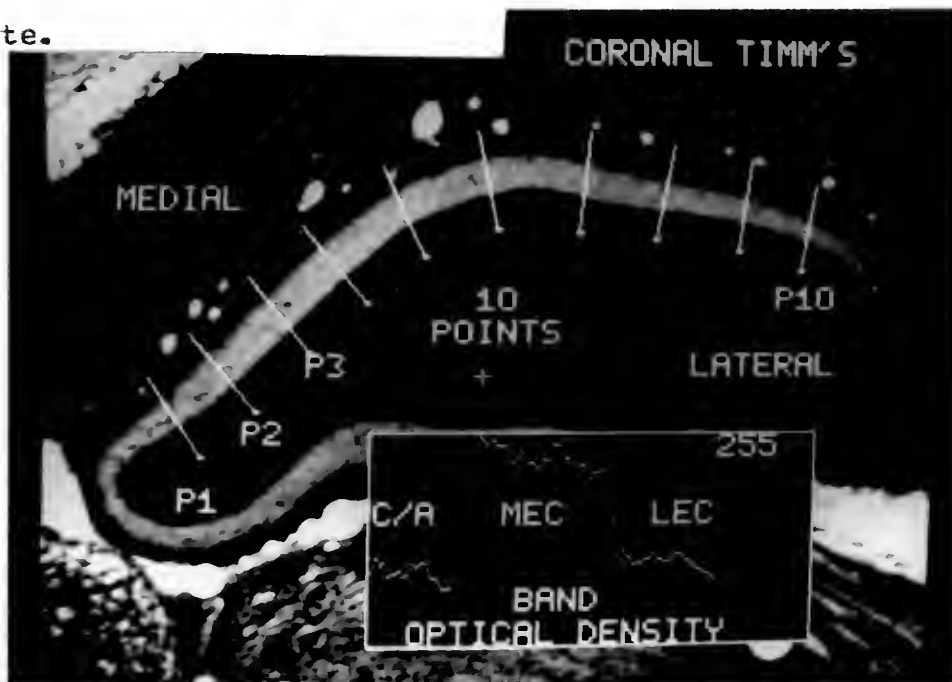


Figure 10: Computer-assisted Timm's Width and Stain Intensity Measurement

Program testing, measurement replication, and testing of this program proved it to be as reliable as making these measurements by hand, with the advantages of speed, objectivity (and thus reliability), and the ability to collect a larger sample.

Measurement software for AChE material.

In the AChE material, the more diffuse nature of the staining pattern required a less automatic approach (figure 11). Here, after measuring bladelength and placing 10% interval markers (this time along the hilus/granule cell layer border), the operator was requested to supply not only the distal extent of the molecular layer, but the borders between 1) the granule cell layer and the compact, AChE-rich supragranular band, 2) the supragranular band and the less dense commissural/associational band, 3) the C/A band and the outer 2/3 region where the AChE is normally slightly more concentrated. This program sampled the Z values of all pixels in boxes 20 pixels wide, along each traverse, for each stain band. The outer 2/3 zone was subdivided into 5 equal boxes for closer examination of the AChE condensation reaction, as well as quantitative description of the pattern in the unlesioned animal and on the side contralateral to entorhinal lesions.

All data were analysed with two-way analysis of variance (CET and ECX) (diet v. lesion) on SAS (Statistical Analysis System), with provisions for testing interactions resulting from 1) medial-lateral gradients or differences, 2) anterior/dorsal-posterior/ventral gradients or differences, and 3) individual animal differences within and between groups. Each measurement point in the 10 by 10 arrays can be compared individually, or collapsed as

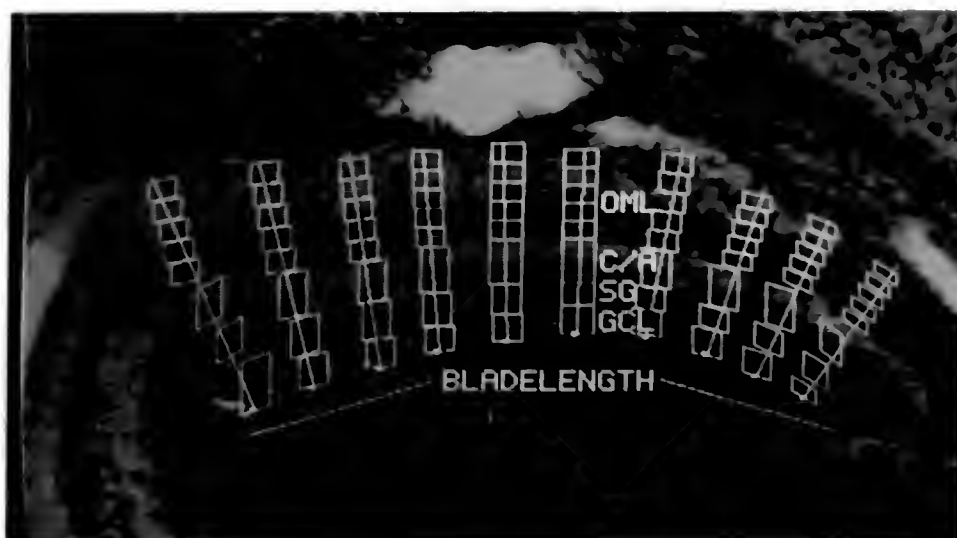


Figure 11: Computer-assisted AChE Band Width and Stain Intensity Measurement

desired. For example, because entorhinal lesion results in a shrinkage of the molecular layer where it is deafferented, we were able to accurately subset the points used for analysis according to a criterion amount of molecular layer shrinkage. This concept is illustrated in further detail in the Results section.

Stain Intensity Normalization.

Because the microscope light level was adjusted to produce optimum video image contrast prior to digitizing each section, it was necessary to normalize the Z values to a constant light intensity. The EyeCom II camera maintains a linear relationship between Z and the light incident on the lens (figure 12), for any particular optical density. Because brain tissue stains appear to pass a greater proportion of the incident light source at higher lamp

voltages, however, it was found that dark regions had different light/Z ratios than lightly stained regions (figure 12). Since the stain bands we measured covered a range of optical densities, it was necessary to correct values by first calculating the slope of the light/Z relationship for the original Z values obtained, then determining the (microscope) light-correction factor according to this specific slope. The specific slope was determined by dividing the raw Z by 57 (the Z obtained at 6.0 volts scope light intensity for an arbitrarily chosen reference section where the optical density is such that Z changes by 30 values per volt), raising the result to the .4 power (the exponential function relating the specific slope to the particular optical density--inset, figure 12), and multiplying by the slope for the reference density (30 Z/volt). Dividing this corrected slope by the difference in scope light voltage (from 6.0) yeilds a normalization quantity that was added (or subtracted) to the original Z value. The following formula was used to normalize the stain intensity raw data:

$$\text{normalized} = \text{raw} + ((\text{raw}/57) ** .4) * 30 \text{ Z levels/volt} * (6.0 - \text{voltage}).$$

normalized=voltage normalized Z value
 raw=raw Z value
 voltage=Olympus BH-2 light voltage used to digitize

Assuming that stain intensity variability averages out with the use of many animals and several sections per animal,

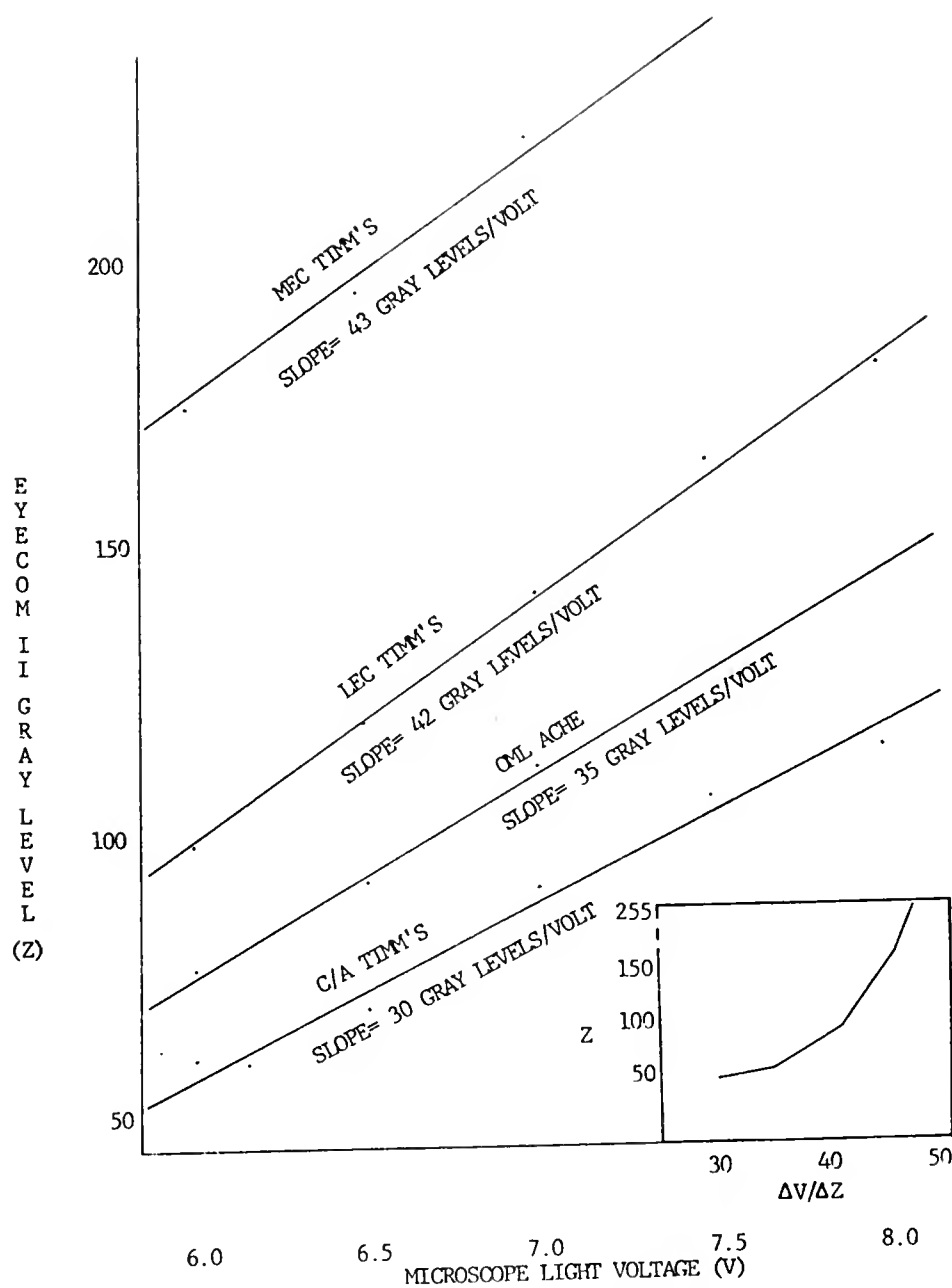


Figure 12: Linearity of EyeCom II Gray Levels

this normalization should be sufficient to allow valid comparisons of the relative stain intensities. Group mean normalized densities were then plotted, and correction factors were determined to correct the densities to any desired level. Because little apparent change in AChE occurs in the granule cell layer or supragranular layer following entorhinal lesion (Storm-Mathisen, '74) adjusting the normalized optical densities by a factor derived from background granule cell layer AChE intensity of each section provides an additional alternative correction. However, if alcohol treatment were to alter either the tissue background stainability (where there is no AChE to stain), or the amount of AChE in the GCL or SG bands, this correction method would mask a real effect. These procedures are illustrated and compared using actual data in the Results section.

Results

Alcohol Consumption

Figure 13 is a graph of the alcohol consumption of two representative animals over the course of the liquid diet administration period. Alcohol consumption patterns are observed to stabilize around 10 to 12 g ethanol/kg body weight/ day by the end of the 20 weeks.

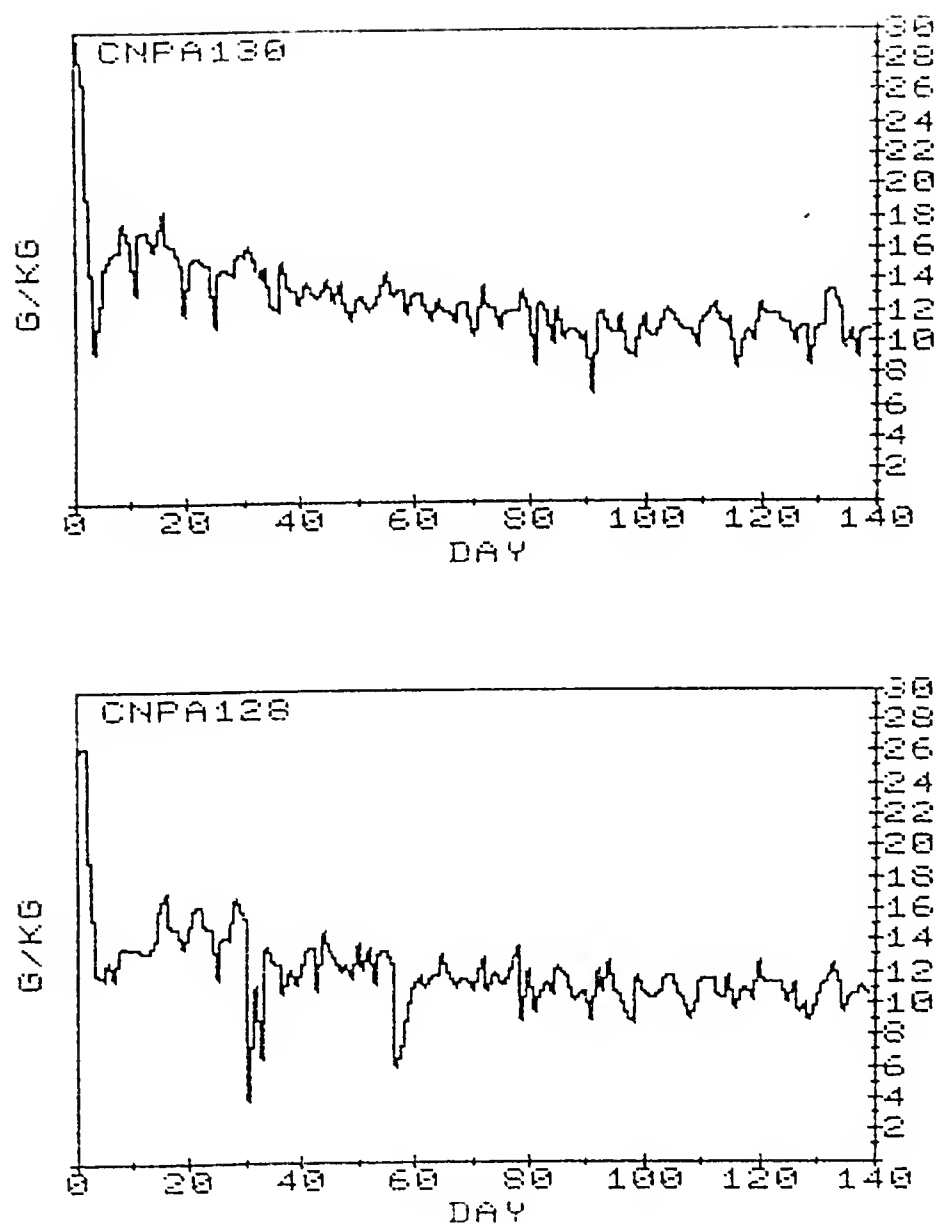


Figure 13: Alcohol Consumption Over the 20 Week Exposure Period

Alcohol Effects: Coronal Timm-stained Dentate

Results from unlesioned animals, using the Timm's stain on coronal sections, will be presented first to illustrate alcohol effects prior to entorhinal lesion. Data from lesioned animals, on the side contralateral to lesioning, in horizontally sectioned AChE material, will be then compared for alcohol effects. Immediately after this, the results from the lesioned side, still using the AChE tissue, will be described.

Timm's Band Widths in Unlesioned Animals.

In unlesioned animals, the intensity and widths of molecular layer bands in coronally sectioned Timm's stained tissue were examined to determine the effects of alcohol consumption alone (table 4). The width of the commissural band was the same in both groups, in the buried blade, but reduced by 4 microns in the exposed blade in the alcchl animals. The buried blade C/A band occupied 25.8% of the molecular layer in the alcohol group, versus 26.0% for controls. The exposed blade C/A band of the alcchl group occupied 26.1% of the molecular layer, as compared to 27.9% in the sucrose group. Thus there may be a small reduction in exposed blade C/A width following long-term ethanol treatment, although these differences were not statistically significant with the group size in our study.

The outer molecular bands corresponding to entorhinal input were only slightly different in the alcohol group. In

TIMM'S UNLESIONED CORONAL WIDTHS

BURIED BLADE				
	C/A	MEC	LEC	ML
SUCROSE	51.8 (1.3)	83.0 (4.8)	67.5 (1.5)	201.0 (6.5)
ALCOHOL	52.6 (2.6)	70.5 (3.4)	70.0 (2.1)	200.4 (4.5)
EXPOSED BLADE				
SUCROSE	55.3 (1.3)	87.2 (3.4)	53.3 (3.0)	195.7 (5.9)
ALCOHOL	51.1 (2.2)	90.8 (3.2)	52.5 (2.0)	194.3 (4.3)

TIMM'S UNLESIONED CORONAL NORMALIZED DENSITIES

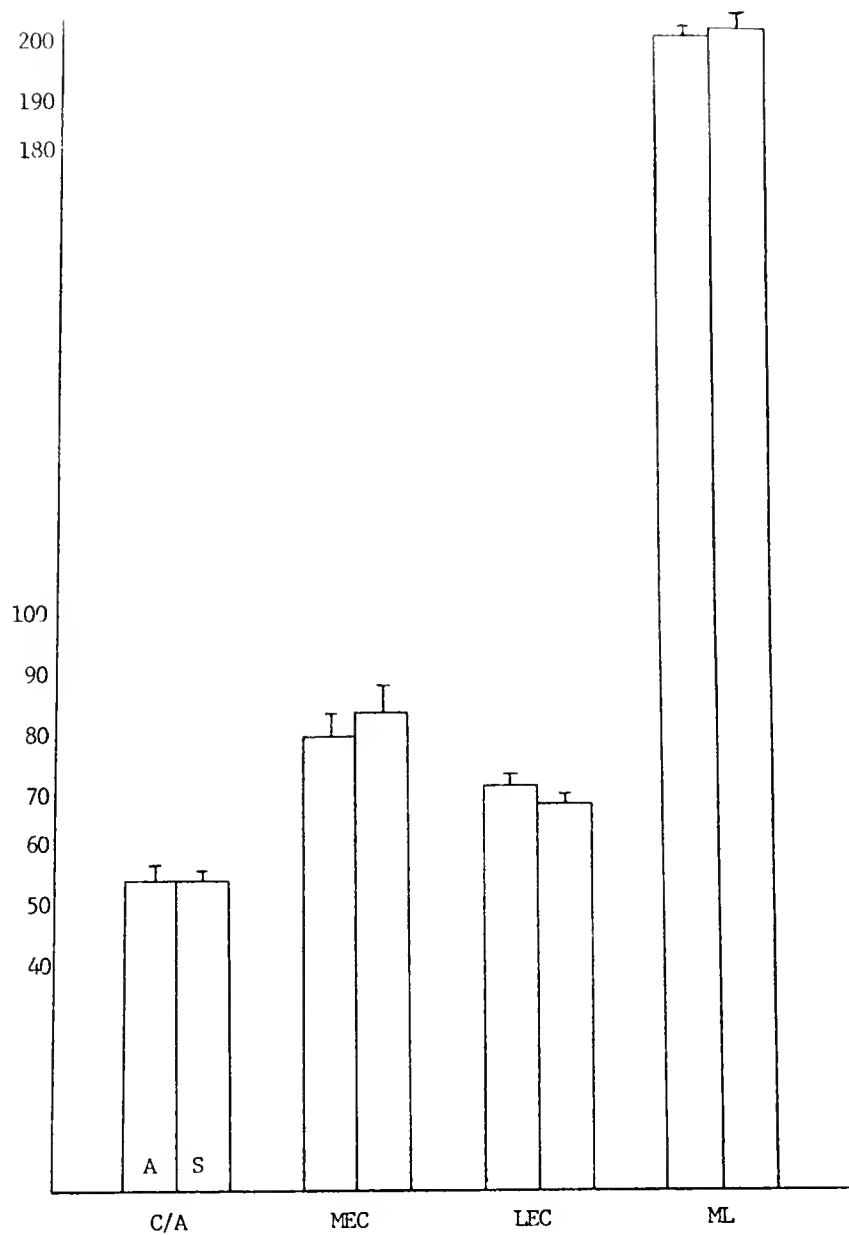
BURIED BLADE			
SUCROSE	163.0 (32.7)	242.7 (40.0)	181.4 (20.8)
ALCOHOL	216.0 (16.9)	340.7 (15.9)	241.4 (21.0)
EXPOSED BLADE			
SUCROSE	238.3 (33.8)	325.7 (32.4)	257.2 (29.7)
ALCOHOL	221.6 (14.4)	316.0 (7.1)	233.6 (7.8)

TABLE 4

Timm's Stain Band Widths and Intensity Measures

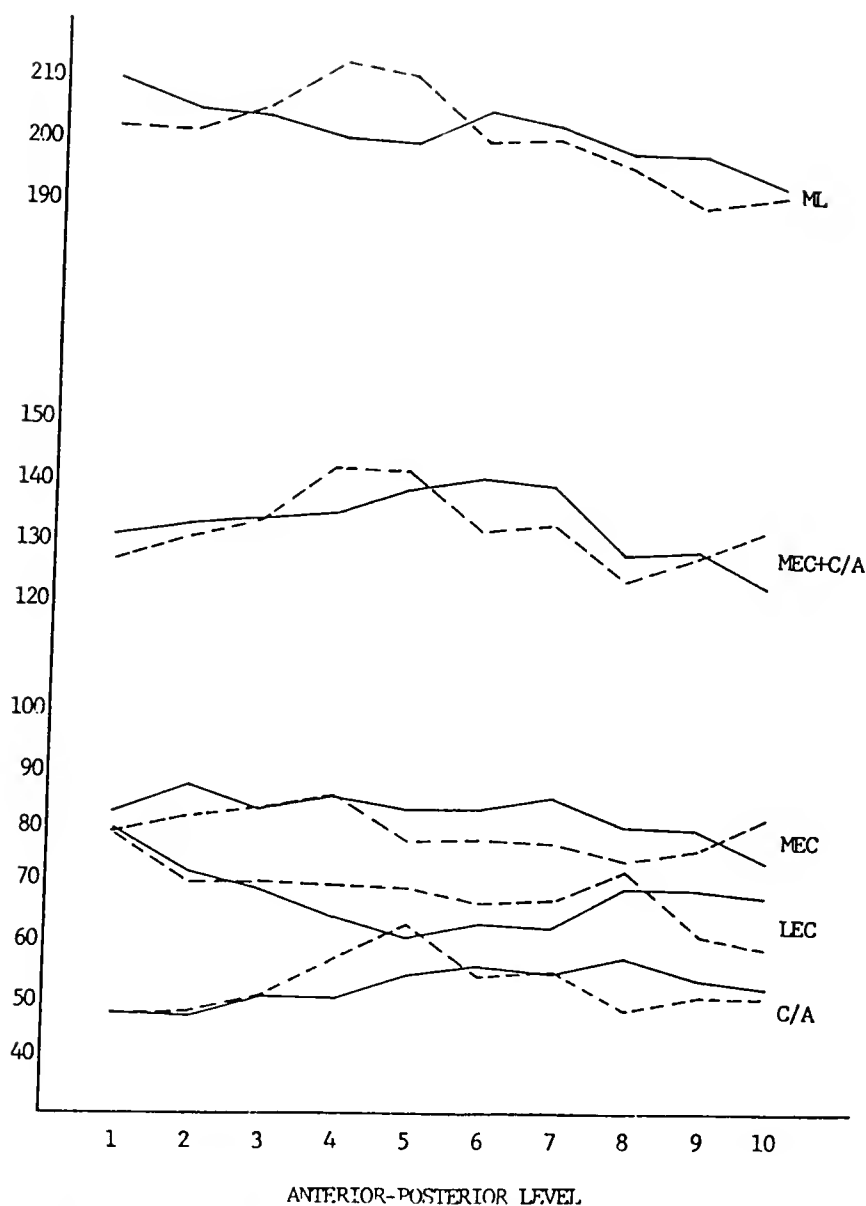
the buried blade, the middle molecular layer (MEC) was slightly smaller (4 μ m), and the outer molecular layer (LEC) slightly larger (3 μ m), in the alcohol group. This pattern was reversed in the exposed blade. Only 1-2 microns difference between total ML width was observed between groups in either blade. The average total length of the granule cell layer of the 10 sections measured was 80 microns (4%) higher in the sucrose group; most of this difference was accounted for by the buried blade length.

When group differences are examined over the 10 A-P levels measured, there seems to be little pattern in the distribution of width differences in either the buried (figure 15) or the exposed blade (figure 17). Collapsed over all A-P levels and examined by crest-tip location, group differences tend to be fairly evenly distributed all



Abscissa, width in micrometers. Upper scale is for ML bars. Mean \pm S.E.M. for all 100 measurement points.

Figure 14: Buried Blade Coronal Unlesioned Timm's Band Widths



Abscissa, mean Timm's band widths at each of the 10 anterior-posterior measurement levels. Solid lines, sucrose group; dashed lines, alcohol group.

Figure 15: Buried Blade Coronal Unlesioned Timm's Widths by A-P Level

along each extent of each blade (figure 18). Density appears to be more variable in this regard (figure 22). However, since systematic crest-tip patterns in the differences were not observed in either width or density for either stain type (Timm's, AChE), no other response variations will be described along this axis of the hippocampal formation.

Timm's Stain Intensity in Unlesioned Animals.

To emphasize the need to normalize the stain intensity data to a constant microscope light level, both the raw and normalized Timm's intensity values will be presented in this section. The results indicate that it is not appropriate to assume that microscope illumination differences average out, even with the use of a large number of tissue sections. These measurements were obtained from 5 sucrose and 5 alcohol animals.

The raw optical density of the two darkly staining Timm's bands (C/A and LEC) appeared to have been increased (i.e., darker) in the alcohol group, in both blades (figures 19, 21). The light middle band was less dense (lighter) in the alcohol group in both blades. Microscope light-level normalization reversed the raw mean intensity differences in the dark bands in the buried blade (figure 20); the alcohol group was found to stain less in all three bands. Normalization did not alter the darker band differences considerably, in the exposed blade, but reversed the MEC raw

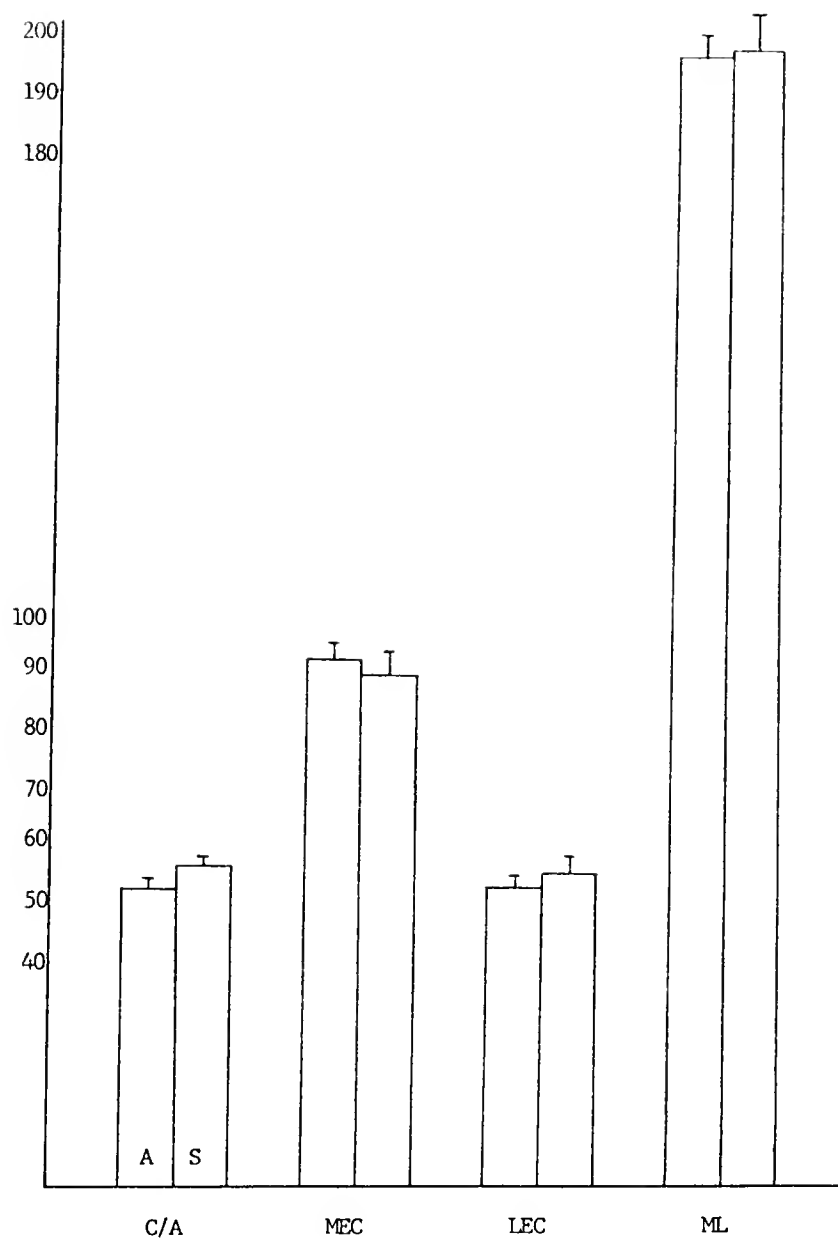
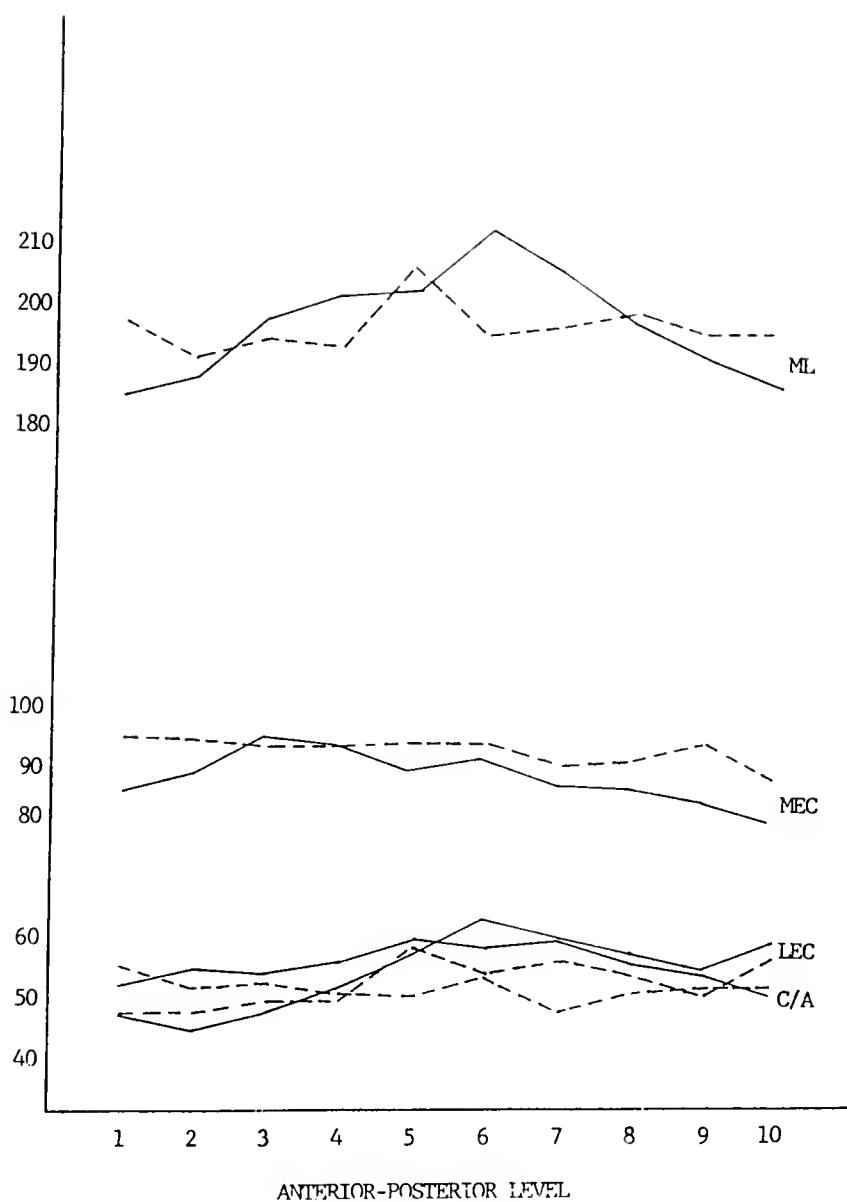
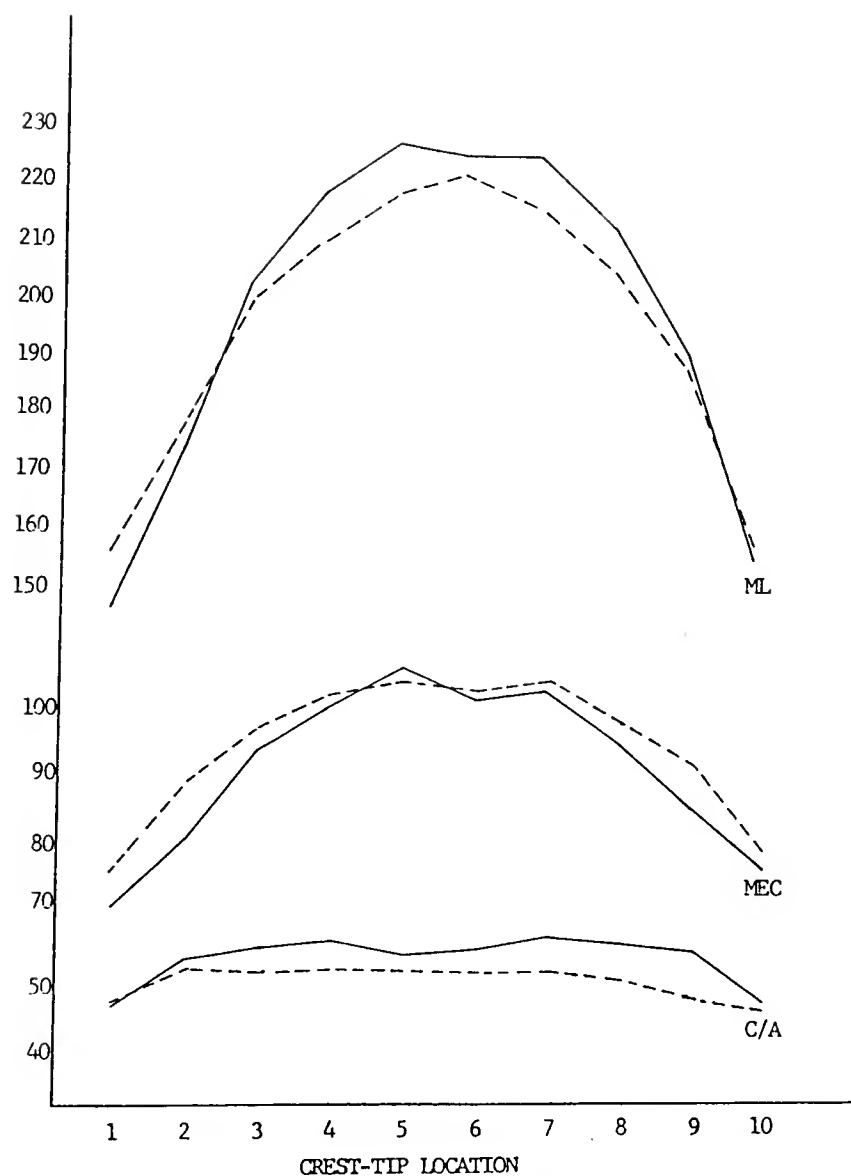


Figure 16: Exposed Blade Coronal Unlesioned Timm's Band Widths



Abscissa, mean Timm's band widths in microns at each of the 10 anterior-posterior measurement levels. Solid lines, sucrose group; dashed lines, alcohol group.

Figure 17: Exposed Blade Coronal Unlesioned Timm's Band Widths by A-P Level



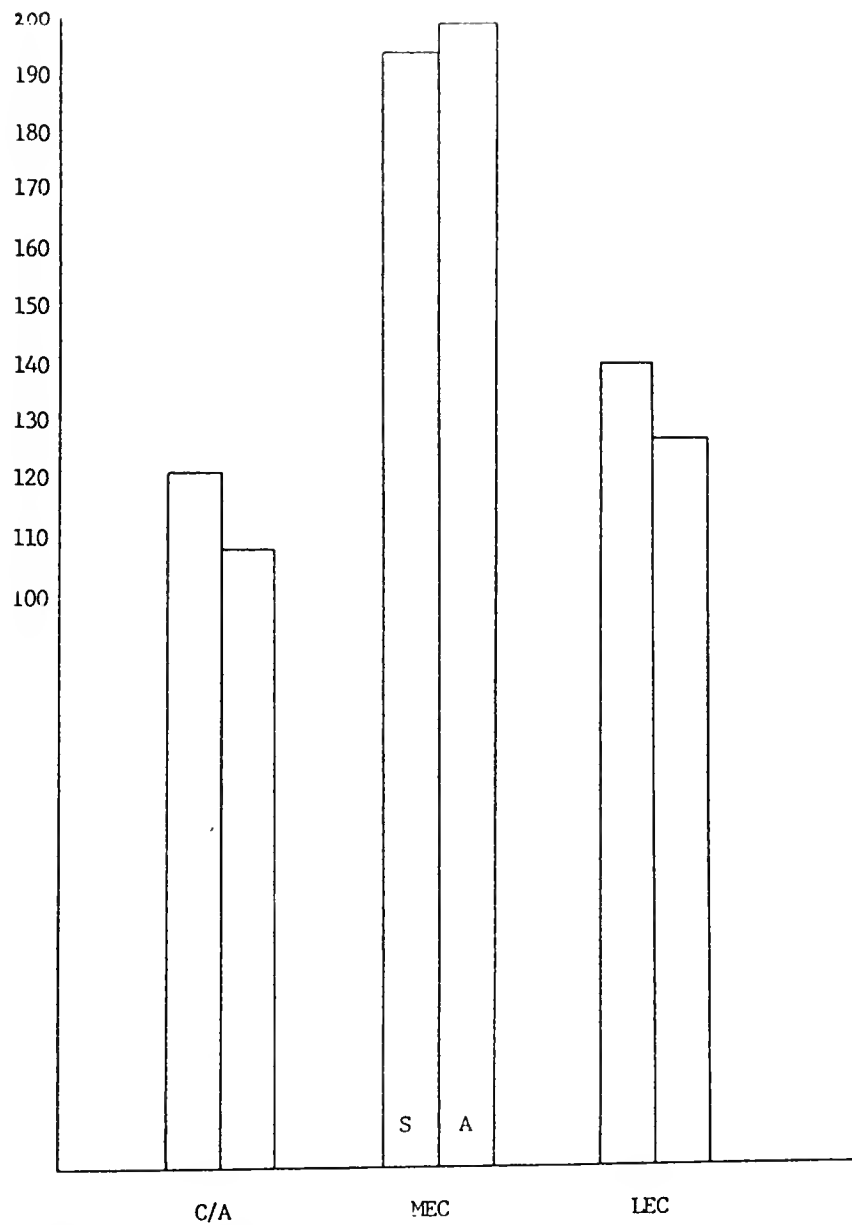
Abscissa, mean Timm's band widths in microns at each of the 10 medial-lateral (crest-tip) levels. Solid lines, sucrose group; dashed lines, alcohol group.

Figure 18: Exposed Blade Coronal Unlesioned Timm's Band Widths by M-L Level

data difference (figure 23). Thus in the buried blade, all three bands were lighter in alcohol animals, while in the exposed blade, all three bands were darker. Normalized stain intensity in the buried blade C/A band was 8% lower (lighter), the medial entorhinal band was 29% lower, and the lateral entorhinal band was 33% less in alcohol animals than controls. In the exposed blade, the normalized C/A intensity was 7% higher (darker) (figure 23), the MEC band was 3% higher, and the LEC band was 13% higher in the alcohol group. Figure 22 gives an indication of the low degree of medial-lateral, or crest-tip variation in stain intensity values and differences, while figure 24 demonstrates how variable the Timm's density may be in the septal-temporal plane.

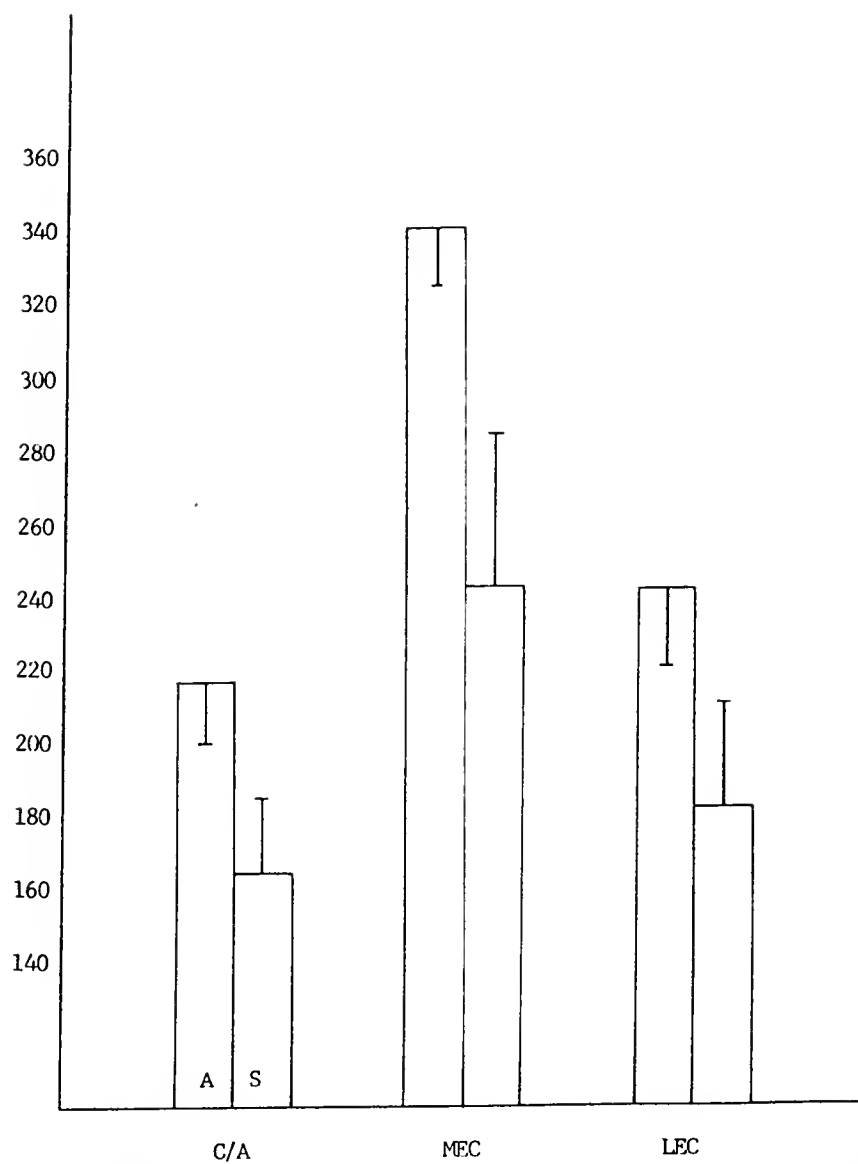
Alcohol Effects: The Contralateral Dentate

In order to better control for individual differences in lesion placement, or size, we subset our 100 point measurement arrays to analyze lesion responses only where there was evidence of molecular layer deafferentation. To do this, only points where ipsilateral molecular layer shrinkage was greater than 15 microns were included in these analyses. Because it has been shown that in adult male Long-Evans rats, the right hippocampus is 2-3% larger on average than the left (Diamond et al., 82), and our lesions were made on the left side, this criterion provides some



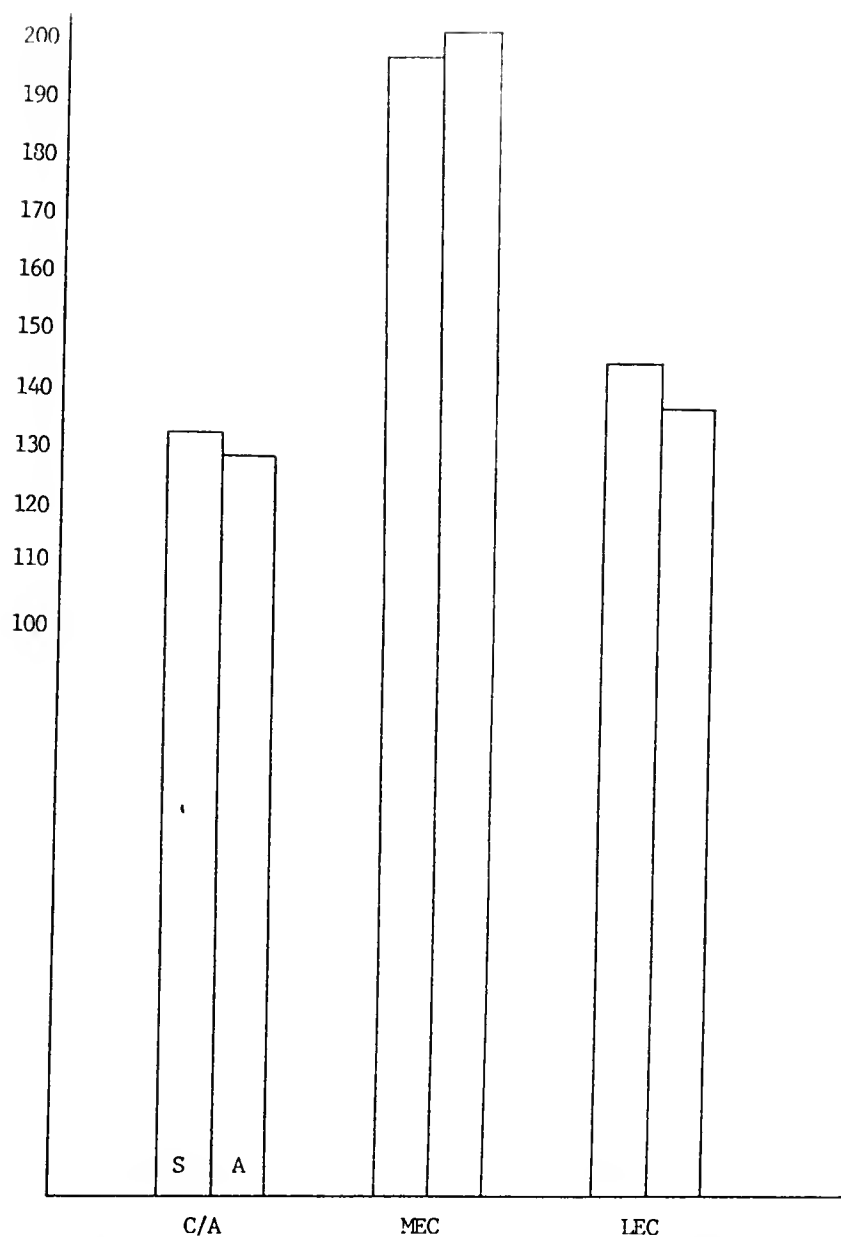
Abscissa, mean Timm's raw stain intensity values,
for all 100 points.

Figure 19: Coronal Buried Blade Unlesioned Timm's Band Raw
Stain Intensity



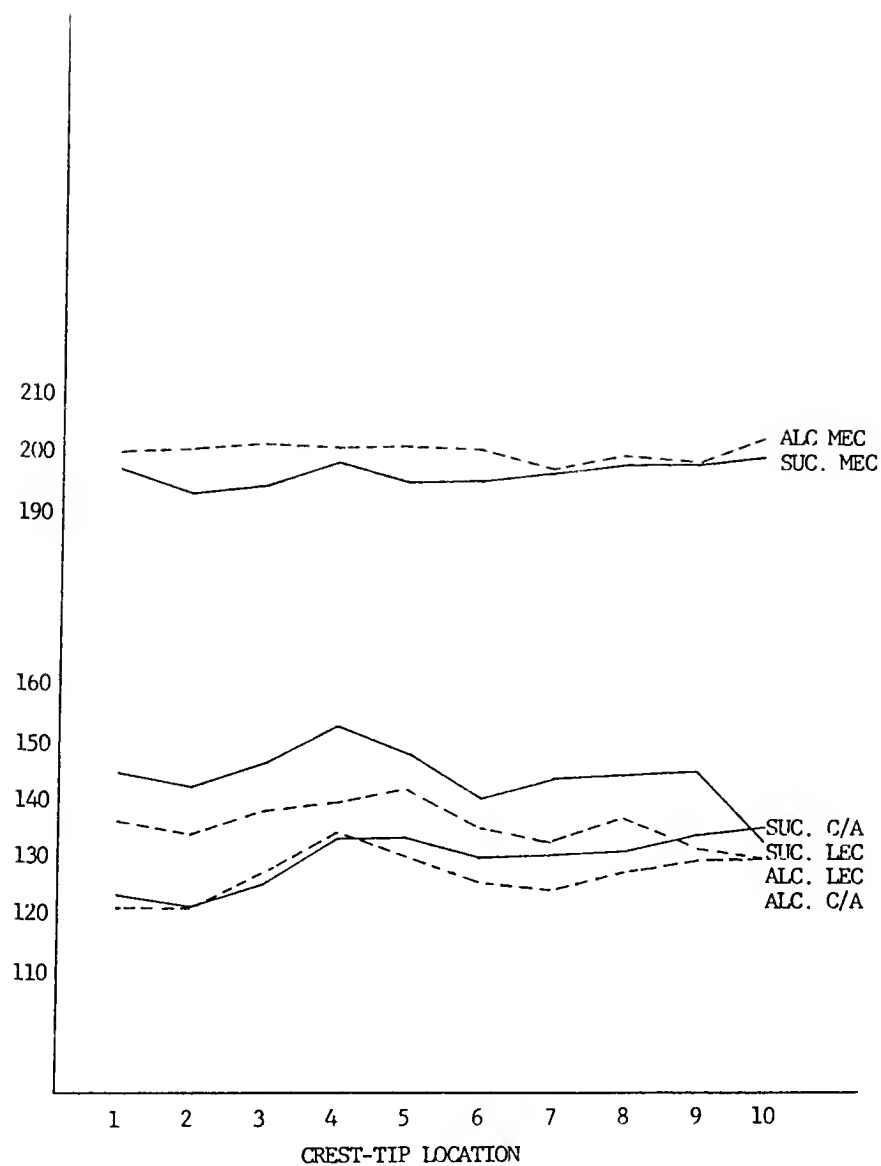
Abscissa, Timm's normalized stain intensity measurements, mean \pm S.E.M. for all 100 points.

Figure 20: Coronal Buried Blade Unlesioned Timm's Band Normalized Stain Intensity



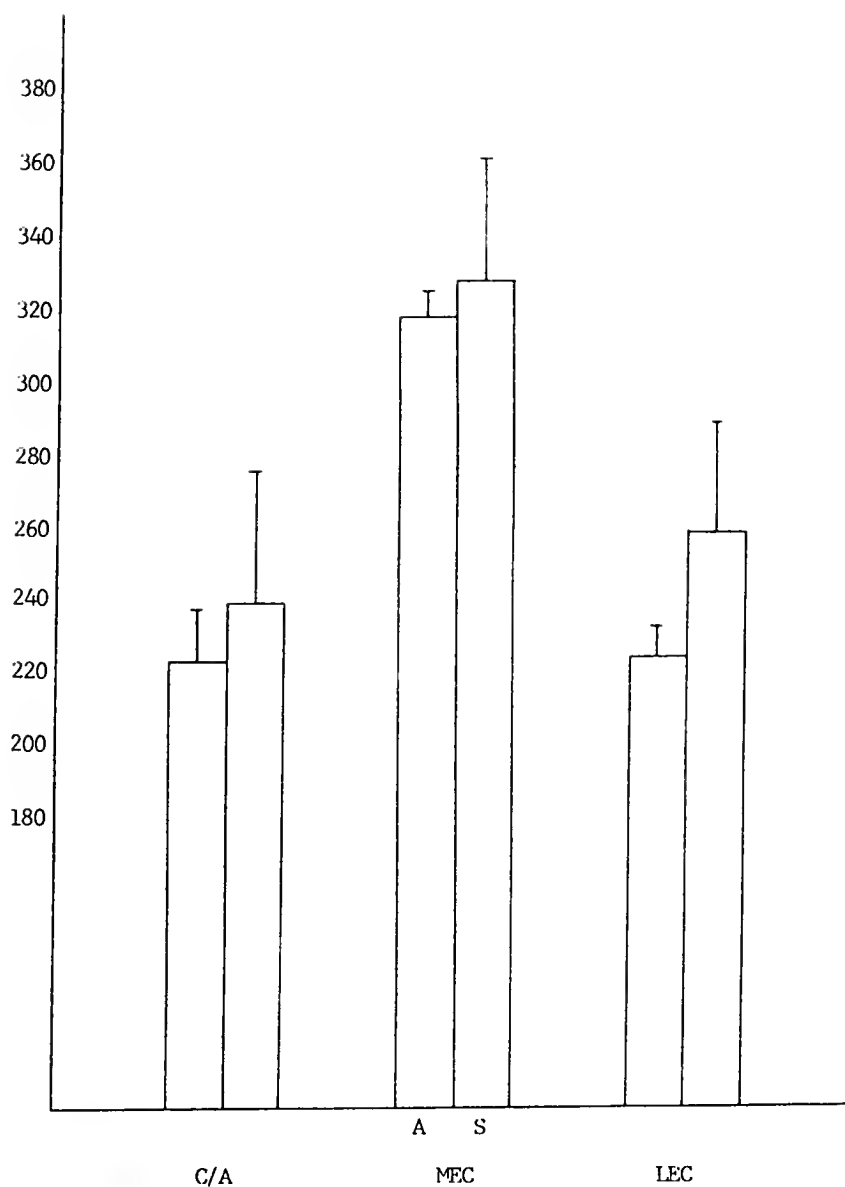
Abscissa, Timm's raw stain intensity measurements, mean \pm S.E.M. for all 100 points.

Figure 21: Coronal Exposed Blade Unlesioned Timm's Band Raw Stain Intensity



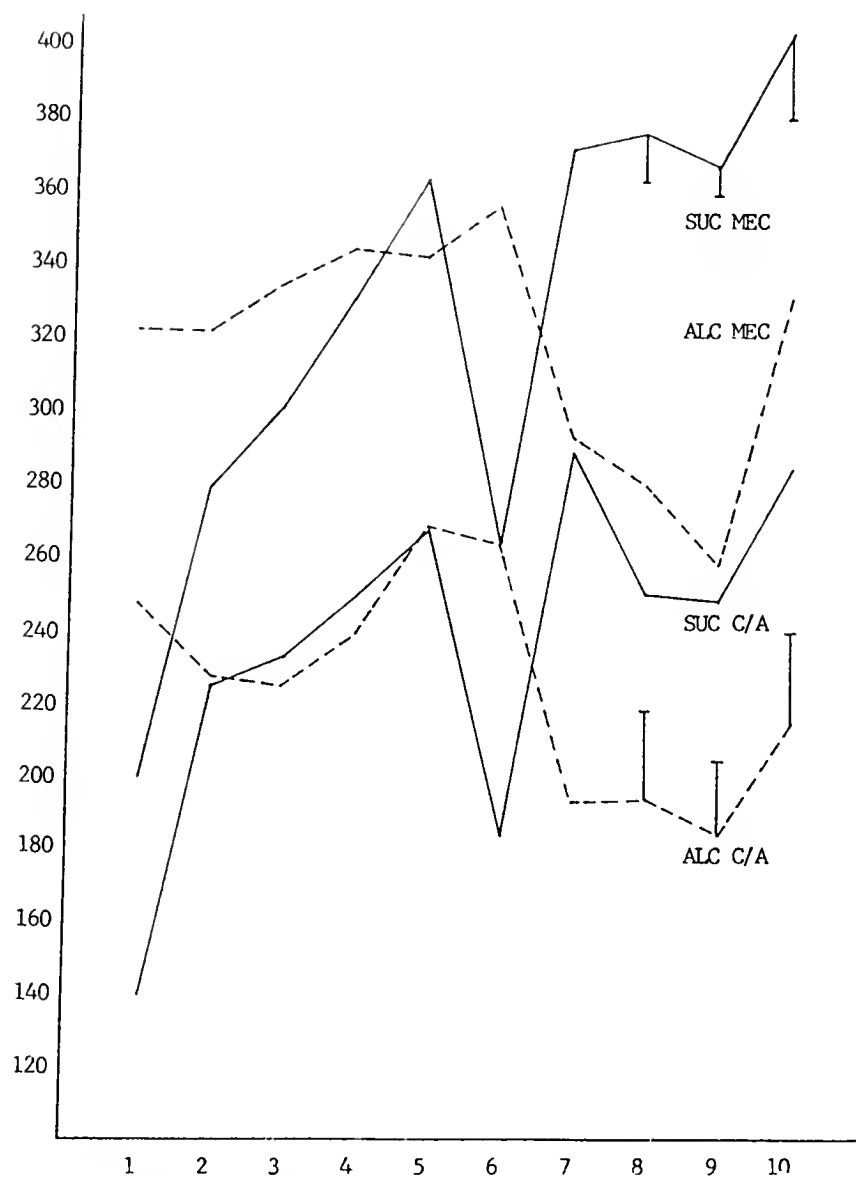
Abscissa, Timm's mean raw stain intensity values, by crest-tip measurement location, exposed blade.

Figure 22: Timm's Intensity Means Along the Medial-lateral Axis



Abscissa, Timm's normalized stain intensity values, mean \pm S.E.M. for all 100 points. Solid lines, sucrose group; dashed lines, alcohol group.

Figure 23: Coronal Exposed Blade Unlesioned Timm's Band Stain Intensity



Abcissa, Timm's normalized stain intensity values, mean \pm S.E.M. by anterior-posterior measurement location. Solid lines, sucrose group; dashed lines, alcohol group.

Figure 24: Timm's Unlesioned Exposed Blade Normalized Stain Intensity by A-P Level

control for natural differences in molecular layer width as well as selecting out locations where an effective deafferentation has occurred. Since the shrinkage averaged more than three times this criterion (Table 5), few measurement points where a deafferentation occurred were eliminated by this subsetting. The results were similar to analyses using all measurement locations, but exhibited less statistical variability. For the comparisons of the contralateral sides, to evaluate alcohol effects presumably uncontaminated with lesion effects, only those contralateral measurement locations that met the MI shrinkage criterion ipsilateral to lesioning were used. That is, only those measurement locations that were used for ipsilateral analyses were used for the contralateral (alcohol effect) analyses. This facilitates direct comparison with the lesion results presented below, and insures that comparisons of lesion effects and interactions are not biased by differences in the locations of the measurements. Virtually identical effects were found when the contralateral comparisons were made using all measurement points.

After lesion and stain quality verification, 10 alcohol and 10 sucrose animals were found suitable for measurement of AChE variables. Since only 7 sucrose and 4 alcohol animals were acceptable for Timm's measurements, measurements from the Timm's material in lesioned animals will not be presented. For easier reference, Table 5

summarizes all the AChE band width data, for both the lesioned and unlesioned sides of both blades, over the entire measurement sample. Table 6 summarizes all the normalized AChE stain intensity data for both blades.

Contralateral Exposed Blade Widths in AChE Material.

On the side contralateral to the lesion, in the exposed blade, the alcohol group exhibited smaller outer molecular layers than the sucrose group (figure 25). No difference in exposed blade C/A width between groups was found. The total molecular layer width, however, was slightly reduced in the alcohol group (3.4%), and since the C/A zone was not different the outer two thirds of the molecular layer must have undergone some shrinkage in the alcohol group (4.3%). This may indicate that some residual deafferentation has resulted from the long-term consumption of alcohol, or that the synaptic reorganization seen contralateral to the lesion in normal animals is altered in alcohol animals. (Alcohol treatment may thus have reduced the outer molecular layer by just about the same amount as the crossed entorhinal projection contributes. This is consistent with the apparent AChE condensation in the outermost fifth of the exposed blade molecular layer contralateral to entorhinal lesion, as described below.) The C/A band occupied 19% of the sucrose group ML and 20% of the alcohol group ML.

Figure 26 shows the dorsal-ventral distribution of differences in the width of exposed blade AChE bands. The

TABLE 5
AChE Stain Band Widths

BURIED BLADE				
	GCL	SG	C/A	OML
UNLESIONED	51.4	42.1	48.5	147.3
SUCROSE CONTRA	40.0 (3.1)	43.9 (1.9)	51.1 (1.0)	167.3 (4.3)
SUCROSE IPSI	37.7 (1.7)	42.9 (2.0)	53.2 (1.0)	118.0 (1.9)
ALCOHOL CONTRA	37.0 (1.2)	44.7 (1.3)	46.6 (1.1)	150.6 (4.6)
ALCOHOL IPSI	36.1 (0.8)	42.8 (1.0)	47.8 (0.9)	106.8 (2.2)
	ML	DG	D-V DISTANCE	
UNLESIONED	195.8	289.3		
SUCROSE CONTRA	218.4	302.2 (9.7)	2515.0 (24.7)	
SUCROSE IPSI	171.2	251.6 (6.0)		
ALCOHOL CONTRA	205.2	286.6 (7.2)	2460.4 (25.0)	
ALCOHOL IPSI	154.6	233.2 (4.3)		
EXPOSED BLADE				
	GCL	SG	C/A	OML
UNLESIONED	46.9	39.3	41.7	167.0
SUCROSE CONTRA	38.3 (1.5)	38.2 (1.5)	45.9 (1.7)	191.4 (5.6)
SUCROSE IPSI	39.3 (1.1)	39.1 (1.6)	51.9 (1.5)	123.2 (4.0)
ALCOHOL CONTRA	40.5 (1.9)	42.1 (1.3)	46.1 (1.7)	103.1 (2.5)
ALCOHOL IPSI	40.0 (1.6)	39.9 (1.5)	50.1 (1.8)	116.1 (3.0)
	ML	DG	D-V DISTANCE	
UNLESIONED	210.7	255.2		
SUCROSE CONTRA	237.3	313.1 (7.7)	2447.0 (29.7)	
SUCROSE IPSI	175.1	253.4 (7.0)		
ALCOHOL CONTRA	229.2	311.6 (5.2)	2476.0 (15.0)	
ALCOHOL IPSI	166.2	245.9 (5.3)		

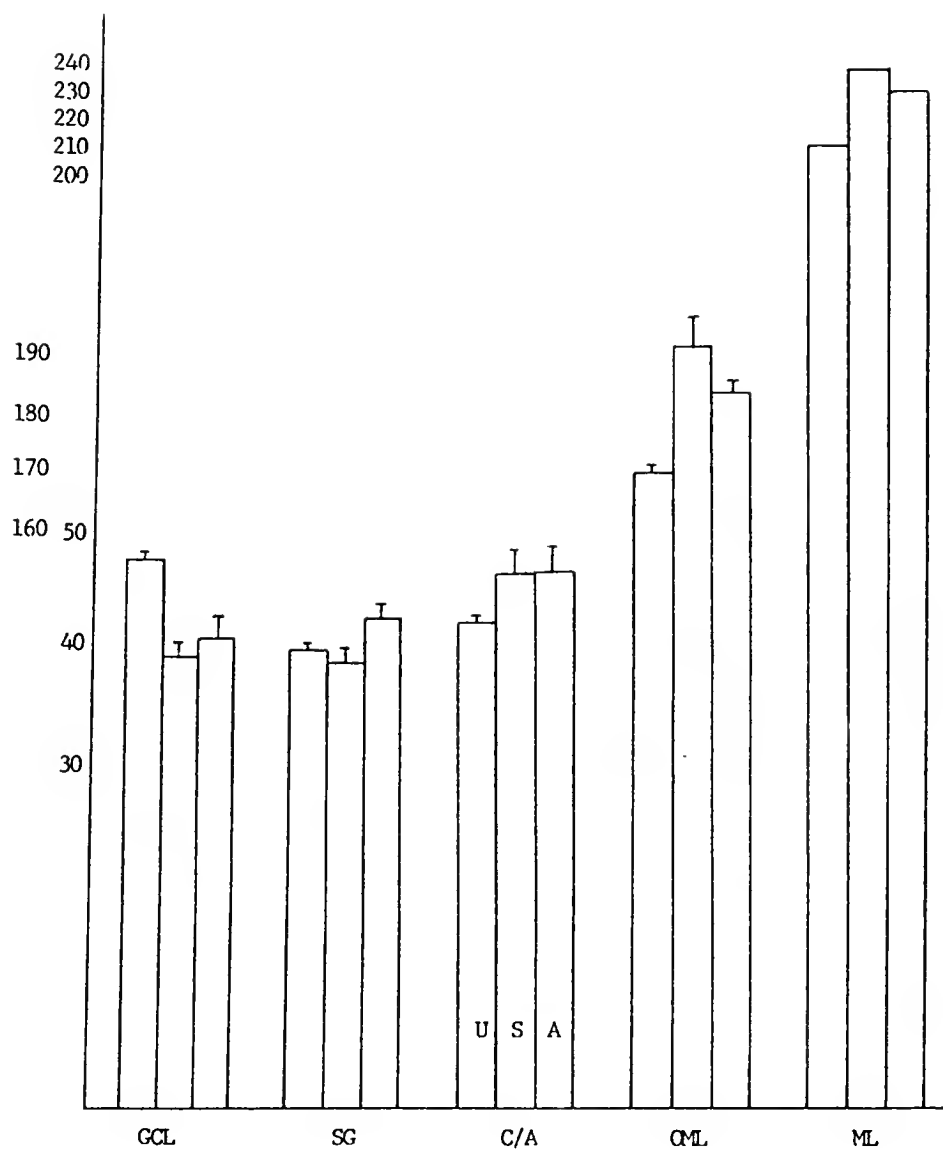
Mean +/- S.E.M. AChE stain band widths, N=10
alcohol and sucrose animals in each group;
5 unlesioned control animals were measured.

TABLE 6

AChE Normalized Stain Intensity

BURIED BLADE					
	GCL	SG	C/A	OML1	OML2
UNLESIONED	115	88	132	124	117
SUCROSE CONTRA	113 (2)	79 (3)	140 (3)	129 (5)	121 (5)
SUCROSE IPSI	114 (4)	87 (4)	151 (4)	76 (5)	88 (9)
ALCOHOL CONTRA	109 (3)	74 (3)	125 (2)	111 (2)	102 (3)
ALCOHOL IPSI	123 (2)	90 (3)	149 (2)	94 (2)	79 (4)
	OML3	OML4	OML5	OML	DG
UNLESIONED	129	145	140	131	124
SUCROSE CONTRA	124 (6)	145 (6)	144 (7)	133 (6)	125 (4)
SUCROSE IPSI	120 (12)	138 (12)	136 (10)	116 (9)	116 (7)
ALCOHOL CONTRA	108 (4)	130 (5)	129 (5)	116 (4)	111 (3)
ALCOHOL IPSI	108 (6)	124 (7)	125 (6)	106 (5)	111 (3)
EXPOSED BLADE					
	GCL	SG	C/A	OML1	OML2
UNLESIONED	117	92	142	128	135
SUCROSE CONTRA	126 (4)	99 (5)	151 (3)	134 (4)	141 (5)
SUCROSE IPSI	124 (2)	99 (5)	150 (3)	109 (4)	103 (7)
ALCOHOL CONTRA	120 (3)	89 (4)	140 (4)	121 (5)	131 (5)
ALCOHOL IPSI	126 (3)	97 (4)	149 (3)	97 (3)	87 (7)
	OML3	OML4	OML5	OML	DG
UNLESIONED	130	156	162	142	134
SUCROSE CONTRA	135 (5)	143 (5)	140 (5)	139 (5)	134 (4)
SUCROSE IPSI	111 (10)	128 (9)	126 (7)	115 (7)	119 (5)
ALCOHOL CONTRA	124 (6)	140 (7)	141 (6)	131 (5)	126 (5)
ALCOHOL IPSI	106 (9)	127 (8)	125 (6)	108 (6)	114 (5)

Mean \pm S.E.M. normalized AChE intensity, N=10
 alcohol and sucrose animals in each group; 5
 unlesioned control animals were measured.



Abscissa, lower right scale, GCL, SG, and C/A widths in micrometers, mean \pm S.E.M. for all measurement points; upper right scale, ML widths; left scale, OML widths. U=unlesioned, S=sucrose, A=alcohol groups.

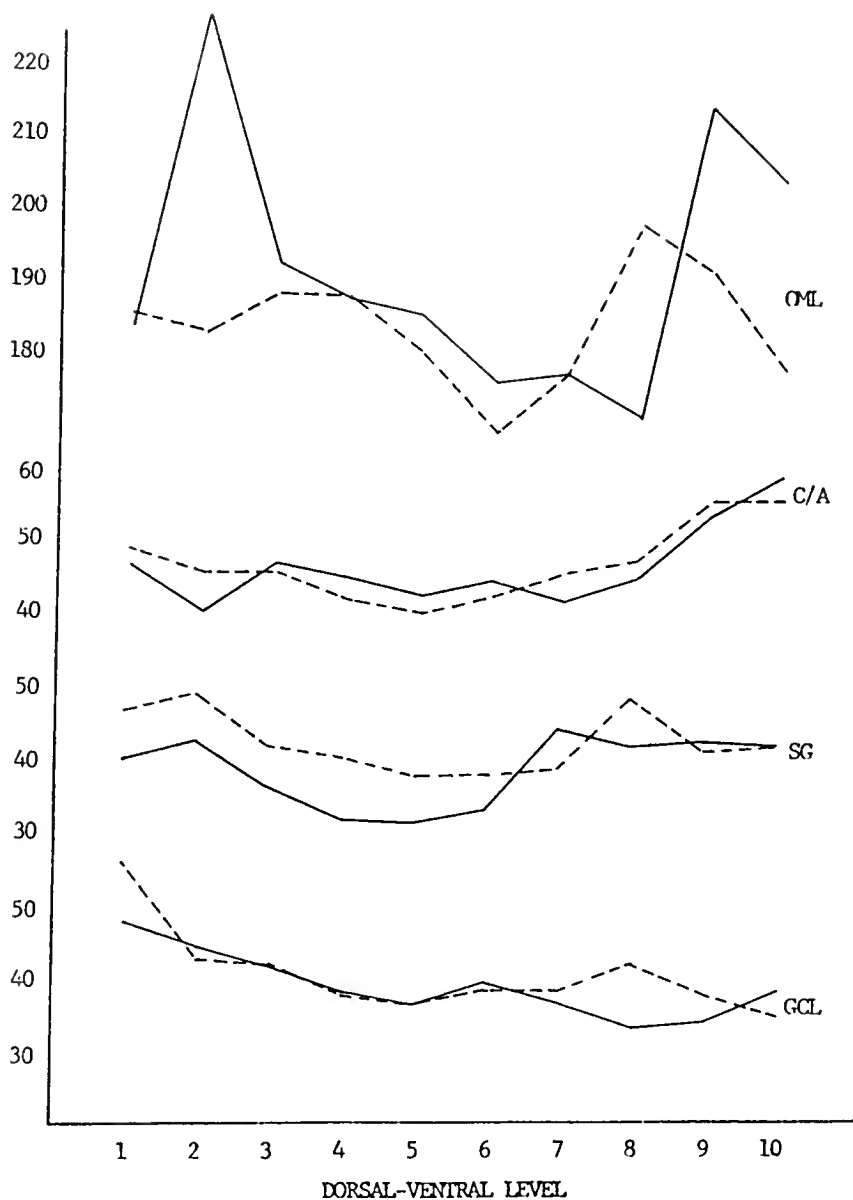
Figure 25: Contralateral Exposed Blade Group Mean AChE Widths

largest group differences in OML width tend to be observed in the most dorsal and most ventral locations. The width of the granule cell layer, supragranular, and C/A bands did not differ significantly at any D-V level.

Contralateral Exposed Blade AChE Stain Intensity.

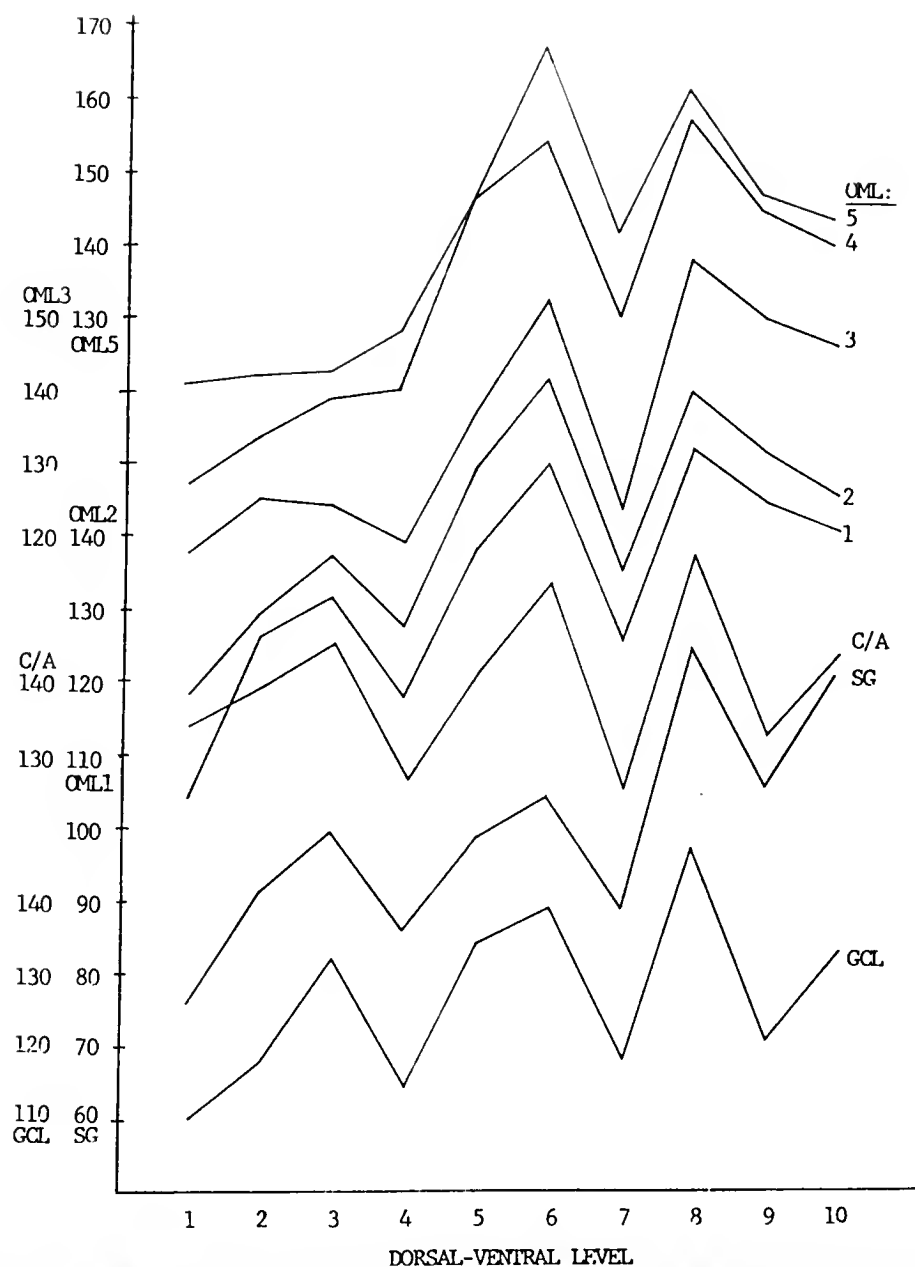
Figure 27 illustrates how the normalized AChE stain intensity values vary for each measured band over the 10 D-V levels, in the sucrose group. While there is generally good correspondance in the D-V patterns across bands, there is also some independence. Since the pattern of AChE staining may be quantitatively associated with the pattern of cholinergic termination in the dentate, these data indicate that considerable D-V variation occurs in the innervation density.

The normalized stain intensity data for the exposed blade contralateral to the lesion indicate that, in the granule cell layer, the alcohol group stains more darkly for AChE at most D-V levels (figure 28). Similarly, the supragranular and C/A bands are also more stain-dense in the alcohol group, but do not exactly follow the same D-V pattern as the GCL. In the outer molecular layer, the patterns deserve more scrutiny. Two general points can be made. First, in both groups, the intensity tends to decrease (lighter staining) at ventral locations compared with dorsal locations, in all fifths of the OML (figures 29, 30). This is interesting because the septal input, partly cholinergic,



Abscissa, mean AChE band width in micrometers; solid lines, sucrose group, dashed lines, alcohol group.

Figure 26: Contralateral Exposed Blade Group Mean AChE Band Widths by D-V Level



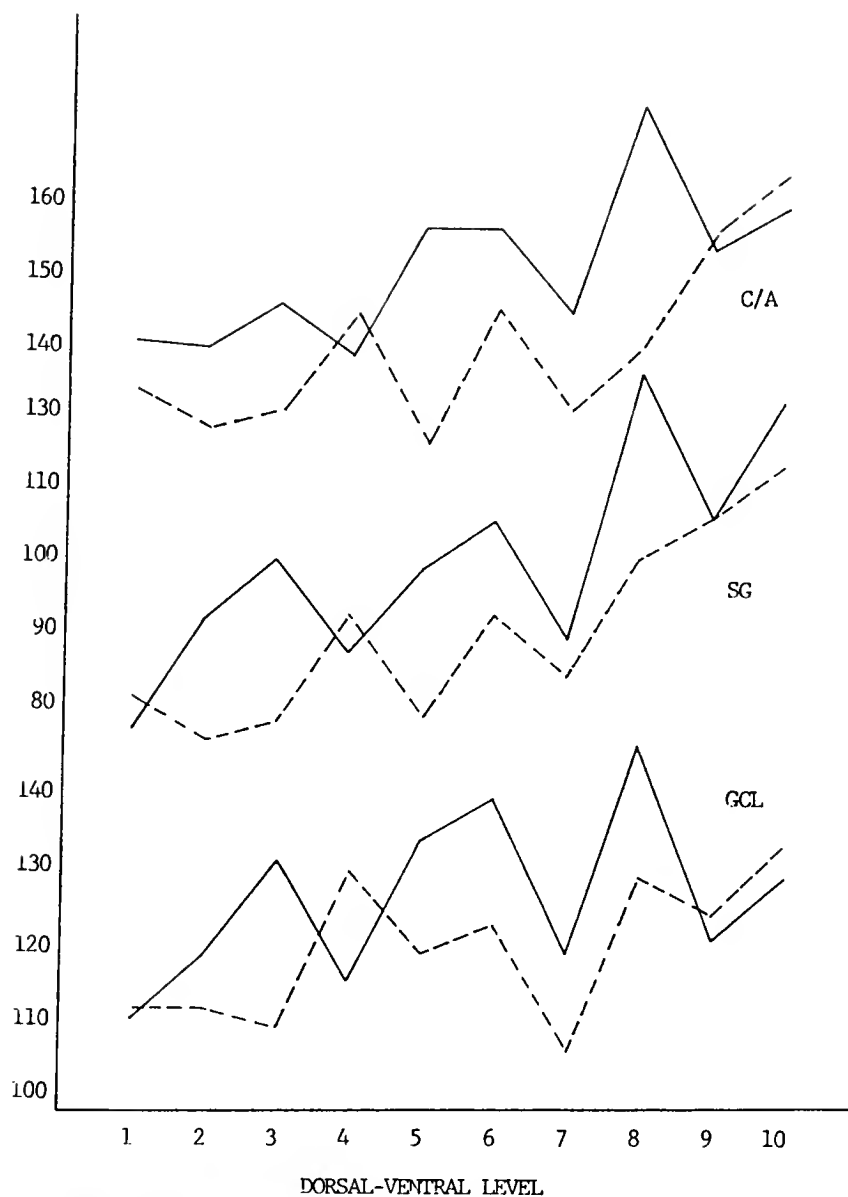
Abscissa, mean sucrose group normalized AChE stain intensity.

Figure 27: Contralateral Exposed Blade Sucrose Group Mean Normalized AChE Stain Intensities by D-V Level

has been reported to innervate the ventral dentate more densely than the dorsal (vide supra). It might thus be expected that more dense AChE staining would be present ventrally. The second point is a bit more complex. A proximo-distal gradient is observed in the magnitude of the group differences. In the three more distal fifths of the OML, the alcohol values are decreased less than in the proximal two fifths, at most D-V levels. In the most distal 20%, the alcohol and sucrose densities are nearly the same. In fact, if the intensities are corrected to the GCL intensity of the sucrose group (assumption: no alcohol effect in the GCL), then the alcohol group intensities in the outer 20% of the OML would be lower (lighter staining) than the sucrose group (not shown, see discussion). Even without such a correction, the alcohol group is lighter at 4 of the 10 D-V levels. As described below, the OML intensity differences of the alcohol group are in the same direction and of a similar degree as the lesion-induced changes in the sucrose group. This suggests that alcohol treatment

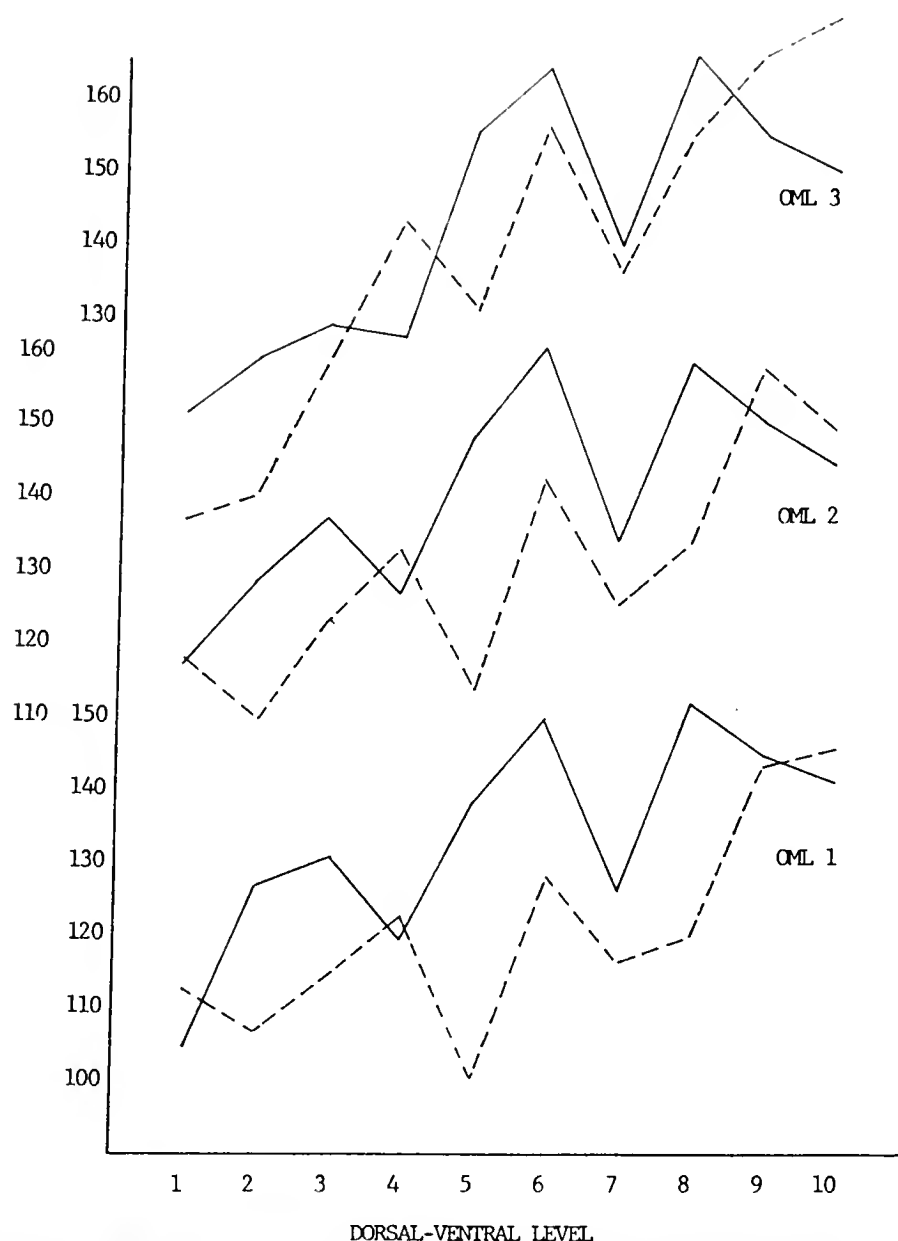
Contralateral Buried Blade Widths in AChE Material.

The contralateral buried blade did not demonstrate as dramatic a difference in total molecular layer band width, but the values for alcohol animals were generally lower than controls (figure 31, table 5). Total ML width was 6.0% lower, and outer molecular layer width 5.2% lower, in the alcohol group than the sucrose. In contrast to the exposed



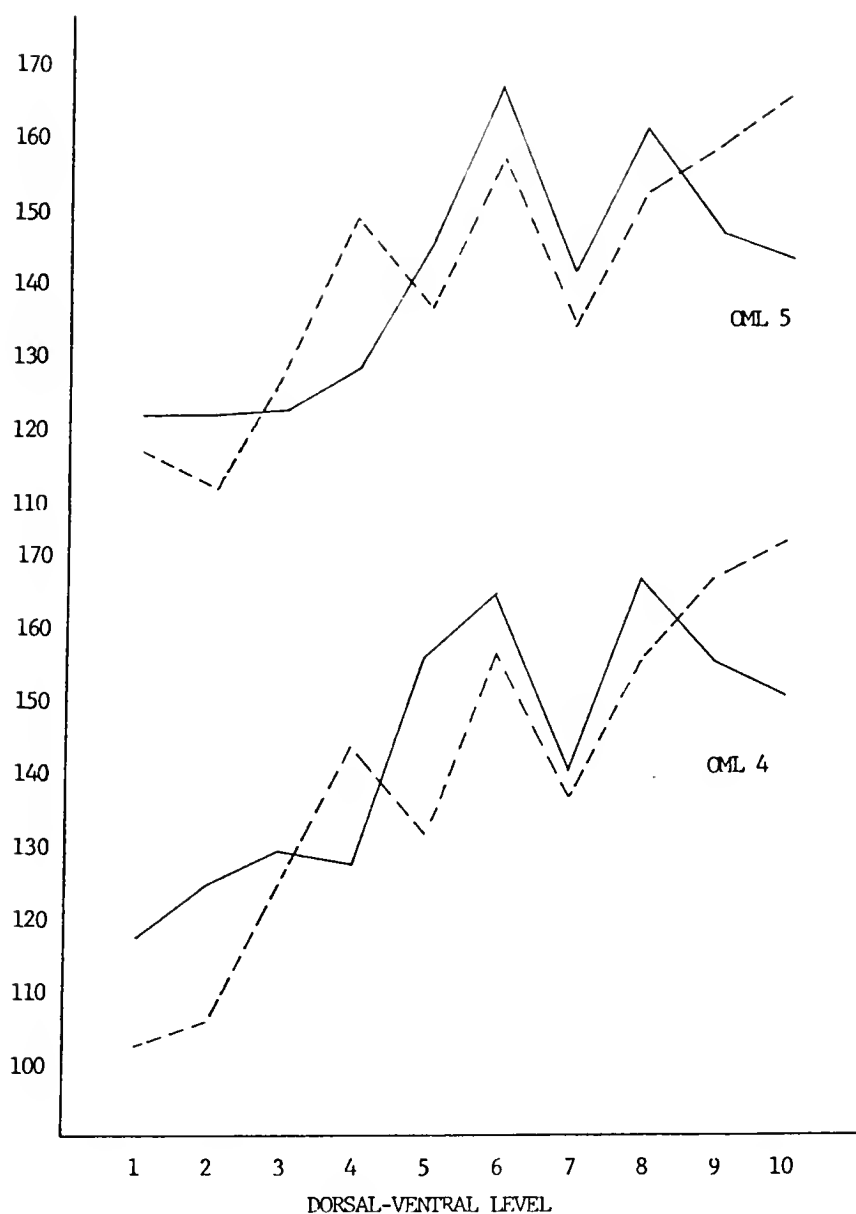
Abscissa, mean normalized AChE intensity; solid lines, sucrose group, dashed lines, alcohol group.

Figure 28: Contralateral Exposed Blade Normalized C/A AChE Intensity by D-V Level



Abscissa, mean normalized AChE intensity; solid lines, sucrose group, dashed lines, alcohol group.

Figure 29: Contralateral Exposed Blade Normalized OML AChE Intensity by D-V Level



Abscissa, mean normalized AChE intensity; solid lines, sucrose group, dashed lines, alcohol group.

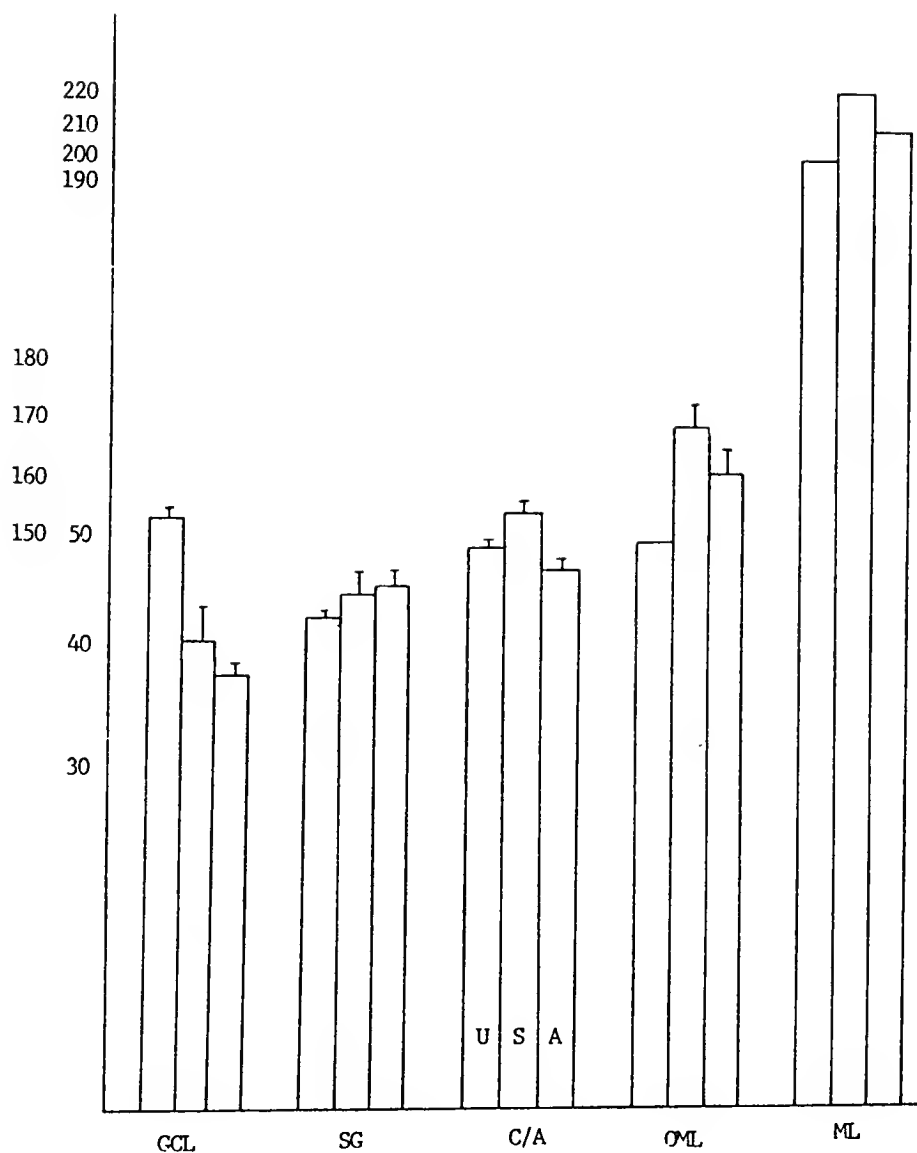
Figure 30: Contralateral Exposed Blade Normalized OML AChE Intensity by D-V Level

blade, however, the C/A zone was 8.8% narrower in the alcohol group than in the sucrose group. The C/A band occupied 23% of the molecular layer in both groups, so no relative decrease in C/A width occurred in the alcohol group. No differences in granule cell layer or supragranular band widths were observed.

When the buried blade contralateral widths are examined at each dorsal-ventral level, it can be seen that AChE stain bands in the alcohol group tend to be slightly narrower at all but the most ventral levels (figure 32). This is different from the exposed blade pattern (figure 26), where the differences were smaller and were observed at the dorsal- and ventralmost levels. The pattern of decreased width is similar in the total dentate width (GCL + SG C/A + OML) (not shown), the total ML width (not shown), and the outer ML width. No significant difference in granule cell layer or supragranular band widths were observed. The decreased C/A width of the alcohol group is more than the GCL or SG differences, and accounts for a substantial portion of the reduction in ML width in the alcohol group.

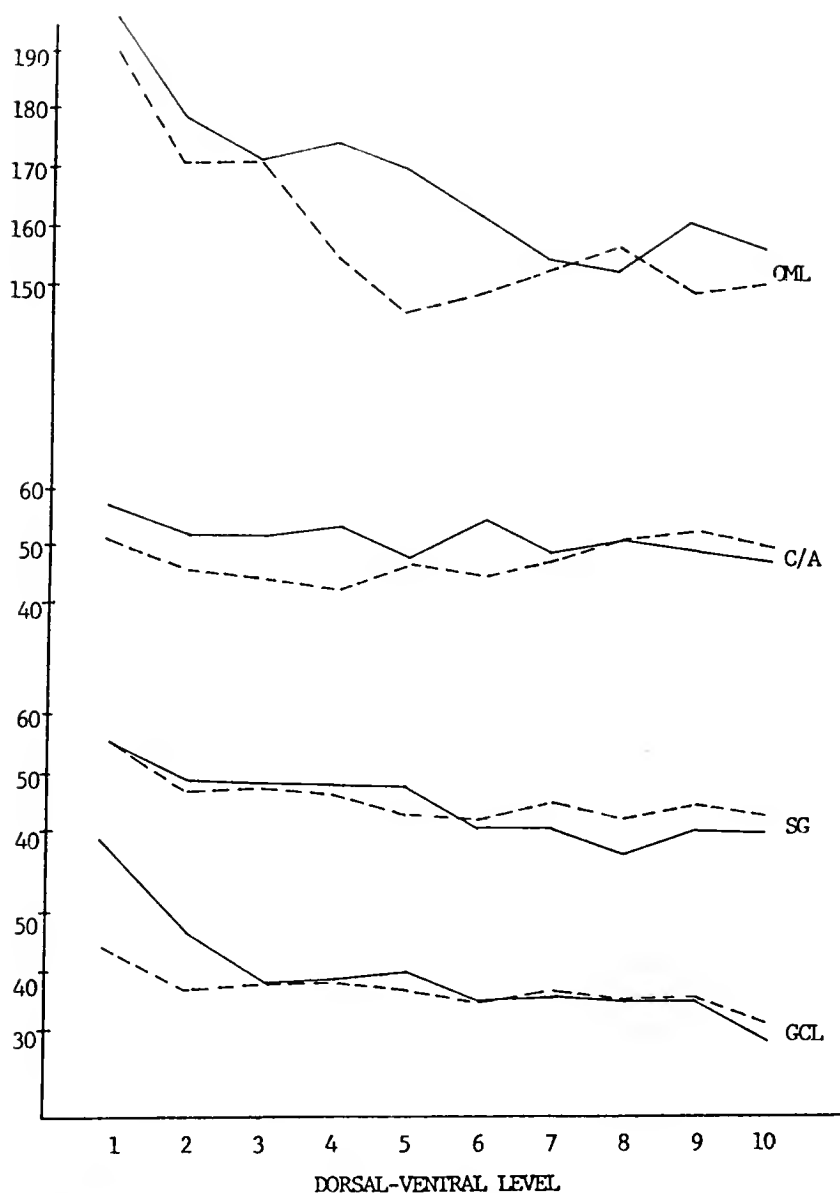
Contralateral Buried Blade AChE Stain Intensity.

Figure 33 presents the normalized buried blade AChE stain intensity measurements for the sucrose control group by D-V level, for each dentate sampling band. As in the exposed blade, there is a strong tendency for each portion of the dentate to vary together, although some independence is observed here as well.



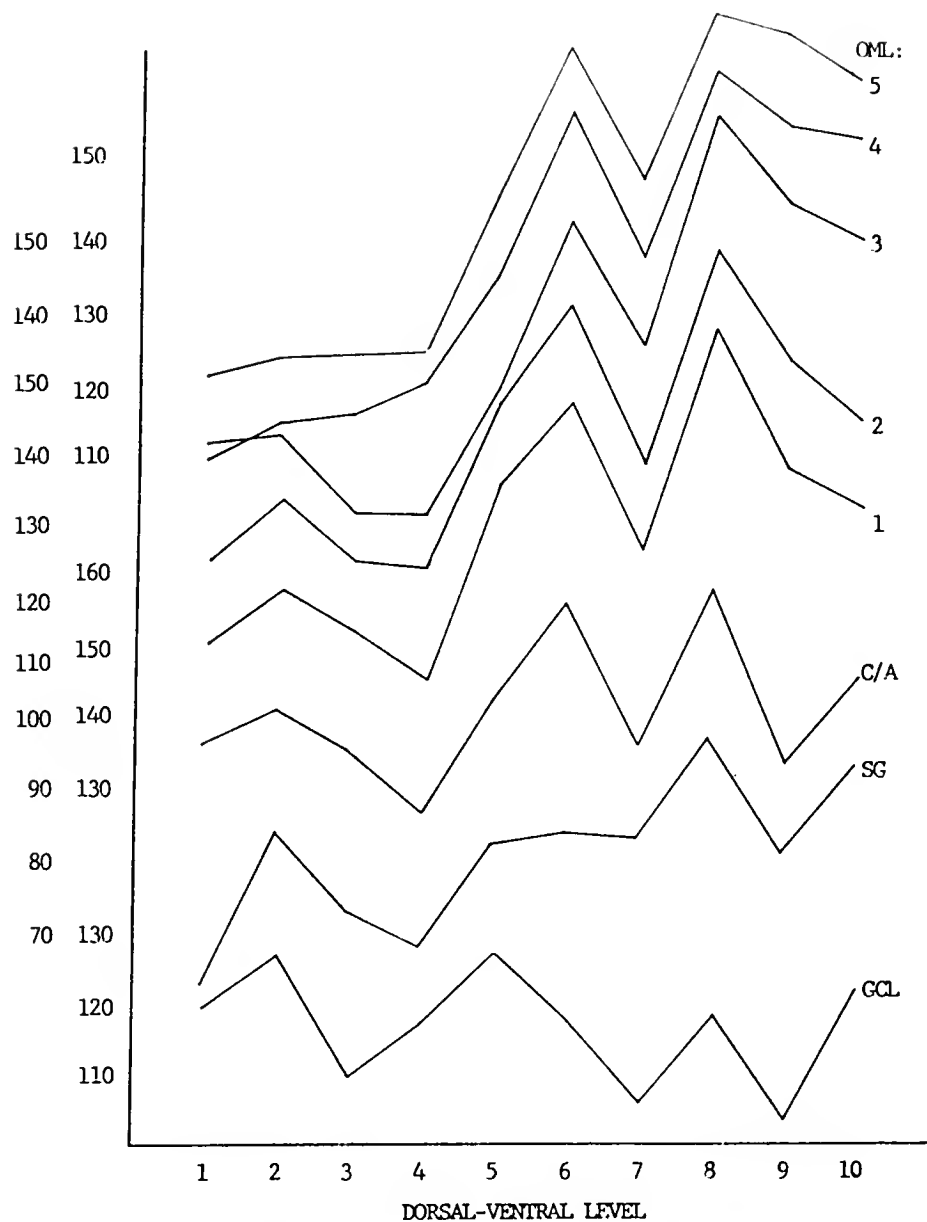
Abscissa, lower right scale, GCL, SG, and C/A widths in micrometers, mean \pm S.E.M. for all measurement points; upper right scale, ML widths; left scale, OML widths. U=unlesioned, S=sucrose, A=alcohol groups.

Figure 31: Contralateral Buried Blade AChE Band Widths



Abscissa, mean AChE band width; solid lines, sucrose group, dashed lines, alcohol group.

Figure 32: Contralateral Buried Blade AChE Band Widths by D-V Level



Abscissa, AChE band mean normalized intensity.

Figure 33: Contralateral Buried Blade Sucrose Group Mean Normalized AChE Stain Intensities by D-V Level

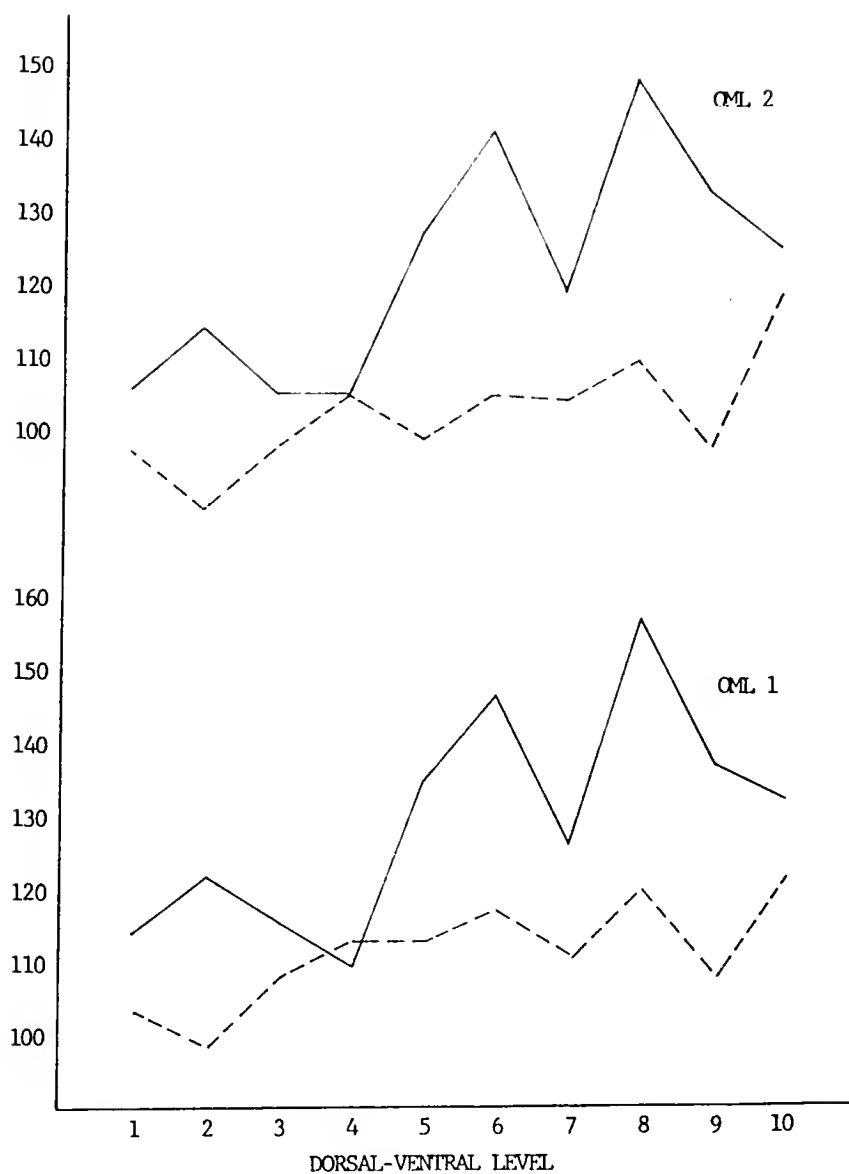
As in the exposed blade, the granule cell layer was darker in the alcohol group at most D-V levels (figure 34). The supragranular band (not shown) followed this pattern. The normalized density of the C/A band was increased (darker) in the alcohol group, and this difference exceeded the GCL and SG differences, being both greater in magnitude and more evenly distributed over the dorsal-ventral extent of our measurement sample. In the outer molecular layer, the alcohol group appears to stain more darkly than the sucrose group, especially ventrally, in all fifths of the OML (figures 35, 36, 37). Proximo-distal and dorso-ventral gradients in the amount of group differences are less clear than in the exposed blade, although the differences tend to be greater proximally and ventrally. As in the exposed blade, both groups tend to exhibit less staining ventrally than dorsally.

Entorhinal Lesions

Our six-stage electrolytic method for unilateral destruction of the entorhinal cortex produced reliable ablations that only rarely encroached upon the subiculum or perirhinal areas. Three dimensional graphs of the molecular layer shrinkage (figure 38), defined as the difference between contralateral and ipsilateral widths, were obtained using SASGRAPH PROC G3D and compared with reconstructions of the lesions at 4 dorsal-ventral levels (figure 7).

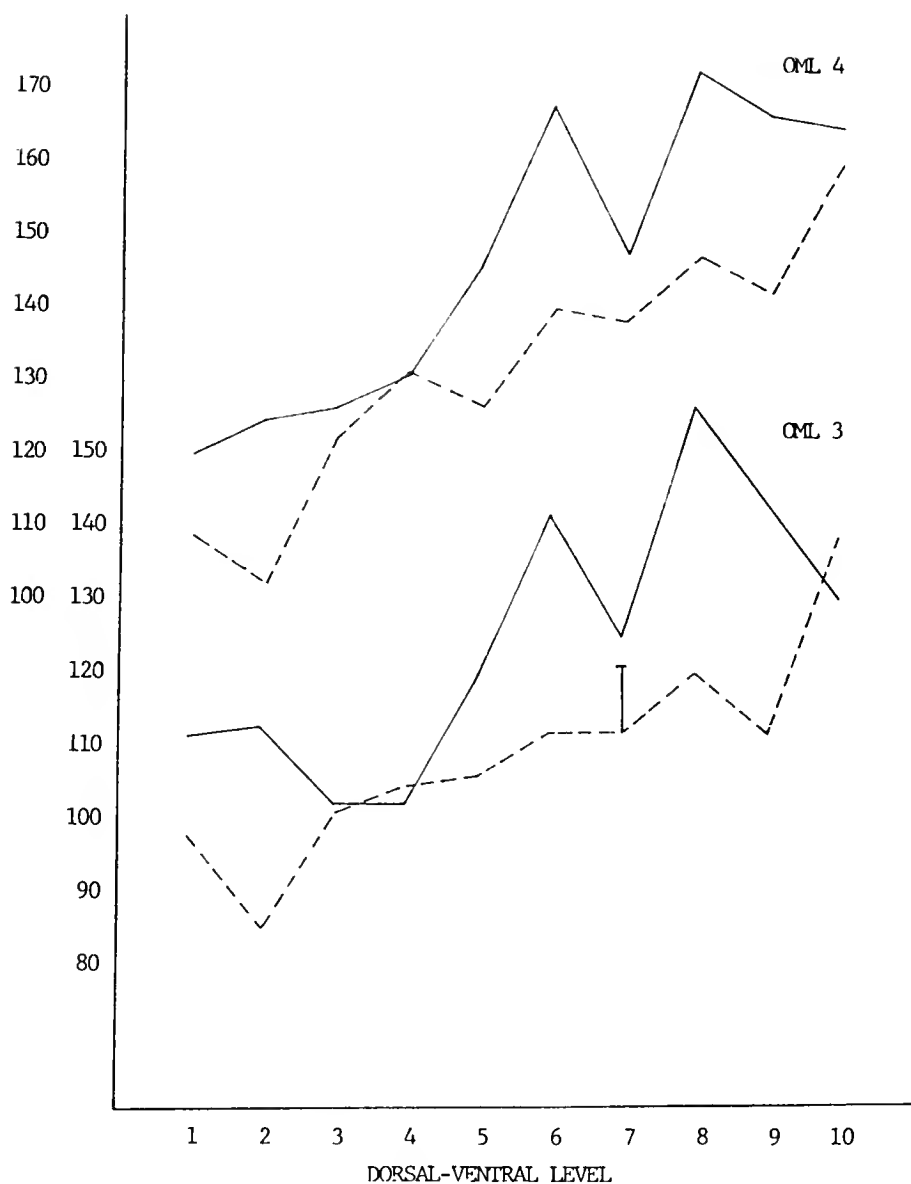
Abscissa, AChE band mean normalized intensity;
solid lines, sucrose group, dashed lines, alcohol group.

Figure 34: Contralateral Buried Blade C/A AChE Band
Intensity by D-V Level



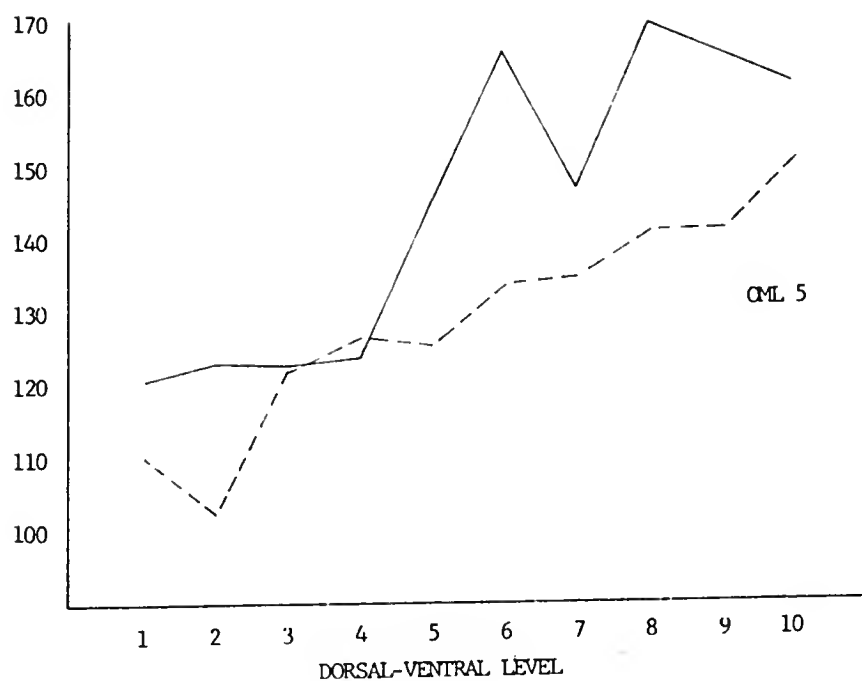
Abscissa, AChE band mean normalized intensity;
solid lines, sucrose group, dashed lines, alcohol group.

Figure 35: Contralateral Buried Blade CML AChE Band Intensity, by D-V Level



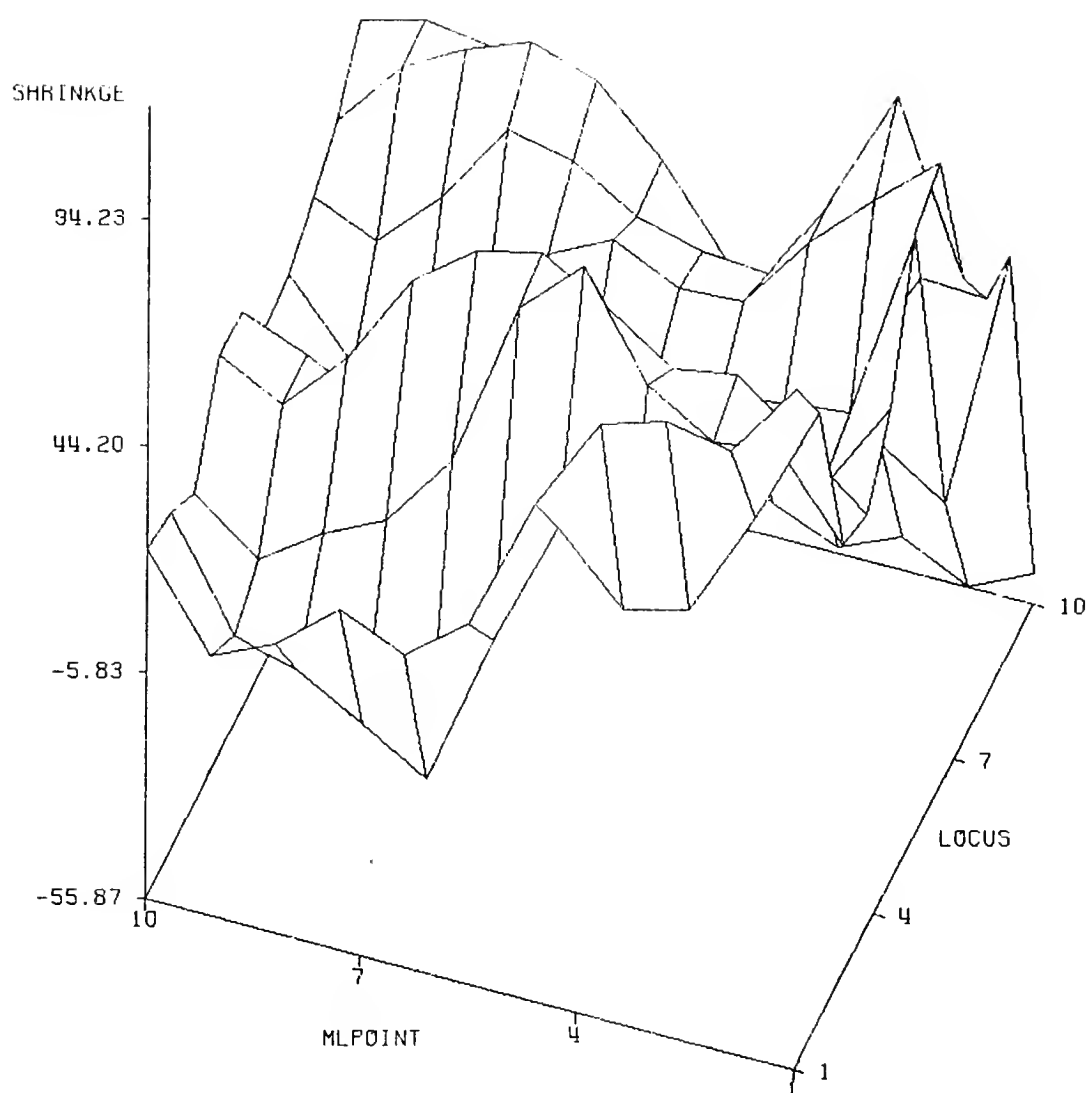
Abscissa, AChE band mean normalized intensity;
solid lines, sucrose group, dashed lines, alcohol group.

Figure 36: Contralateral Buried Blade OML AChE Band Intensity, by D-V Level



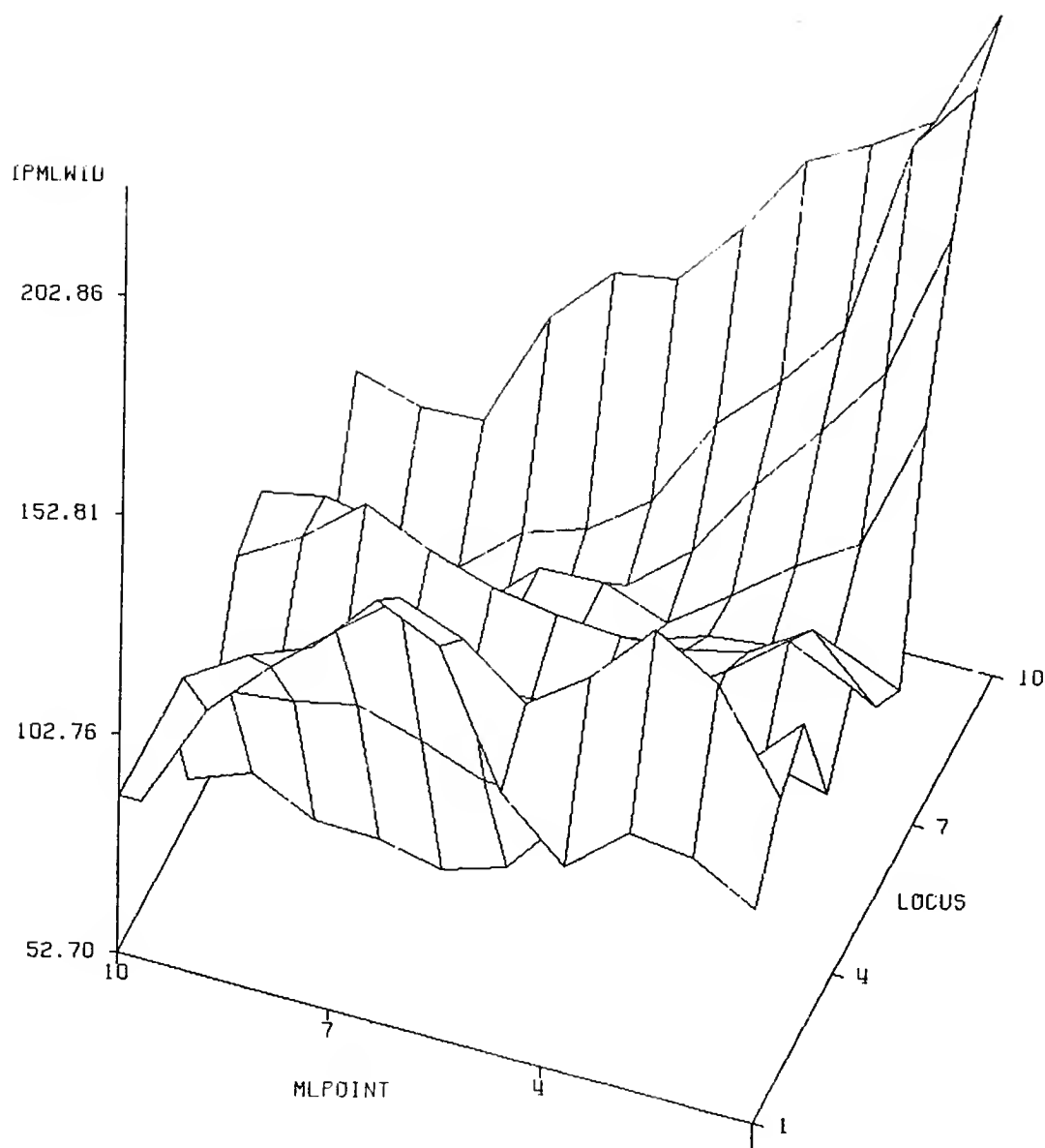
Abscissa, AChE band mean normalized intensity;
solid lines, sucrose group, dashed lines, alcohol group.

Figure 37: Contralateral Buried Blade OML AChE Band
Intensity, by D-V Level



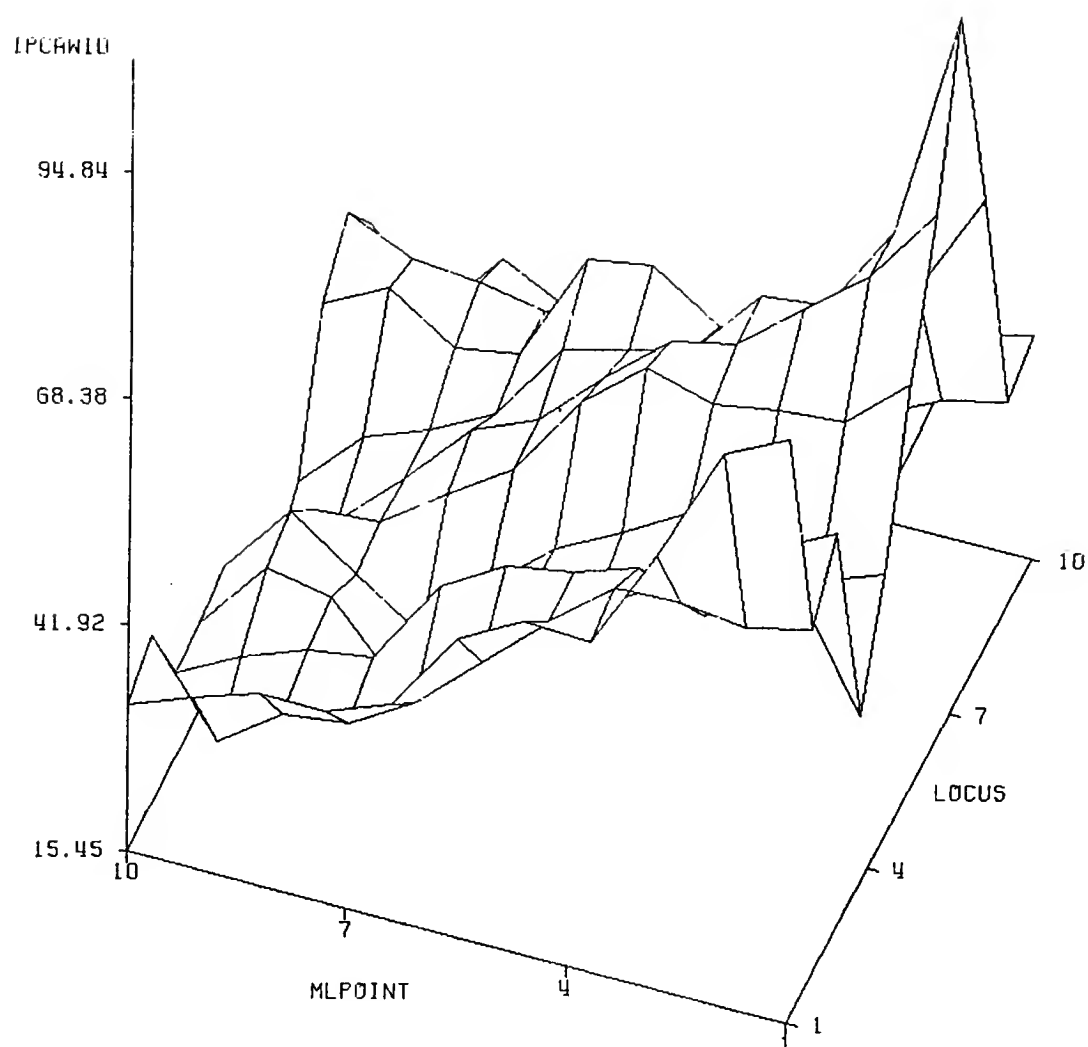
SHRINKGE, contra minus ipsilateral ML width; MLPOINT, cell layer crest-tip location; LOCUS, dorsal-ventral measurement location.

Figure 38: Molecular Layer Shrinkage Following Entorhinal Lesion



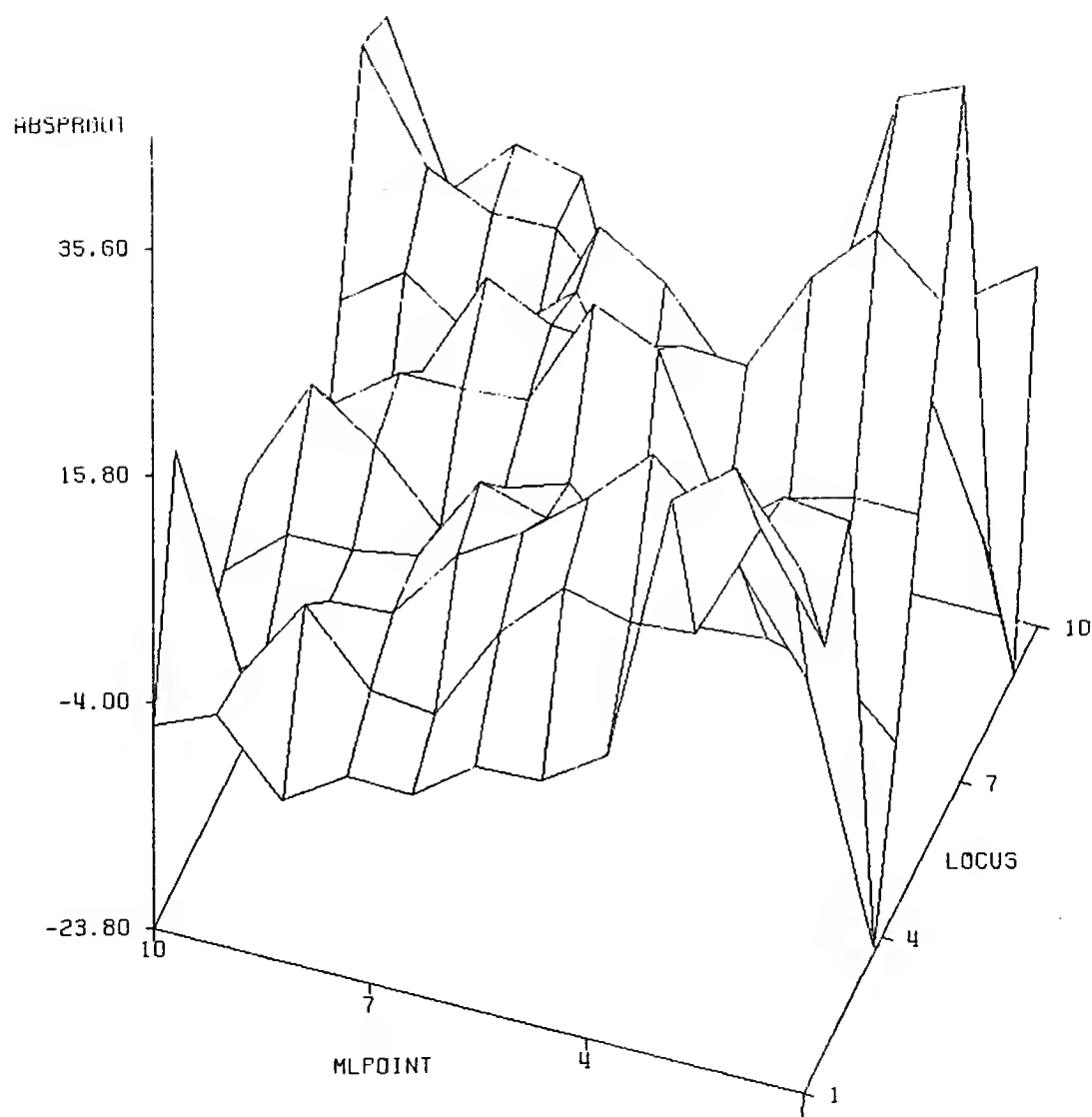
IPMLWID, ipsilateral molecular layer width; MLPOINT, cell layer crest-tip location; LOCUS, dorsal-ventral measurement location.

Figure 39: Molecular Layer Width Following Entorhinal Lesion



IPCAWID, ipsilateral C/A width; MLPOINT, cell layer crest-tip location; LOCUS, dorsal-ventral measurement location.

Figure 40: AChE C/A Band Width Following Entorhinal Lesion

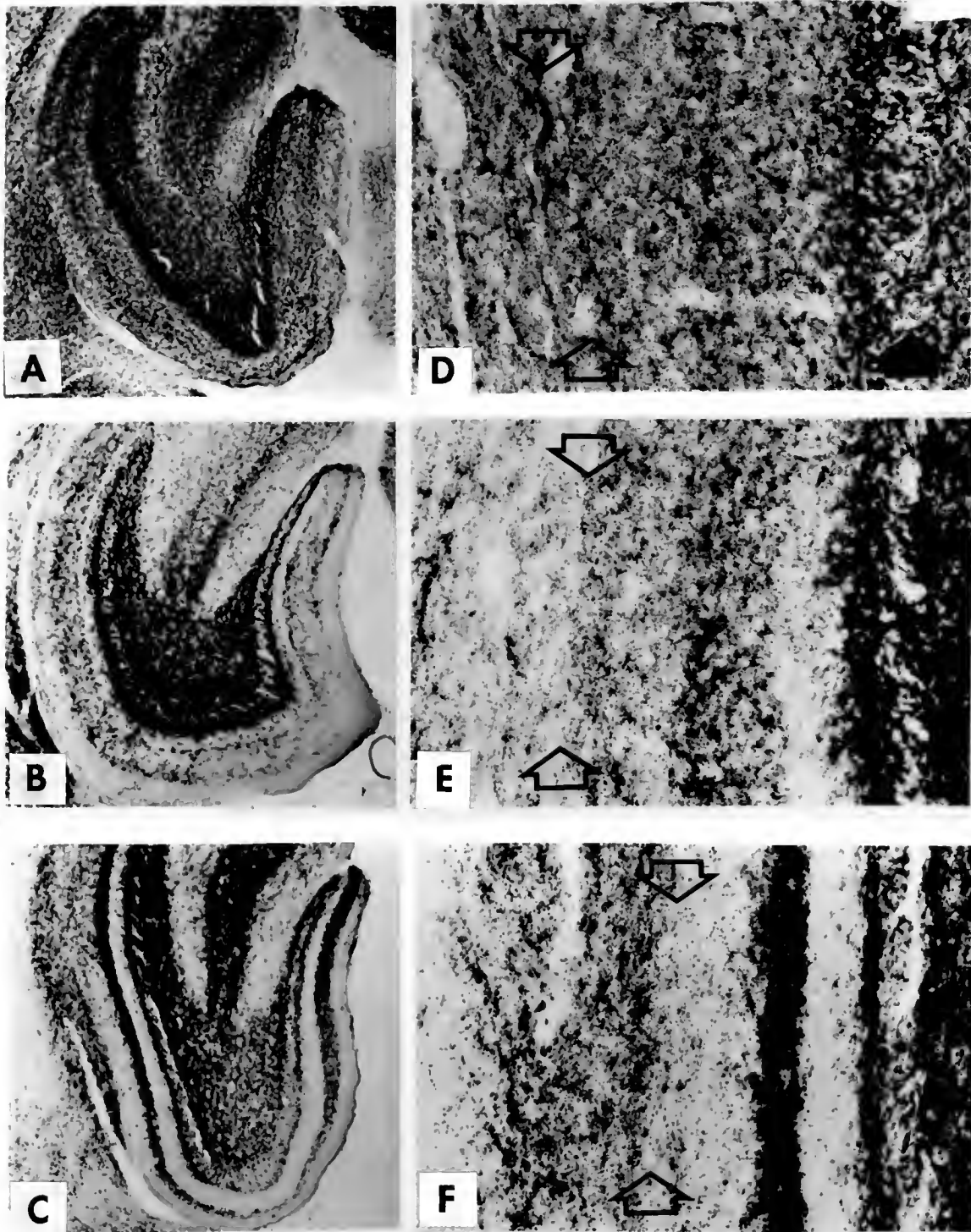


ABSPROUT, ipsilateral C/A width minus contralateral;
 MLPOINT, cell layer crest-tip location; LOCUS,
 dorsal-ventral measurement location.

Figure 41: AChE C/A Band Expansion Following Entorhinal Lesion

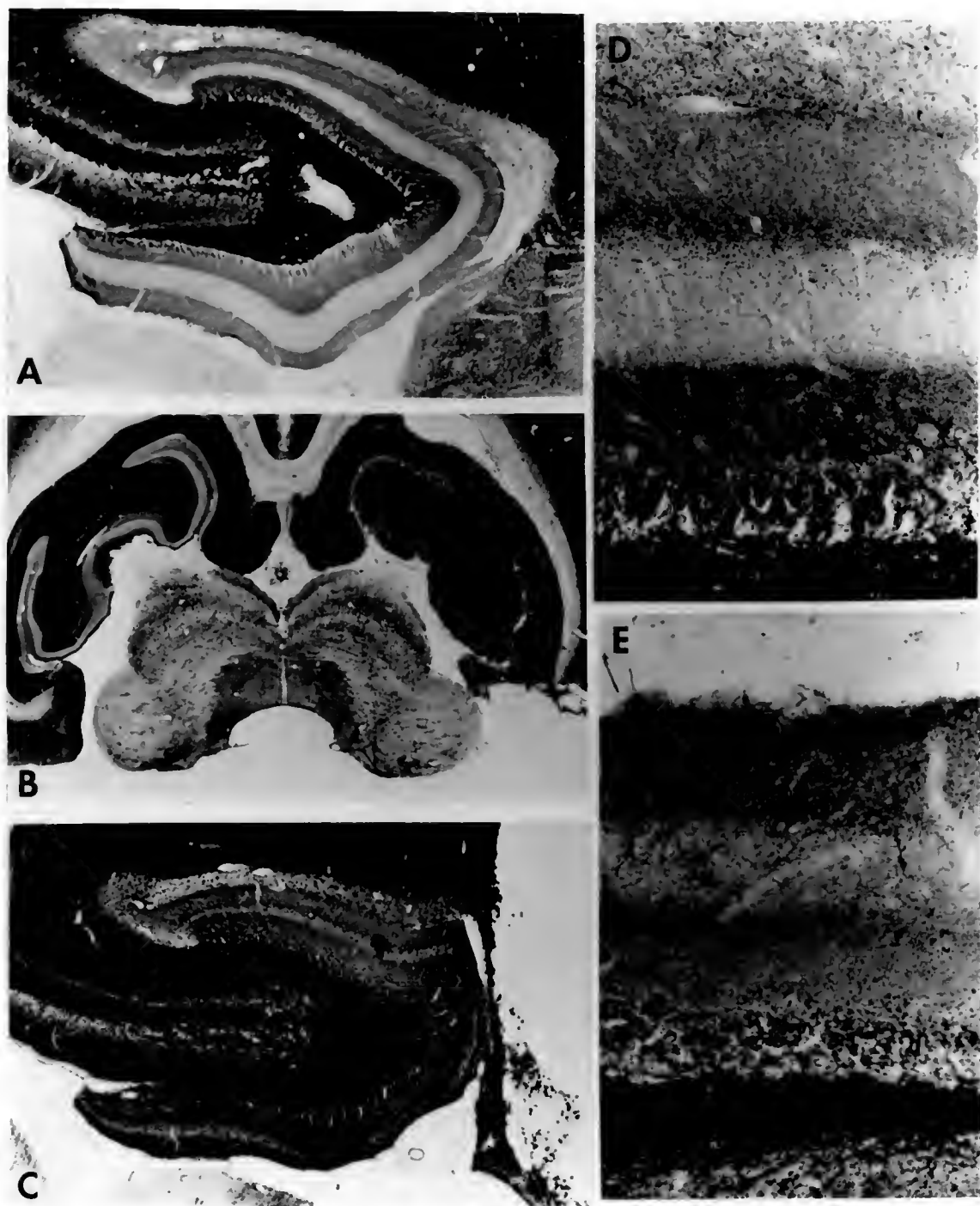
This type of graph (figures 38-41) is useful for representing the relationship between the location and magnitude of the entorhinal lesion, the molecular layer shrinkage, and the sprouting response. It also illustrates the width variation pattern within the dentate that we have previously described (King et al., in press). We found a mean molecular layer shrinkage of about 15% over all 100 measurement points (before subsetting by criterion shrinkage) in animals selected for further analysis on the basis of nearly complete and restricted total entorhinal lesions.

The sprouting response is apparent in the AChE-stained material. As others have reported, we find a clearing of reaction product from the inner portion of the molecular layer on the lesioned side, an absolute and relative expansion of this band, and a condensation of reaction product in the outer molecular layer (figure 42). In Timm's stained material, the outer molecular bands on the lesioned side lose their distinct definition and shrink; reactive astrocytes are often seen in this zone (figure 43). Qualitative differences in the width or density of the inner band are not obvious.



A,D, unlesioned animal AChE dentate stain pattern; B,E, contralateral side; C,F ipsilateral side in lesioned animal. Left column, low power magnifications; right column, higher magnification of ML. Dark arrow indicates GCL, open arrows indicate location of the fissure.

Figure 42: AChE Stain Patterns in Unlesioned and Lesioned Animals



A,D, contralateral dentate; C,E, ipsilateral. B shows lesioned (right) and unlesioned dentate at a dorsal level. Reactive astrocytes can be seen in the CML in C and E.

Figure 43: Timm's Stain Patterns in Unlesioned and Lesioned Animals

Unlesioned vs. Contralateral AChE Patterns

To evaluate the use of the contralateral dentate as a within-animal control for the effect of unilateral entorhinal lesions, comparisons between several unlesioned animals and the contralateral side of lesioned animals were made. Measurements on AChE-stained horizontal sections from 5 unlesioned animals were made using the same procedure as for the animals in the lesion experiment. Examination of these data will also allow comparison of the various stain intensity normalization and correction methods evaluated.

No statistically significant differences in the widths of AChE stain bands were found when non-lesioned animals were compared with the unlesioned side of animals with unilateral entorhinal lesions. Width values for all bands are very similar to those reported by other investigators (West et al., '81), with a total molecular layer width of about 200 microns (Table 5). However, the pattern of AChE staining in the molecular layer indicates that the unlesioned side does undergo some reactive change in response to contralateral lesion, as previously reported (Hoff et al., '81). When the stain intensity values are normalized for microscope light level and the unlesioned group is corrected to the mean stain intensity of the granule cell and supragranular zones of lesioned animals, significant clearing of AChE from the commissural/associational zone is observed (figure 47). This correction produces the minimum C/A band optical

density difference, and the clearing response is correspondingly greater if group densities are uncorrected or corrected to any other band or the mean dentate AChE intensity. For example, Figure 41 shows the raw density data for each AChE band in unlesioned animals and contralateral to the lesions in the sucrose group animals. All of the unlesioned bands have lower mean values than the sucrose animals. Is this because there is really less AChE staining in the lesioned sucrose group, or might it be an artifact of histochemical processing differences between groups? If it is the latter, then simply adding the average group difference to all the unlesioned group means would correct for this error. Figure 45 shows this correction applied to the buried blade values shown in Figure 44. The unlesioned group (dashed line) was adjusted by minimizing the difference in the granule cell and supragranular bands, where contralateral lesion effects would be least expected. As with the raw data means, a clearing of AChE from the C/A band is apparent even when the values are brought closer together. This correction method, however, does not compensate for the amount of light used to illuminate the tissue sections under the microscope. Since this variable could affect the digitized gray level corresponding to a particular stain intensity, it is necessary to normalize the density data to a constant level of microscope light intensity. As described in the Methods section, this

normalization procedure was applied to the raw, uncorrected data shown in Figure 44. As Figure 46 shows, although the pattern of group differences changes slightly, there is still a clearing observable in the sucrose group C/A band. When both the light-normalization and lesion-neutral-band correction techniques are applied, the results are again very similar (figure 47).

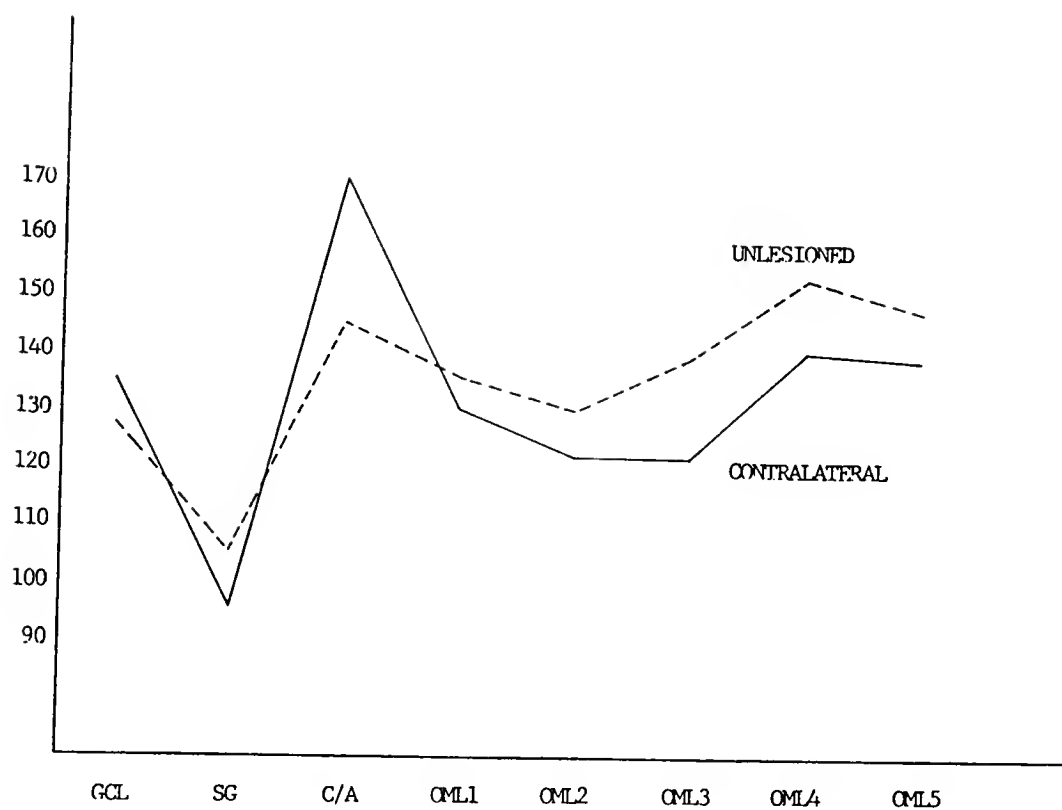
In conjunction with this clearing, we find mean C/A width values to be not significantly different from unlesioned animals (figure 25), suggesting that the clearing of AChE in the C/A zone in response to partial outer molecular layer deafferentation may not be dependent upon expansion of the C/A zone. Percent occupation of the molecular layer by the C/A band, which increases on the lesioned side, may even be slightly reduced on the contralateral side in sucrose and alcohol groups in both blades of the dentate, when compared to unlesioned animals. When only the dorsalmost 3 sections were compared, however, a small increase in C/A zone width was observed between unlesioned and contralateral groups (not shown). This indicates that in the portion of the dentate where the deafferentation might be expected to be greater on the basis of afferent projection patterns (Steward, '76), a small expansion of the C/A zone may have occurred that is beyond our statistical resolving power.

There may also be some AChE effects in the distal 50% of the outer molecular layer, especially in the exposed blade,



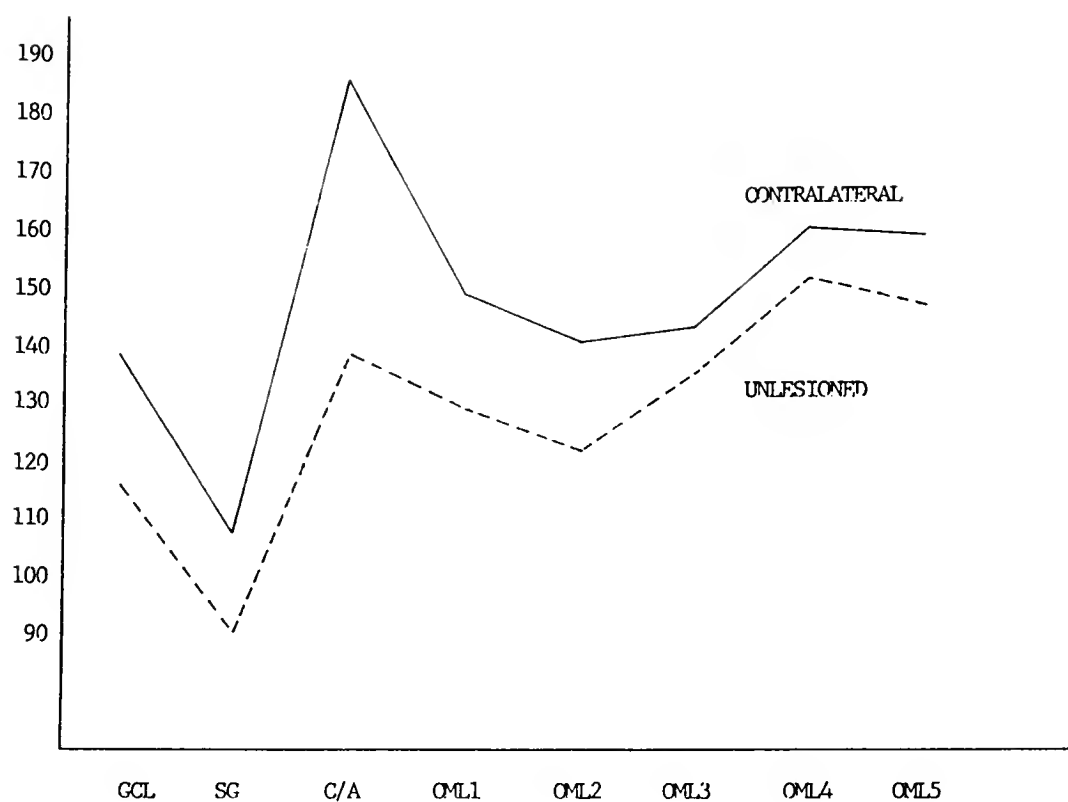
Abscissa, raw AChE stain intensity. Only sucrose animals (solid lines) were used for contralateral data; dashed lines, unlesioned control group.

Figure 44: Raw AChE Stain Intensity, Unlesioned vs. Contralateral Dentate



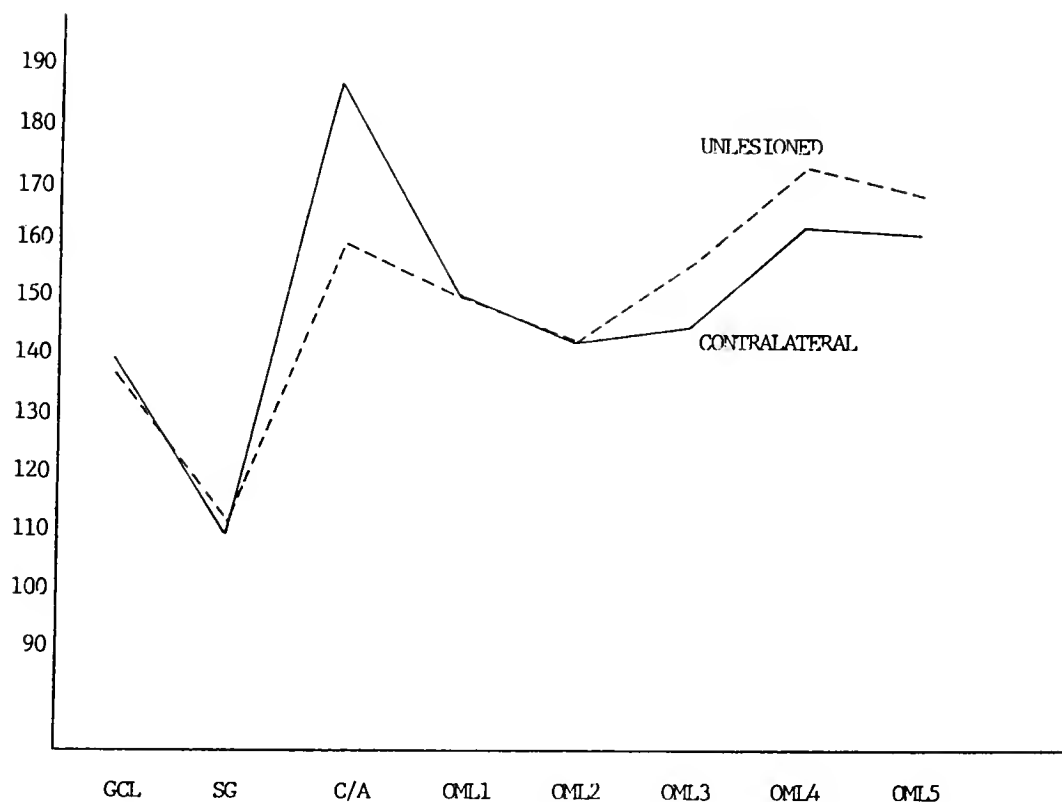
Abscissa, buried blade AChE stain intensity corrected by mean GCL/SG difference. Sucrose animals (solid lines) were used for contralateral data; dashed lines, unlesioned control group.

Figure 45: Corrected AChE Stain Intensity, Unlesioned vs. Contralateral Dentate



Abscissa, buried blade normalized AChE stain intensity. Sucrose animals (solid lines) were used for contralateral data; dashed lines, unlesioned control group.

Figure 46: Normalized AChE Stain Intensity, Unlesioned vs. Contralateral Dentate



Abscissa, buried blade normalized AChE stain intensity corrected by mean GCL/SG difference. Sucrose animals (solid lines) were used for contralateral data; dashed lines, unlesioned control group.

Figure 47: Normalized and Corrected AChE Stain Intensity, Unlesioned vs. Contralateral Dentate

although this failed to reach significance in our study. The pattern of stain intensity in this zone is suggestive that a redistribution of enzyme occurs, leading to a higher density of AChE product in the most distal molecular layer (figures 44, 47). This has been shown to be where the crossed entorhinal-dentate axons contact the contralateral granule cell dendrites most heavily (Steward and Scoville, '76).

Synaptic Reorganization Effects

Buried Blade Widths in AChE Material.

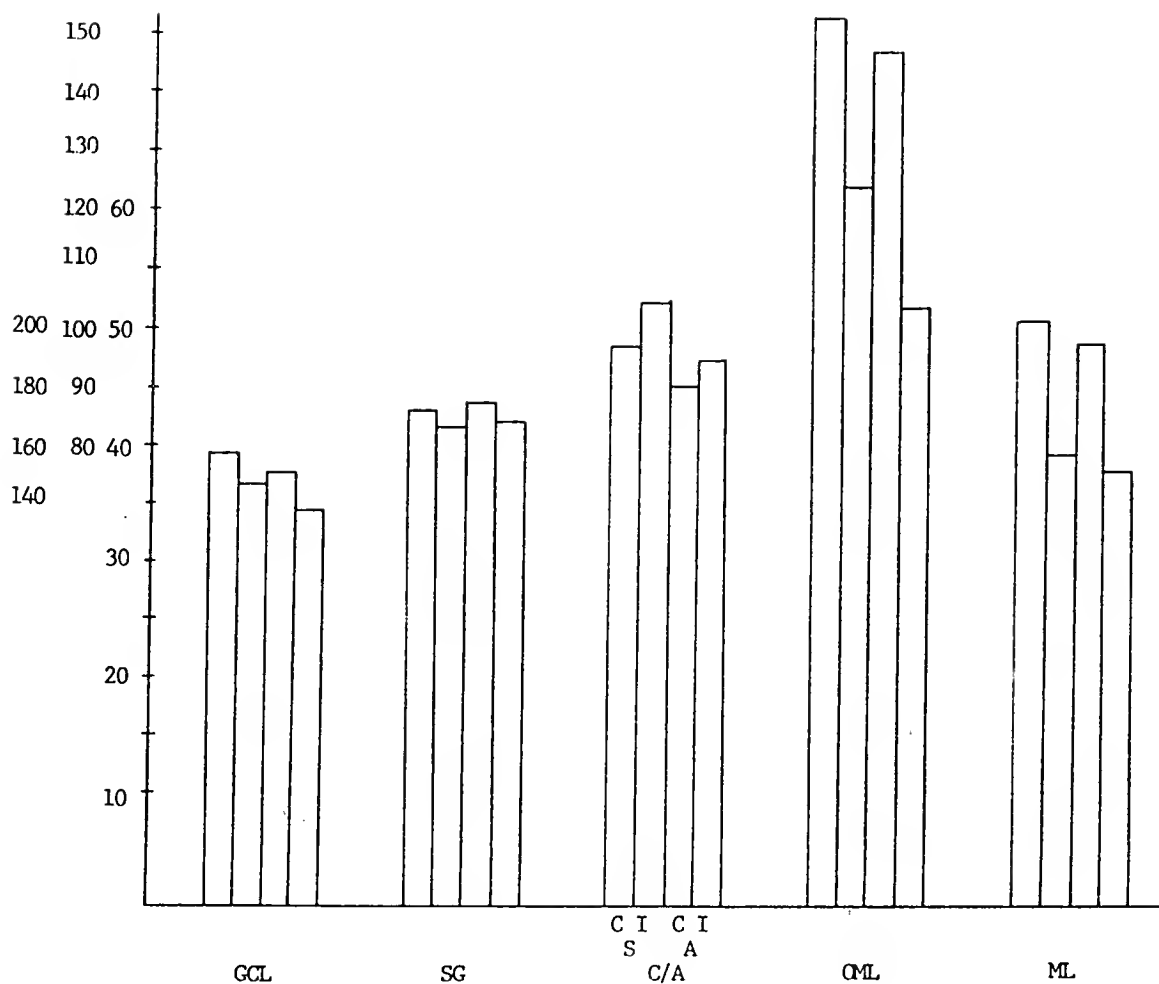
Lesion effects were determined by comparing the lesioned dentate with the contralateral side, at the same measurement location, in the same animal. In the buried blade, entorhinal lesion resulted in a 22% shrinkage of the molecular layer in the sucrose control group, and a 25% shrinkage in the alcohol group (figure 48). The mean absolute shrinkage was 47 microns for the sucrose and 51 microns for the alcohol group. The group differences in shrinkage were not statistically significant. Nor were the larger group differences in the amount of shrinkage in the buried blade outer molecular layer (A: 33%, S: 29%) significant. The two groups can thus be considered to have received equivalent lesions. Figure 49 shows very nicely that a uniform shrinkage occurs in both groups across D-V levels. Differences in the ipsilateral ML widths are

largely accounted for by differences on the contralateral side between groups.

No lesion-induced differences in granule cell layer or supragranular band width were observed. In the sucrose control group, analysis over all measurement points where shrinkage was greater than 15 microns revealed that the buried blade C/A zone increased an average of 2.1 microns, compared to the contralateral side, following the entorhinal lesion (figure 48). The alcohol group, in contrast, exhibited only about half (1.1 microns) the absolute C/A expansion of controls. This represents a relative increase of 4.1% in the sucrose and 2.4% in the alcohol groups. In keeping with the published literature on dentate reactive synaptogenesis, the largest C/A increases occur at the more dorsal levels (figure 50), although the sucrose group demonstrated a substantial increase at the ventralmost 2 levels. Considerable variation across measurement levels is observed in both groups; it cannot be determined whether this is an artifact of the particular lesion locations in these animals or a characteristic feature of dentate reactive synaptogenesis.

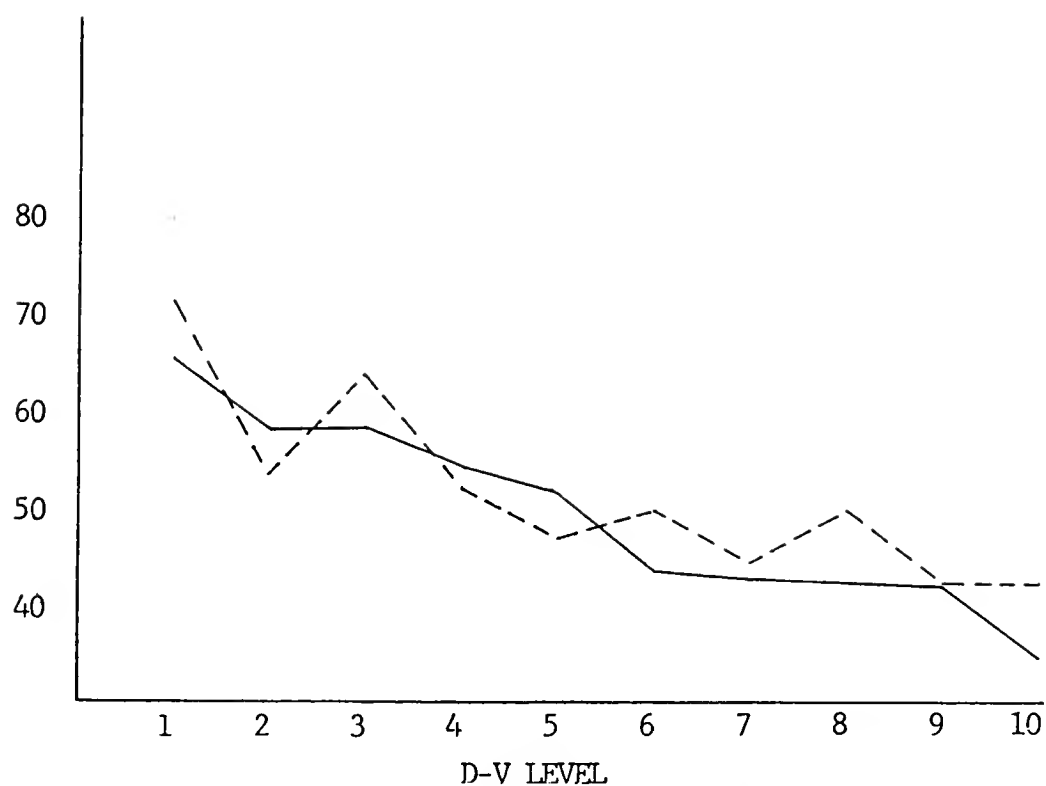
Buried Blade AChE Intensity.

As shown in Figure 51, the normalized stain intensity of the granule cell layer decreased (lightened) ipsilateral to the lesion in the sucrose group, at most D-V levels (figure 52). In the alcohol group, which was more dense (darker)



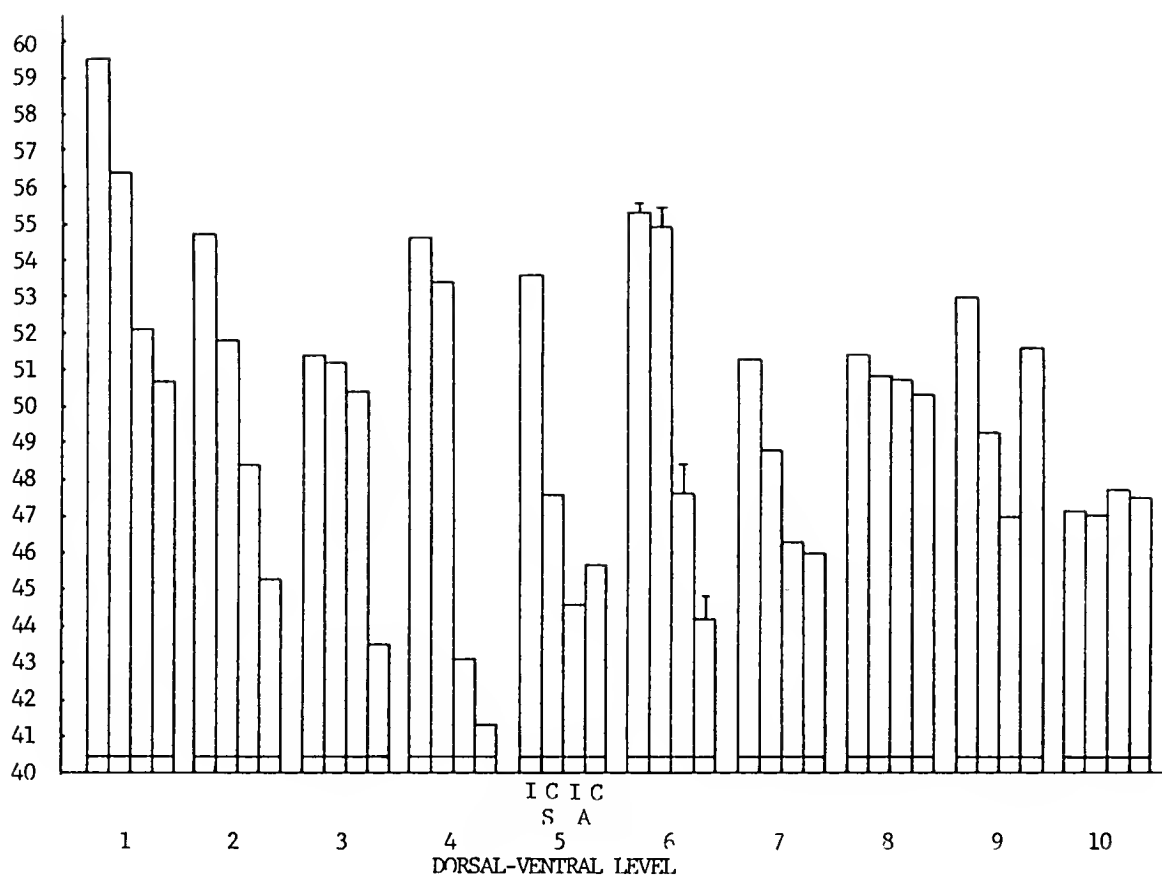
Abscissa, mean width in micrometers, \pm S.E.M.. Leftmost scale, ML; middle scale, OML; rightmost scale, all other bands. C=contralateral, I=ipsilateral; S=sucrose, A=alcohol group.

Figure 48: Buried Blade AChE Stain Band Width Changes in Entorhinal Lesioned Animals



Abscissa, contralateral minus ipsilateral OML width, in micrometers, showing shrinkage at each D-V level. Dashed line, alcohol group.

Figure 49: Buried Blade Lesion-induced OML Shrinkage by D-V Level

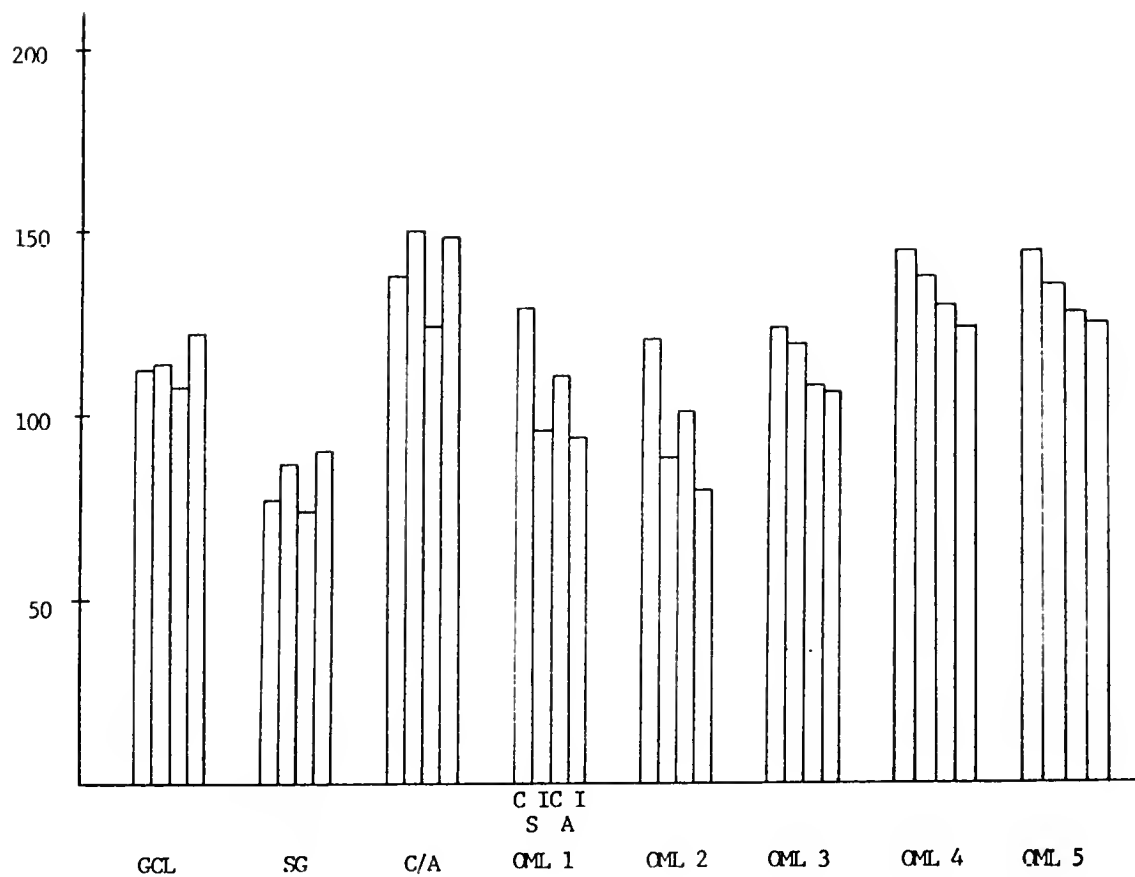


Abscissa, group mean C/A band width, in micrometers, \pm S.E.M.. C=contralateral, I=ipsilateral; S=sucrose, A=alcohol group.

Figure 50: Buried Blade AChE C/A Band Widths, Ipsi- and Contralateral, by D-V Level

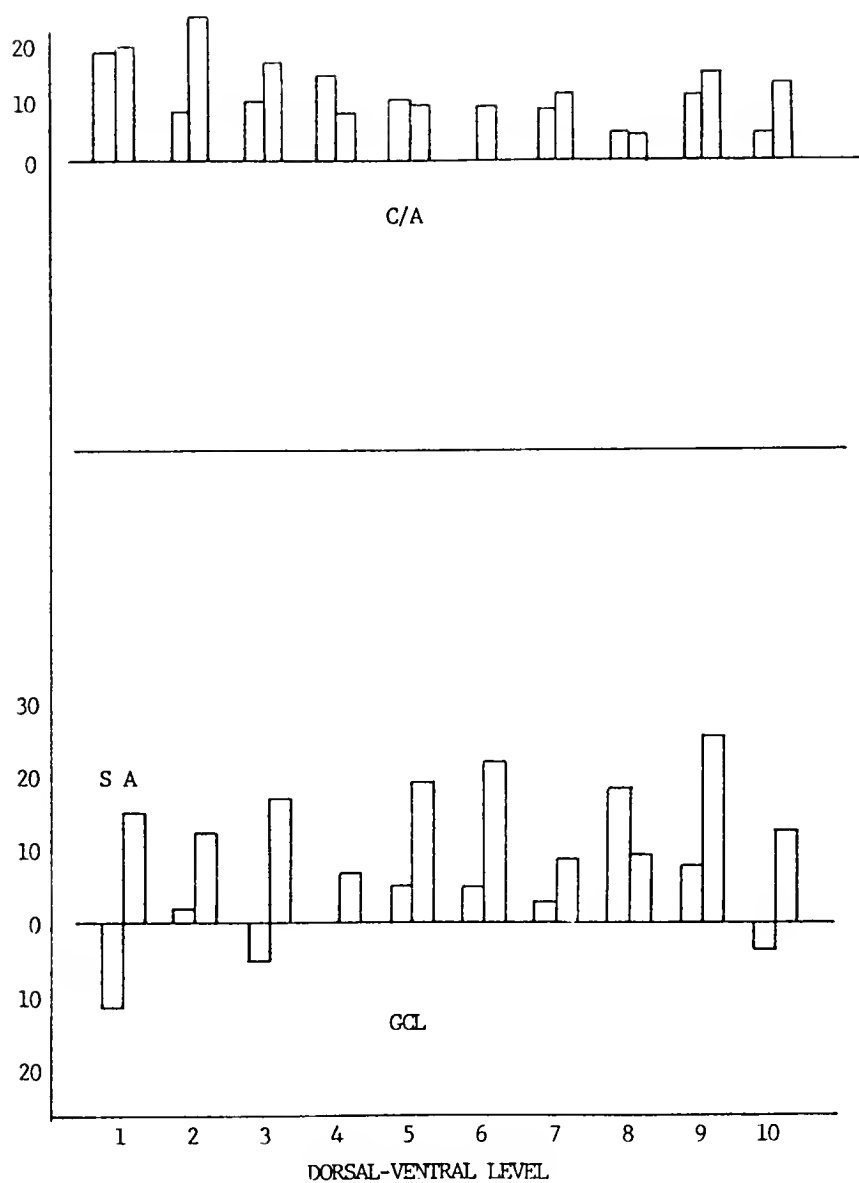
contralaterally than the sucrose group, a greater decrease in AChE intensity was seen in response to the lesion. Alcohol group values, at all but one D-V level, showed that less staining was present than either contralaterally or in either side of the sucrose group. Furthermore, while the clearing that occurred in the sucrose group followed the contralateral variations in intensity at different D-V levels, the alcohol group GCL clearing was noticeably less tied to contralateral variations. Similar changes and patterns are observed in the supragranular band (not shown).

The C/A band of the sucrose group showed the characteristic clearing ipsilateral to the lesion. The clearing did not appear to be closely associated with the amount of sprouting that was measured, although some correspondence between the D-V levels where clearing and sprouting were greatest is evident. In the alcohol group, although there is only half as much sprouting, the clearing does not appear to be much different from that of the sucrose group at most D-V levels (figure 52). Here there is also less correspondence between the loci where sprouting is greatest and the amount of clearing. Ventrally, even where the alcohol group C/A band is even narrower ipsilaterally than it is contralaterally, a substantial clearing is still apparent. If it is assumed that no density changes occur ipsilateral to the lesion (cf. Storm-Mathisen, '74), and the ipsilateral GCL densities of both groups are set equal to



Abscissa, ipsilateral and contralateral normalized AChE stain intensity means, \pm S.E.M.. C=contralateral, I=ipsilateral; S=sucrose, A=alcohol groups.

Figure 51: Buried Blade AChE Band Stain Intensity Responses to Entorhinal Lesions

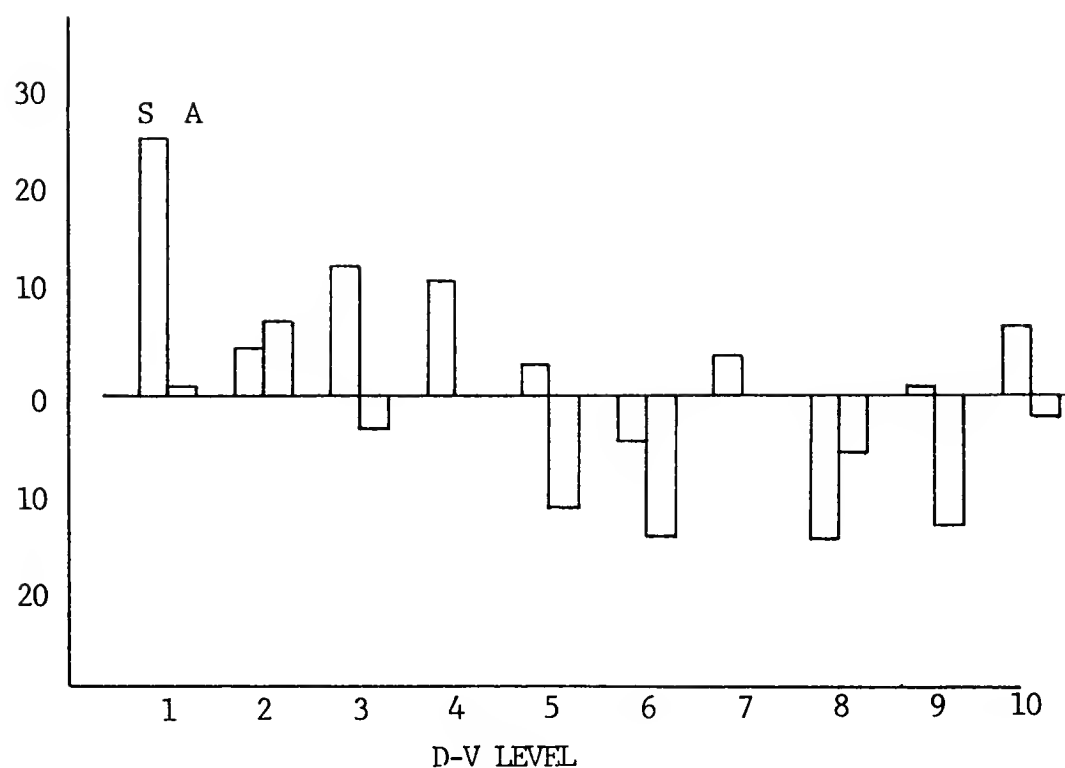


Abscissa, ipsilateral minus contralateral normalized AChE intensity; positive bars indicate clearing of AChE and vice versa.

Figure 52: Buried Blade AChE GCL and C/A Band Stain Intensity Responses to Entorhinal Lesion

the contralateral GCL density, then the amount of clearing observed is greatly reduced in the alcohol and little changed in the sucrose group (figure 53). Even after subtracting out the GCL clearing, however, the correspondence between sprouting and clearing is poor in the alcohol group. It is rather improved in the sucrose group.

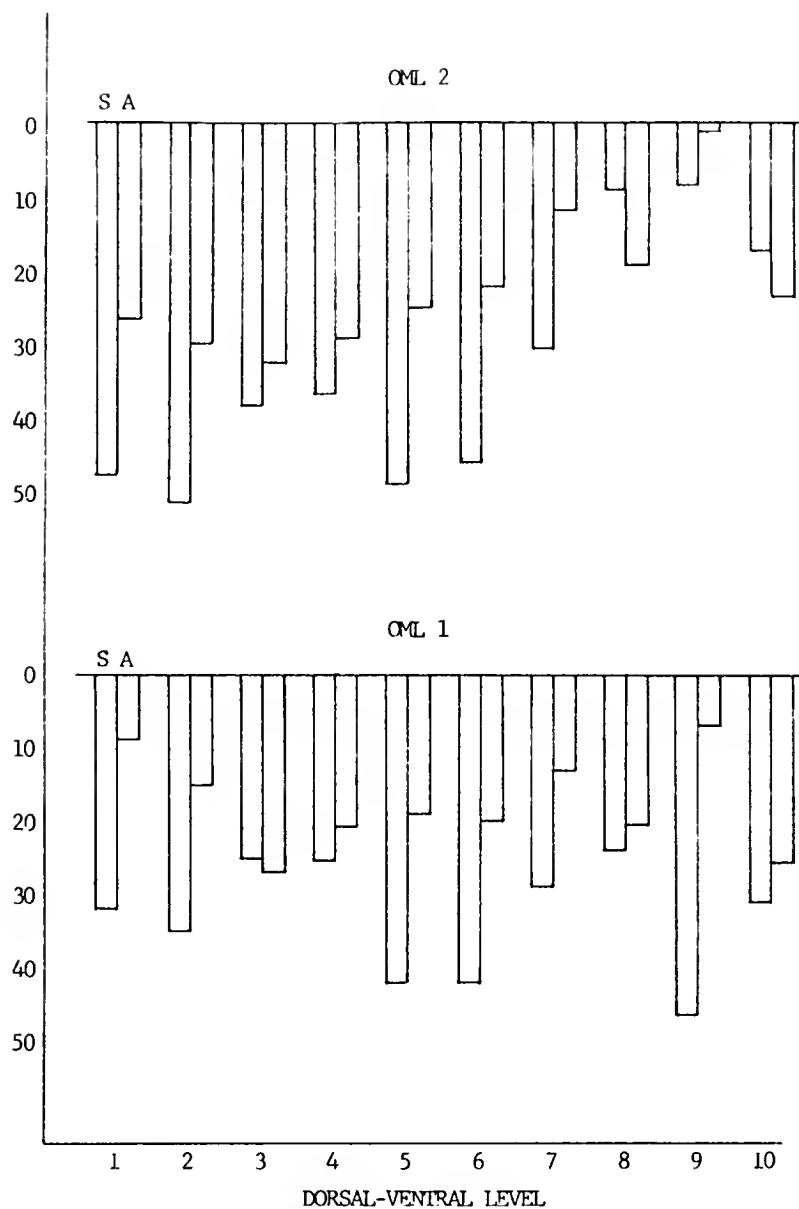
In the buried blade outer molecular layer, the differences between groups in their density responses to lesion tend to be smaller relative to the amount of lesion-induced change (figures 54, 55, 56). In the proximal 20%, the sucrose group undergoes the characteristic condensation of AChE staining; the amount of condensation is similar at most D-V locations. Less condensation is observed in the alcohol group. However, the alcohol group demonstrates darker staining contralateral to the lesion, and the ipsilateral densities at most levels are the same as or darker than the sucrose group ipsilaterally. Thus, the lesion deafferentation may have induced the alcohol animals to complete a condensation response already initiated, and perhaps even surpass the final cholinergic termination density of the sucrose group. In the second 20% of the OML, the pattern of OML1 condensation is evident at dorsal levels, but ventrally both groups show less condensation and there is more of an increase in AChE stain density (darkness) in the alcohol group. Here the ipsilateral alcohol group staining is also greater than the sucrose



Abscissa, ipsilateral minus contralateral normalized AChE intensity corrected for GCI response; positive bars indicate clearing of AChE and vice versa.

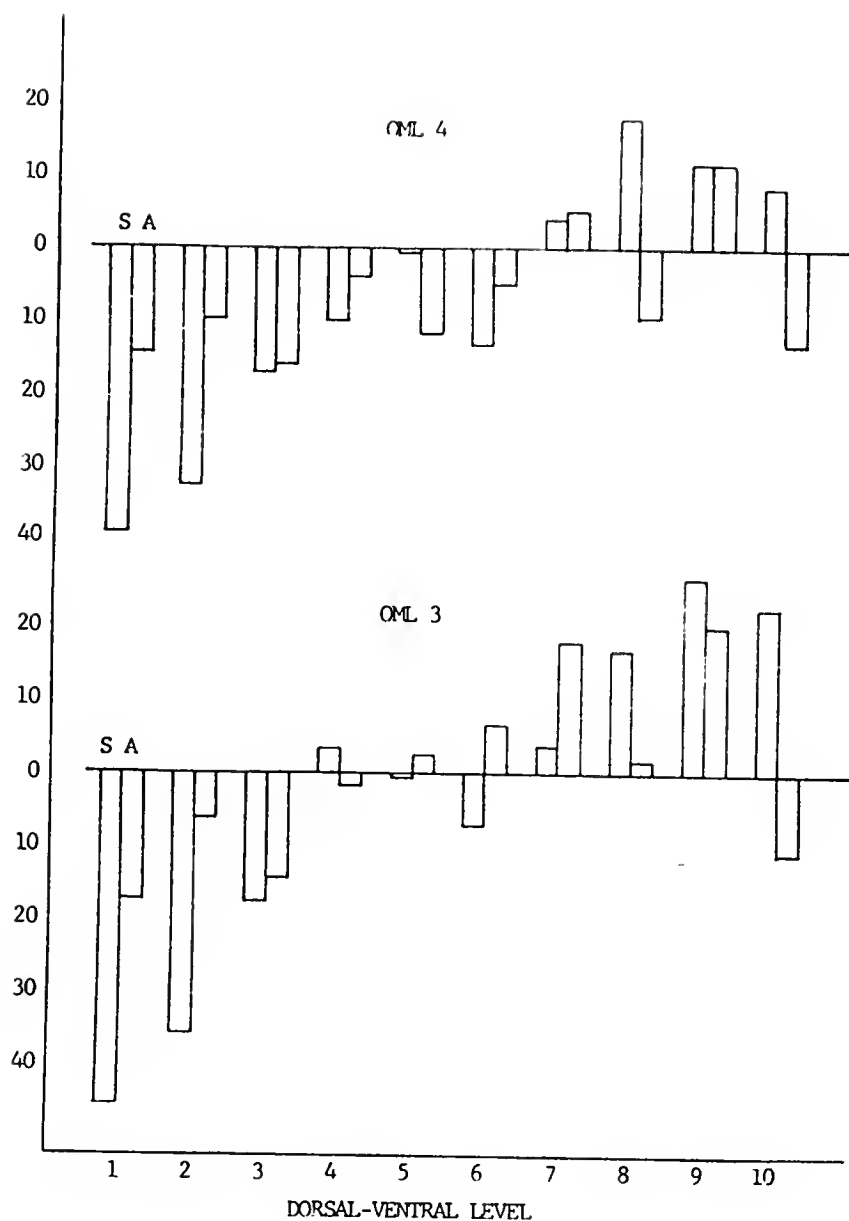
Figure 53: Buried Blade AChE GCL and C/A Band Stain Intensity Responses to Entorhinal Lesions by D-V Levels

group. In the middle 20% of the OML, a dorsal-ventral gradient in the response begins to show up more convincingly. Dorsally, both alcohol and sucrose groups demonstrate a condensation. Although it is less in the alcohol group, here too the ipsilateral absolute intensity values are about equal in both groups. At mid-dorsoventral levels, neither group differs from the contralateral side. Ventrally, however, both groups exhibit a clearing of AChE. As for the condensation in this third fifth of the ventral OML, the alcohol group normalized intensity values fail to reach those of the sucrose group. In the fourth 20% of the OML, this gradient is also evident, although the sucrose group neither condenses as much dorsally nor clears as much ventrally as in the more proximal fifths. The alcohol group, however, fails to condense as much dorsally and clear as much ventrally as the sucrose group. In the distalmost 20%, this pattern is again repeated. Here the alcohol group shows hardly any difference between ipsi- and contralateral density in the ventral 6 levels, although the sucrose group changes are smaller as well. These results indicate the alcohol group is impaired relative to the sucrose group in its response to partial deafferentation, both in the deafferented zone (OML) and outside it (C/A). In addition, they describe heretofore unrecognized dorsal-ventral and proximo-distal gradients in the response of normal animals.



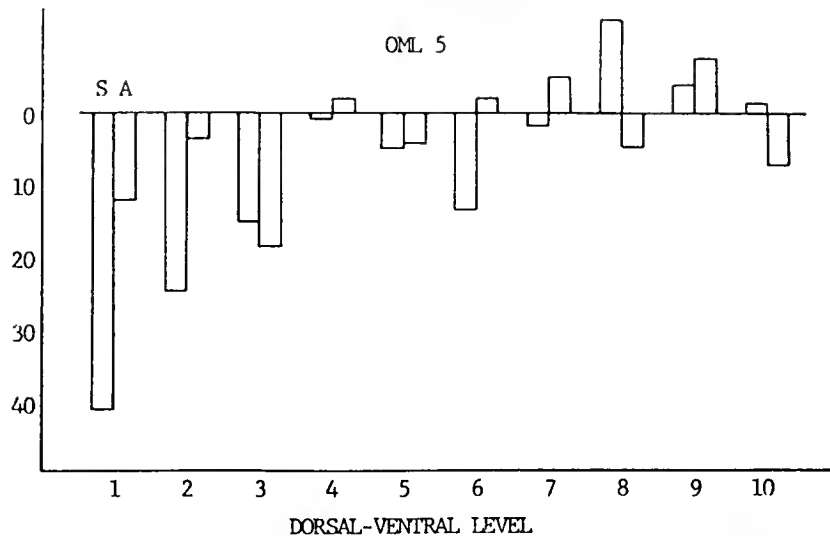
Abscissa, ipsilateral minus contralateral normalized AChE intensity; positive bars indicate clearing of AChE and vice versa.

Figure 54: Buried Blade AChE OML Band Stain Intensity Responses to Entorhinal Lesions by D-V Levels



Abscissa, ipsilateral minus contralateral normalized AChE intensity; positive bars indicate clearing of AChE and vice versa.

Figure 55: Buried Blade AChE OML Band Stain Intensity Responses to Entorhinal Lesions by D-V Levels



Abscissa, ipsilateral minus contralateral normalized AChE intensity; positive bars indicate clearing of AChE and vice versa.

Figure 56: Buried Blade AChE OML Band Stain Intensity Responses to Entorhinal Lesions by D-V Levels

Exposed Blade AChE Widths.

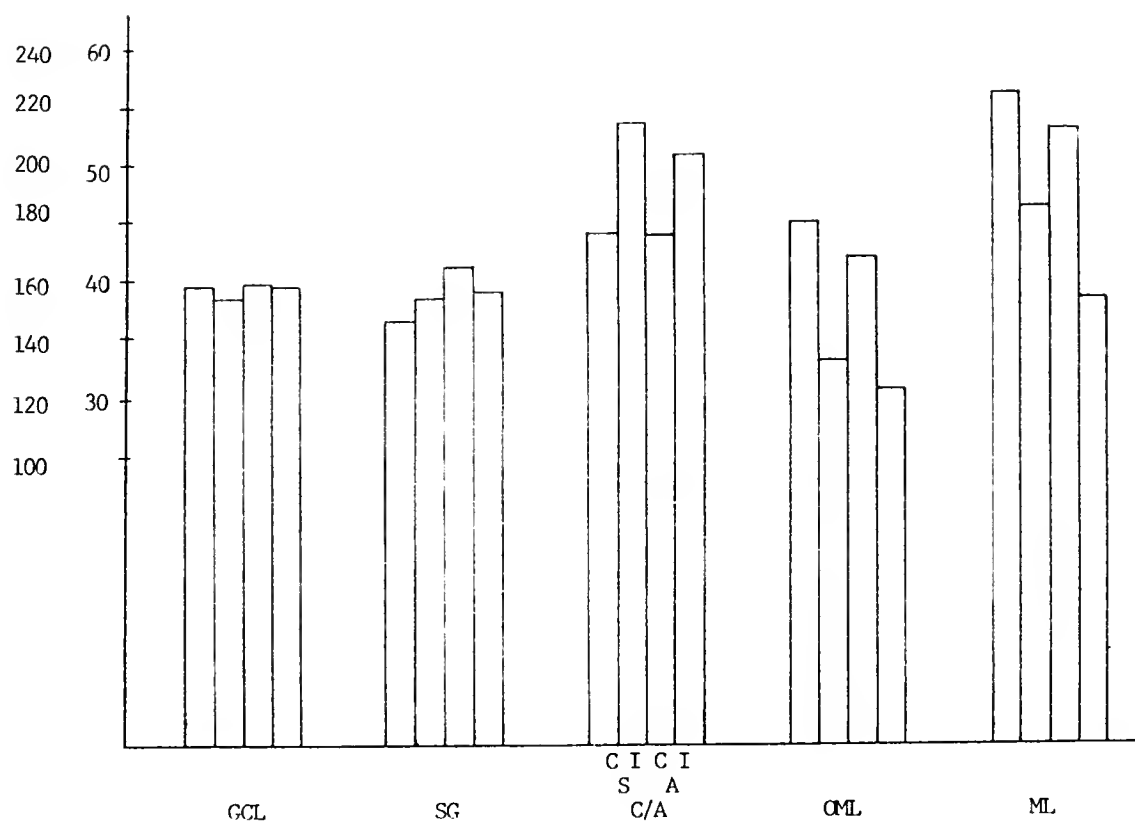
In the exposed blade, lesioning resulted in a total ML shrinkage of about 62 microns, or 26%, in the sucrose group (figure 57). In the alcohol group these values are 63 microns and 27%. As in the buried blade, a uniform shrinkage was seen across D-V levels, with somewhat more shrinkage at the most dorsal levels (figure 58). Differences in ipsilateral molecular layer width were largely accounted for by contralateral differences between groups. Also as in the buried blade, no differences in granule cell layer or supragranular band widths were observed. C/A expansion in the exposed blade was greater for both groups, even with a relatively smaller lesion: 6.0

microns in the control animals, compared with 3.7 microns in the alcohol animals. This corresponds to an increase of 13.1% and 8.0% increase over contralateral C/A widths in sucrose and alcohol groups, respectively. Over the 10 D-V levels, considerable variability can be seen in the amount of C/A expansion that occurred (figure 59) in both groups.

These differences in sprouting are further emphasized by the fact that although the alcohol group showed nearly the identical amount of ML shrinkage as the sucrose group, they still showed 38% less C/A expansion. This tends to negate the possibility that the buried blade results were explainable by the fact that the alcohol group merely had larger lesions. Either the alcohol group is less capable of executing the same amount of C/A expansion as the sucrose group for a given deafferentation, or they have less reactive C/A expansion because they were less deafferented, in which case they exhibit less reinnervation of the OML by the contralateral entorhinal cortex than the sucrose group does for a larger lesion. This could show up in equivalent amounts of ML "shrinkage", which is in fact the final sum of both shrinkage and the crossed entorhinal sprouting.

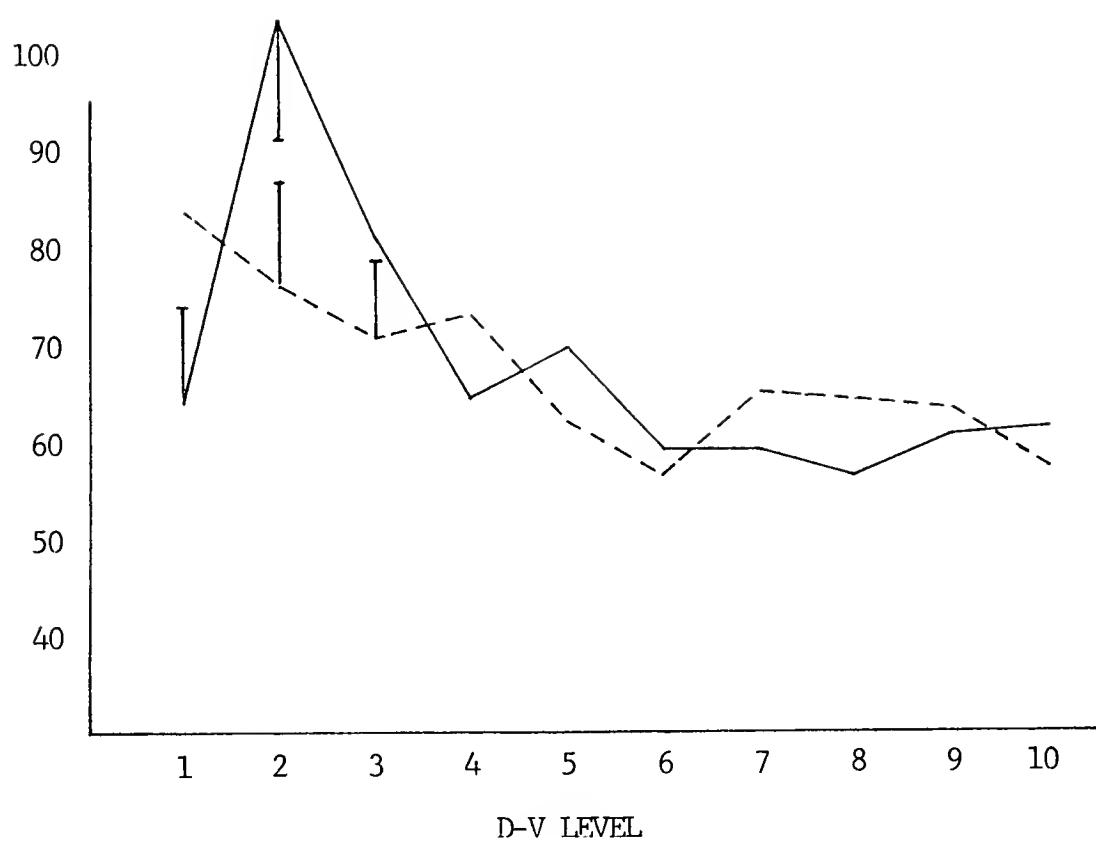
Exposed Blade AChE Stain Intensity.

The alcohol group showed a slight decrease in AChE staining in the granule cell layer ipsilateral to the lesion (figure 60), with more D-V variability than the sucrose group (figure 61). Similar changes appeared in the supragranular



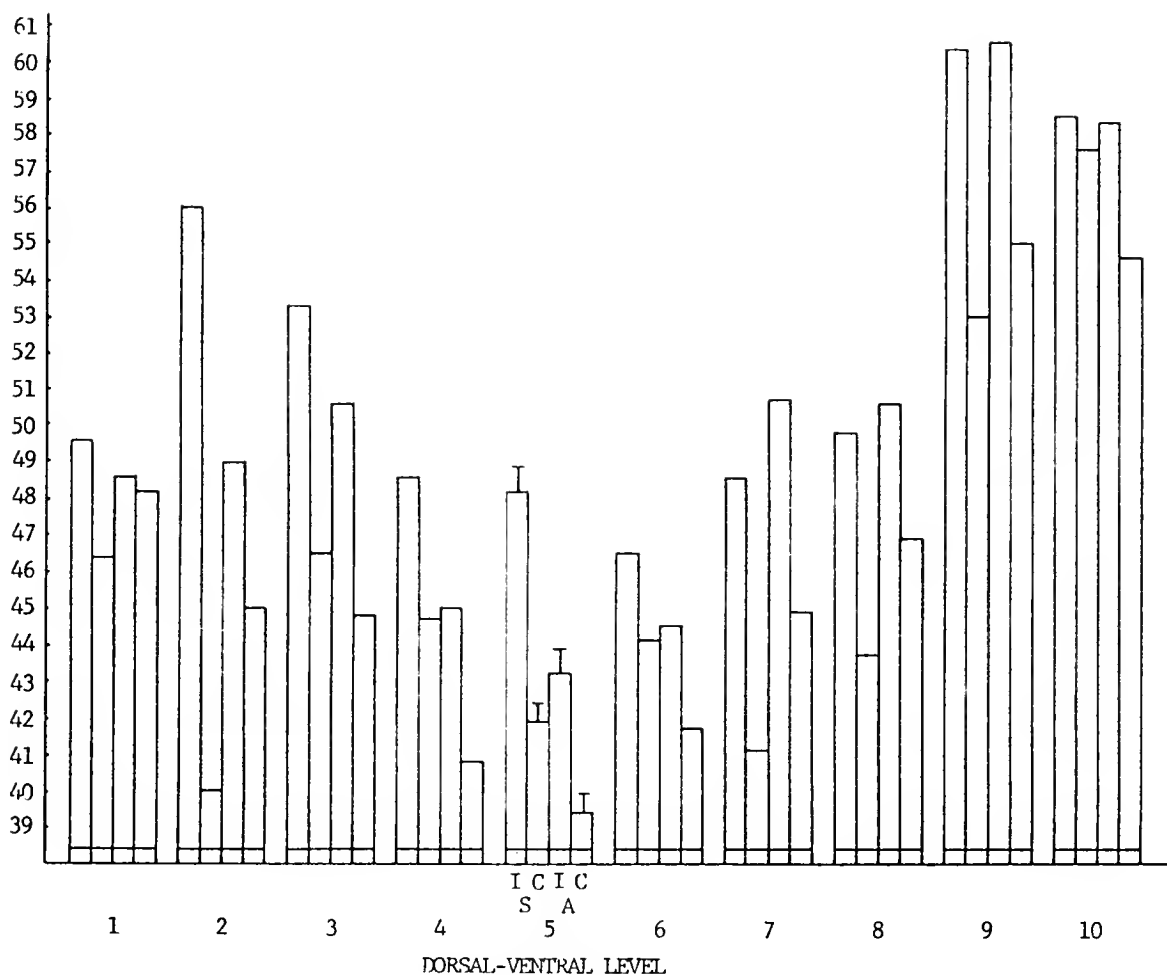
Abscissa, ipsilateral and contralateral AChE stain band group mean widths, in micrometers. C=contralateral, I=ipsilateral; S=sucrose, A=alcohol groups.

Figure 57: Exposed Blade AChE Band Width Responses to Entorhinal Lesions



Abscissa, contralateral minus ipsilateral OML width in micrometers. Dashed line, alcohol group.

Figure 58: Exposed Blade OML Shrinkage in Response to Entorhinal Lesion, by D-V Level

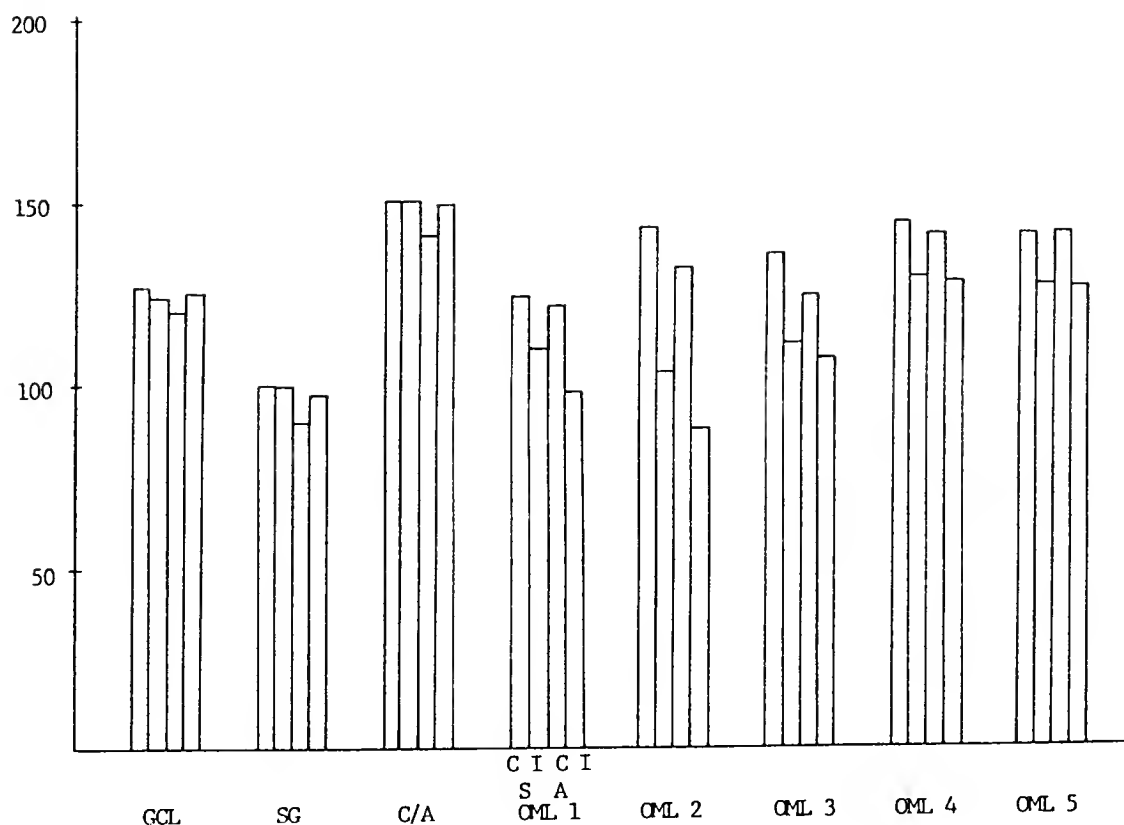


Abscissa, ipsilateral and contralateral AChE C/A stain band group mean widths, in micrometers. C=contralateral, I=ipsilateral; S=sucrose, A=alcohol groups.

Figure 59: Exposed Blade AChE C/A Band Width Responses to Entorhinal Lesions, by D-V Levels

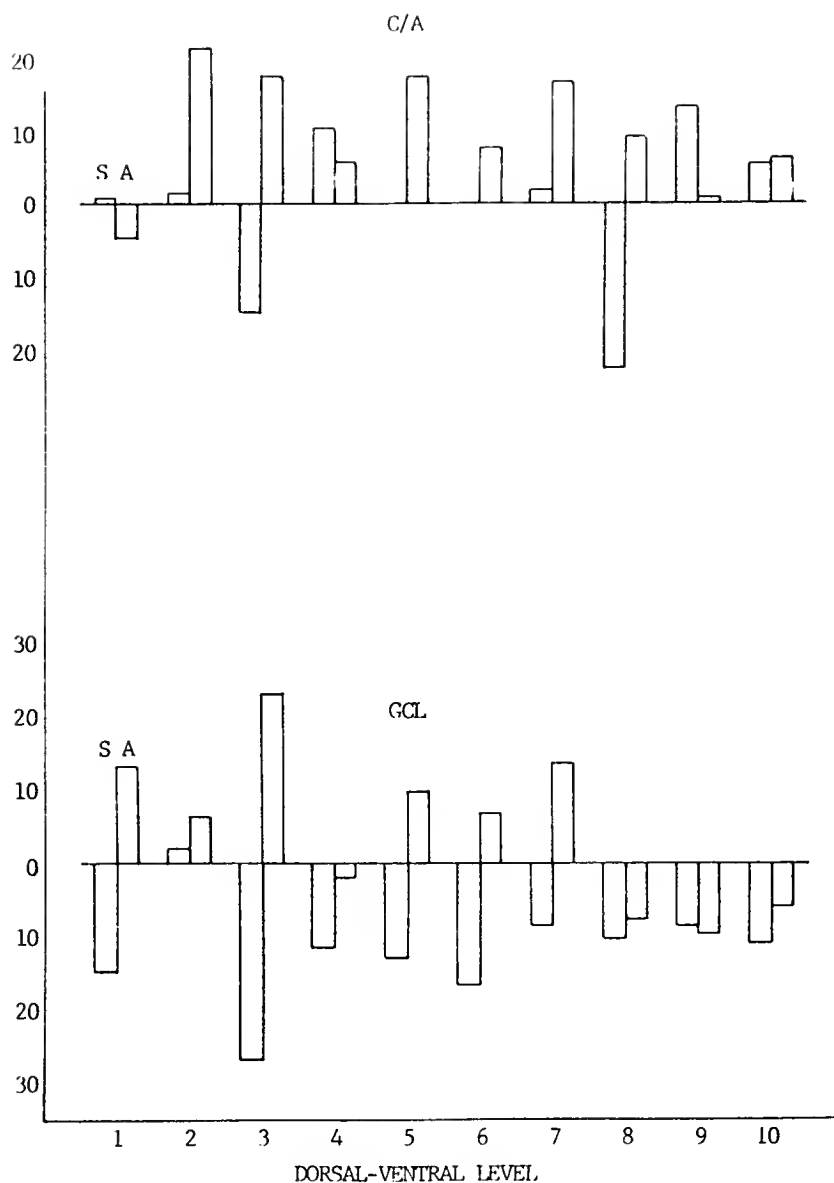
band. In the C/A band, the sucrose group showed variable clearing across D-V levels (figure 61). The alcohol group, in contrast, demonstrated more clearing in the exposed blade than either group in either blade. As in the buried blade, however, if the ipsilateral densities are corrected to the contralateral GCL values, subtracting out the GCL density difference within groups from the C/A data, then the alcohol group exhibits less clearing than the sucrose group at all but three D-V levels (figure 62), and actually shows negative clearing at one level. However, we are not convinced that this correction is entirely valid, as it does not improve the correspondence between sprouting and clearing at any particular D-V level, and necessitates extracting what may be a real effect in the GCL and SG bands.

In the outer molecular layer, in contrast to the buried blade, an increase in AChE intensity is evident in all 20% proximo-distal intervals, at nearly all D-V levels (figures 63, 64, 65). Condensation is more pronounced in the proximal 40% than the distal 60%, and the differences between groups are largely accounted for by the contralateral density differences: the amount of condensation is roughly equivalent at all D-V levels. Unlike the inner 40% in the buried blade, the alcohol group densities ipsilateral to the lesion are higher (darker) than the sucrose group. Distally, both groups tend to reach



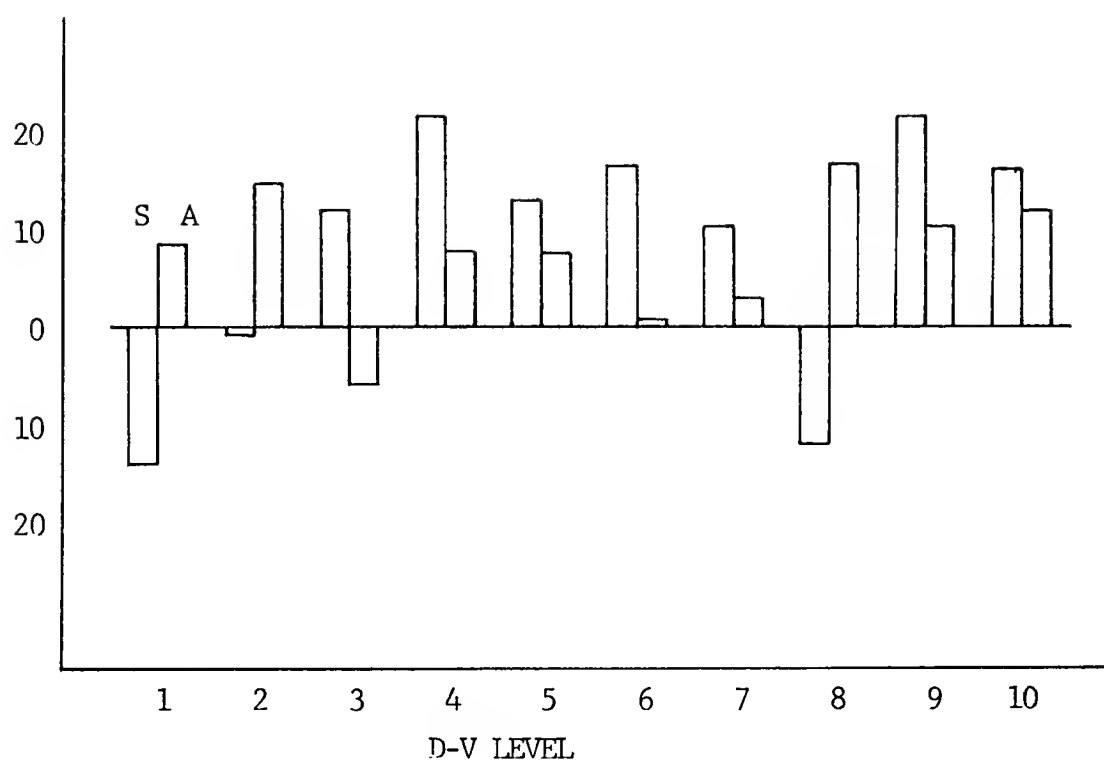
Abscissa, ipsilateral and contralateral normalized AChE stain intensity. C=contralateral, I=ipsilateral; S=sucrose, A=alcohol groups.

Figure 60: Exposed Blade AChE Stain Intensity Responses to Entorhinal Lesions



Abscissa, ipsilateral minus contralateral AChE stain intensity. S=sucrose, A=alcohol group.

Figure 61: Exposed Blade AChE C/A Band Stain Intensity Responses to Entorhinal Lesions, by D-V Levels



Abscissa, ipsilateral minus contralateral AChE stain intensity, normalized and corrected for GCL response. S=sucrose, A=alcohol groups.

Figure 62: Exposed Blade AChE C/A Band Stain Intensity Responses

nearly equivalent densities. In the ventral dentate, where in the buried blade the sucrose group showed clearing of AChE in the distal OML bands, this clearing only occurs at the ventralmost two levels. The alcohol group fails to match this clearing, and becomes more AChE dense at almost all D-V levels in OML3-5.

Discussion

As summarized in Tables 4, 5, and 6, several main findings can be described. First, long-term ethanol consumption appears to increase Timm's staining in the exposed blade of the dentate gyrus of rats, while decreasing Timm's staining in all 3 buried blade bands. Second, the alcohol group exhibited more AChE staining in both blades of the dentate, in all sampling bands, on the side contralateral to the deafferentation. These stain intensity effects were not accompanied by major changes in stain band width, although a small reduction of the molecular layer may have occurred. In the lesioned animals, chronic ethanol exposure appeared to result in a residual impairment in synaptic reorganization in response to entorhinal deafferentation. C/A band expansion was reduced by about 50% in the buried blade, and by about 30% in the exposed blade. AChE stain intensity changes in response to lesion did not appear grossly different between groups, but the alcohol group tended to exhibit as much (buried) or more

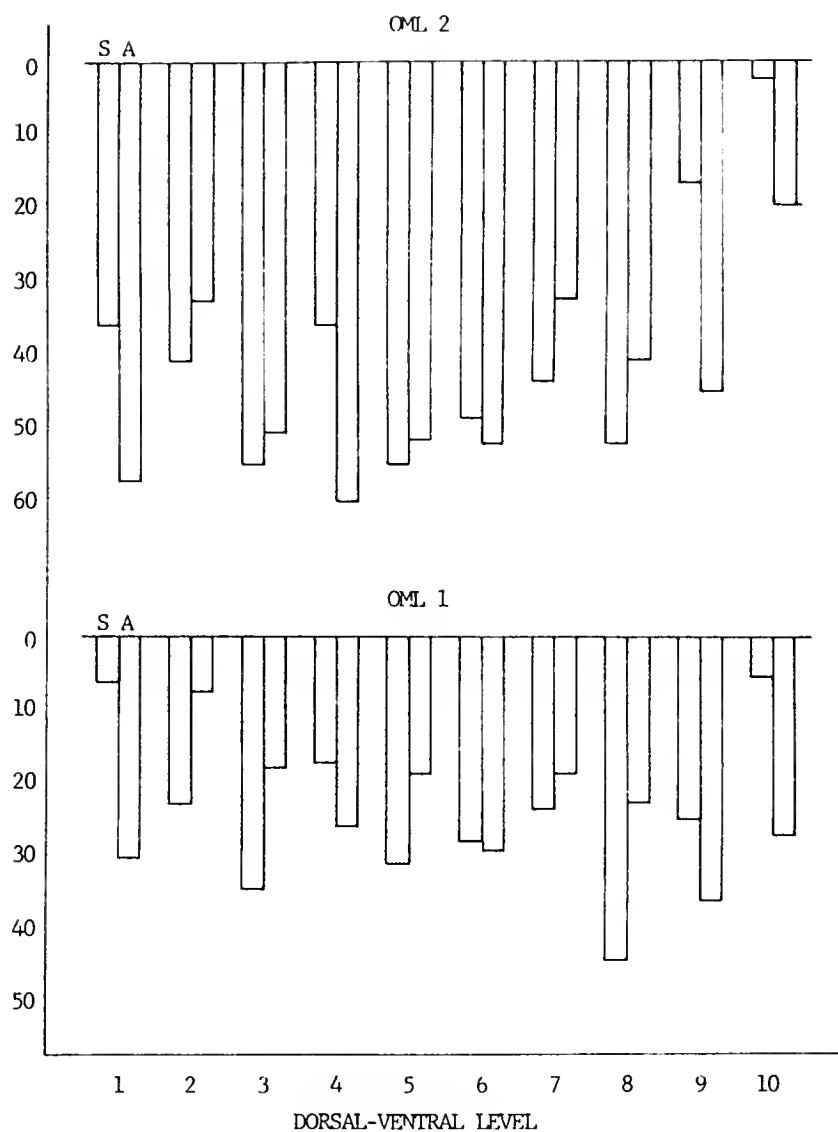


Figure 63: Exposed Blade AChE OML Band Stain Intensity Responses to Entorhinal Lesions

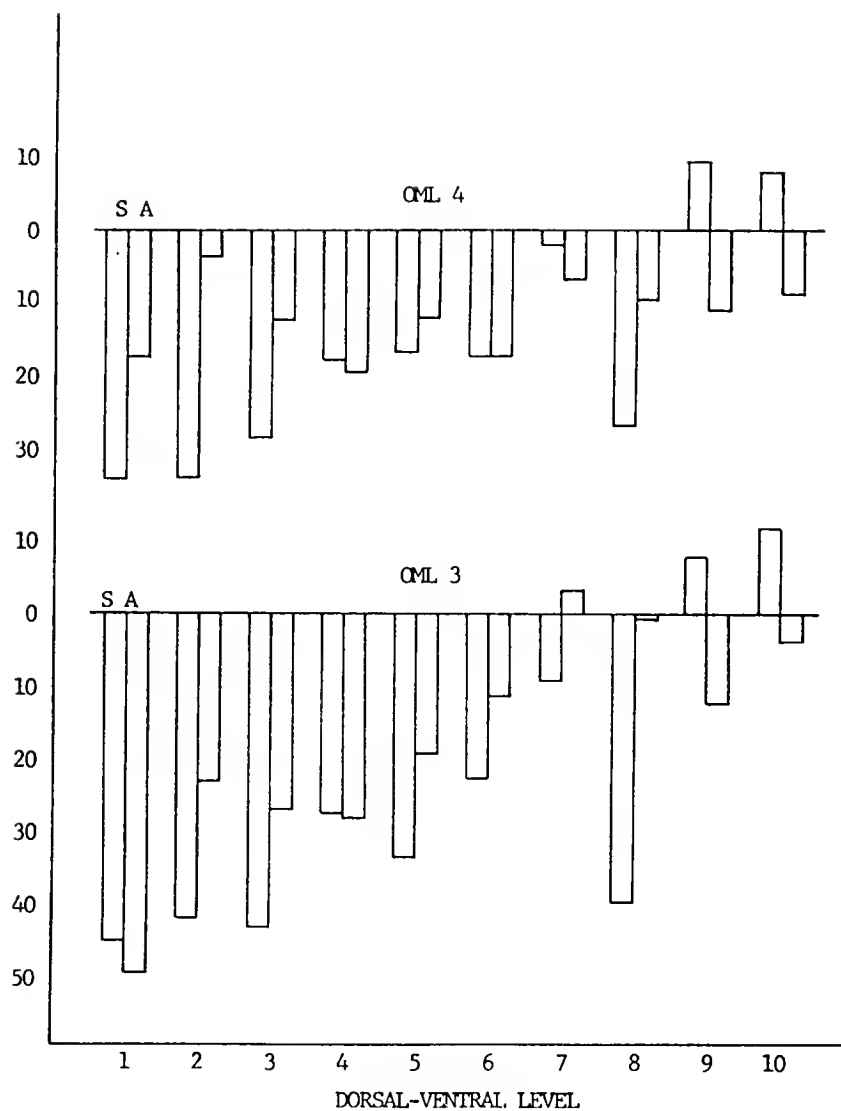


Figure 64: Exposed Blade AChE OML Band Stain Intensity Responses to Entorhinal Lesions

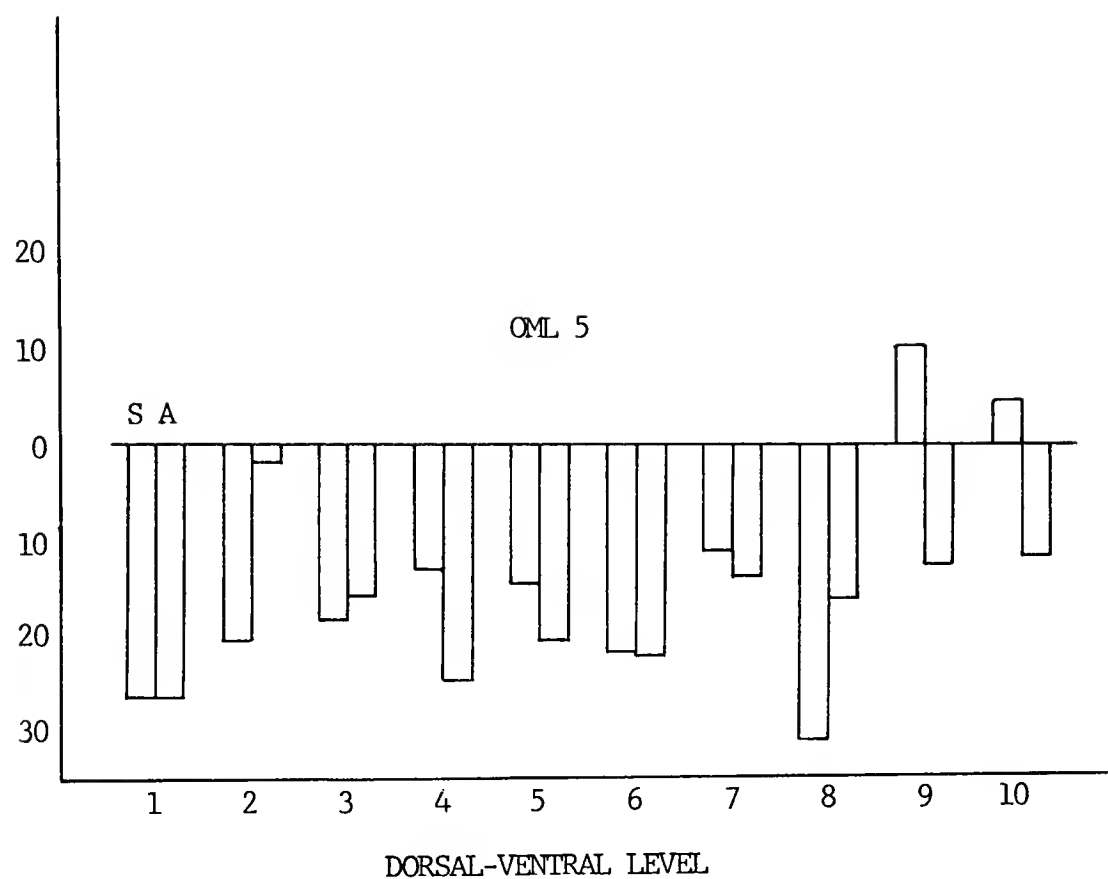


Figure 65: Exposed Blade AChE OML Band Stain Intensity Responses to Entorhinal Lesions

(exposed) C/A clearing but smaller changes in OML AChE intensity than the sucrose group. Together the lesion results indicate that 1) there is more elimination of AChE from the C/A band in alcohol animals, 2) there is less sprouting of C/A terminals in the alcohol animals, and 3) there may be less sprouting by the contralateral entorhinal cortex in alcohol animals.

Chronic Ethanol Consumption and Timm's Patterns in Dentate

The Timm's pattern in the unlesioned groups indicated that ethanol treatment had little effect on the afferent band widths, except for the C/A band in the exposed blade, which was 9.2% narrower in the alcohol group. In contrast, stain intensity appeared to be markedly altered. While it is still not known what the Timm's reaction product means in physiological terms, it has been associated with presynaptic structures in the hippocampus using electron microscopy (although in the terminals of granule cells, and not their afferents (Danscher, '81)). Thus these results are consistent with the fact that with sufficiently sensitive measures, some electrophysiological effects of long-term ethanol consumption have been found in the dentate gyrus. If the ML Timm's intensity is indicative of the amount of synaptic input to the granule cells, then the Timm's intensity changes may be causally related to the shrinkage, in alcohol animals, of the OML current sink that occurs with

stimulation of entorhinal afferents (Abraham and Hunter, '82), or with the relative reduction in granule cell population action potentials recorded in response to particular stimulation current patterns (asymptotic portion of input/output function, paired pulse synaptic potentiation, frequency potentiation, and developing long-term potentiation (Abraham and Hunter, '82; Abraham et al., '84; Durand and Carlen, '84)).

If the Timm's intensity results were reversed, that is, if the exposed blade had been lighter than the buried blade, then it would have to be considered possible that some leaching of the reaction product occurred from the exposed blade during tissue processing. Since the exposed blade was found to be darker, it would appear that this is not a problem. Of course, the intensity results in both blades could be partly due to differential tissue density, or composition, such that more or less leaching occurred in one group. This possibility must be considered to be a consequence of the diet and not merely a random histological artifact.

AChE Patterns in the Contralateral Dentate Gyrus

Few investigators have attempted to measure AChE in the dentate gyrus. Several qualitative descriptions of dorsal-ventral concentration gradients have suggested that the ventral dentate stains more darkly than the dorsal (cf.

Milner et al., '84). Our measurements of stain intensity suggest that this is not the case. As Milner et al. ('84) point out, however, substantial variation in stain intensity can be observed across many D-V levels. We find that this substantiates our measurement of marked peaks and dips at particular D-V levels in both groups. In particular, a very sharp increase in AChE intensity appears to occur at level 7, (see figures 27, 33) and is accompanied by large decreases dorsally and ventrally. That this does occur in both groups suggests that this is a real anatomical feature of the ventral dentate, and not a chance fluctuation. If this is the case, then this would provide an excellent internal landmark by which to match experimental tissue sections. Such a peak of AChE intensity could have led previous investigators to the conclusion that the ventral dentate stains more darkly. Other implications may seem more odious to hippocampal physiologists, for such focal peaks and dips in AChE would mean that, among other things, transverse slices used for electrophysiological studies are not all equivalent, as they are now commonly considered, even though the septohippocampal afferents are invariably completely removed. Although most slice studies use sections more dorsal than where the ventral AChE peak occurs, the fact that our methods revealed such patterns in both groups, and both blades, argues that the smaller fluctuations that tend to occur dorsally are also real. The

assays of Storm-Mathisen ('74) support this possibility; in addition to reporting a 35% greater increase in ML AChE activity at his level 7 compared to level 5 (Table II), he shows substantial variation in the AChE activity per dry weight between levels 4 and 6 (Table III). The functional significance of such an organization is not known, but it could serve either to normalize the relative amount of ACh release to random D-V variations in septal input density, or to focus cholinergic transmitter effects into, perhaps, some unit of organization analogous to the proposed hippocampal lamellae. This could in fact provide an effective means for increasing the relative synaptic specificity over that attained by the spatial targeting of actual synapses. An alternative explanation for the peaks may be that the cholinergic axons enter the dentate from the fimbria collectively at particular locations (cf. Milner et al., '84).

The alcohol group exhibited more AChE staining than the sucrose group, on the unlesioned side. As pointed out in the Results, there are two possible reasons for this. Either there is a real increase in AChE, or the apparent increase is due to some histological difference between groups that changes the background color of the stained tissue where there is no AChE. Since the group differences vary across the sampling bands (greater in the C/A than the GCL, SG, and OML), it must be considered more likely that

alcohol treatment produced a reorganization of the cholinergic input to the dentate. The recovery experiment spine density data support not only the notion that there could be an increased synaptic density of cholinergic input to the dentate, but that it could show the proximo-distal gradient shown by the AChE intensity difference. A finer appreciation for the actual magnitude of this change must await the development of AChE stain density standards relating stain intensity directly to tissue AChE concentration.

The apparent increase in AChE in the alcohol group may be responsible for the increased paired-stimulus potentiation of the granule cell population action potential, in response to entorhinal afferent stimulation, as was discovered in this laboratory (Abraham and Hunter, '82). It has been reported recently that experimental paired-pulse stimulation of the septal input to the dentate can potentiate not only this pathway, but the entorhinal input as well (McNaughton and Miller, '84). If there is indeed a proliferation of cholinergic septal terminals in the dentate, then this potentiation might be enhanced in ethanol-treated animals. This might be easily tested by comparing the relative potentiation enhancement of the commissural hilar afferents to that of the entorhinal pathway, within alcohol-treated animals.

Inhibited Reactive Synaptogenesis in Alcohol Animals

For the lesion experiment, there are some precedents for comparison. The results of Jim West's laboratory at the University of Iowa are similar to our own. They found that 2 weeks of ethanol before and 9 days following entorhinal lesion led to a more pronounced inhibition of C/A sprouting. Their sample, however, consisted of a single coronal section of the dorsal dentate gyrus, which may contribute to the difference in results. The most probable cause for different results, however, is that our animals were exposed to alcohol only prior to lesioning, for a much longer duration, and with an interposed interval without alcohol exposure. Thus the present study should be a better indication of residual alcohol effects.

The West et al. ('82) measurements of AChE stain bands in normal and lesioned control sides are also worth comparing to our own, even though their measurements were made in coronal material. They report a control group supragranule layer width that is less than what we measured in horizontal sections (25.1 ± 0.57 v. our 42.9 ± 1.1). In reacting to ECX, it shrinks to $22.8 \pm .7$ microns, while ours shrinks less than 2 microns averaged over 10 D-V measurement locations. The outer zone of their report corresponds to our definition of the outer molecular layer (OML), and their width values of 135.8 ± 2.2 to 140.1 ± 1.7 (left v. right) is similar to our value of 153.3 ± 3.8 , in the horizontally sectioned tissue. Lesion is followed by shrinkage to

82.8 \pm 2.2 to 88.0 \pm 1.7, while we found that the OML in horizontal sections averaged 123.7 \pm 2.8 on the lesioned side. Our ML shrinkage values are also corroborated by Scheff et al., ('80b), who find 14.6% shrinkage after more extensive lesions including the parasubiculum, which was avoided in this experiment.

In contrast to long prelesion exposure to alcohol, the 2 week plus 9 day ethanol exposure of West et al. ('82) did not lead to decreased widths in the dentate molecular layer. The ethanol exposure group also showed less outer zone shrinkage after lesions, in the animals of West et al. ('82). In contrast, our alcohol group had slightly less buried blade OML shrinkage than the sucrose controls, yet we still find an inhibition of C/A sprouting. Although the values for C/A expansion reported here are smaller than those found by other investigators, this is probably attributable to the greater age of the animals in this study at the time of lesion. Declines in both the rate (McWilliams and Lynch, '83) and amount (Scheff et al., '80b) of reative synaptogenesis during adulthood have recently been documented, and since these animals were over 9 months old when lesioned, it is not surprising that they demonstrated less sprouting than the younger animals used in many previous studies (cf. Cotman et al., '81).

Lesion-induced AChE Intensity Changes

The results we describe for the AChE material of control animals are consistent with those previously reported (Storm-Mathisen, '74; West et al., 82). Storm-Mathisen reported a 50-60% increase in AChE activity per tissue volume or weight, in carefully dissected ML sections. This increase was reported to be localized to the deafferented zone, where we measured an increased AChE optical density. Storm-Mathisen ('70) has also correlated the actual tissue levels of AChE with the relative staining intensity. It is possible, then, to infer that changes and group differences in AChE stain intensity represent real effects on concentrations of the enzyme. Since transecting the primary pathway from the septum to the hippocampus prevented the AChE changes following entorhinal lesions, synaptic reorganization among the at-least-partly cholinergic septohippocampal afferents would apparently explain the changes in both AChE and the synthetic enzyme for acetylcholine (choline acetyltransferase, ChAc, Storm-Mathisen, '74). The impaired response in the alcohol group implies that the septohippocampal projection may have been damaged by prior ethanol exposure and not able to execute normal reorganization patterns. This is supported by the increased AChE intensity in the alcohol animals on the contralateral side. If the septohippocampal fibers have already been induced to reorganize by ethanol treatment,

they may be less able to subsequently reorganize in response to entorhinal deafferentation. For example, the increased AChE in the C/A band on the contralateral side in alcohol animals may mean that the C/A terminals that sprout ipsilateral to the lesion have more difficulty displacing the cholinergic terminals because of their sheer numbers. They may accomplish the displacement within the original C/A band, as indicated by the AChE clearing response, but then be unable to extend as far into the deafferented zone as normal animals.

Because of the evidence linking pathology of cholinergic systems in the CNS with memory disorders (e.g., Henke and Lang, '83), with ethanol exposure (Nordberg et al., '82), and the memory disorders that are observed in chronic alcoholics, our results suggest that long-term exposure to ethanol may lead to memory dysfunctions in part via damage to cholinergic systems. However, since sprouting was inhibited in the alcohol group in the C/A zone, non-cholinergic systems may be equally affected. Alternatively, cholinergic, or perhaps even noncholinergic, septohippocampal afferents could normally play a facilitative role in the synaptic reorganization of the commissural and associational terminal field. In this case, ethanol-related damage to septohippocampal afferents might compromise the sprouting of hilar afferents more indirectly.

The pattern of AChE reorganization in the OML ipsilateral to the lesion has never been quantitatively described in as much detail. While the proximal OML condensation of AChE is characteristic of the dentate response to entorhinal deafferentation, the dorsal-ventral gradient of the changes in AChE intensity are much more subtle. The diminished condensation at temporal levels, described above for the outer 40% of the OML, may reflect simply that a less effective deafferentation occurred more ventrally. This is consistent with the graphs of OML shrinkage over D-V levels. Alternatively, since there are D-V gradients in the AChE intensity on the control side, it is possible that the synaptic reorganization is different in the ventral dentate than the classically described dorsal patterns.

Buried and Exposed Blade Differences Before and After Lesions

The differential Timm's stain response in unlesioned animals may appear suspicious. In fact, Irle and Markowitz ('83) who identified a progression of granule cell loss over long term ethanol exposure, report that the exposed blade loses neurons earlier and more dramatically than the buried blade. Thus the Timm's phenomenon may reflect a preferential susceptibility of the exposed blade to neurotoxic alcohol effects. This is in keeping with a long tradition of neuropathologists who noted the proximity of CNS pathology in alcoholics to the cerebrospinal fluid

spaces (Victor et al., '71). Since the exposed blade is suspended in the cisternal space, it may be one of the more sensitive structures. There are other grounds for accepting that differences exist between buried and exposed blades; different afferent connection patterns (vide supra) have been described, and a gradient in granule cell neurogenesis from the buried crest to the exposed crest have been found (Bayer, '80). Furthermore, substantial blade differences in both magnitude and direction of several electrophysiological variables have been described in sucrose control animals in previous experiments from this laboratory (Abraham and Hunter, '82), and the effects of chronic ethanol on these variables show blade differences as well. Blade differences in the innervation of the dentate by cholinergic axons have also been reported (Milner et al., '84; see also Chen et al., '83), and may account for the differences in AChE intensity responses described above.

The developmental gradient from buried to exposed blade may also explain some of the different alcohol and lesion effects. The absolute expansion of the C/A band was much larger in the exposed blade. A developmental continuum for C/A expansion has been described such that more is observed in young animals than in adults (Cotman et al., '73). Thus, if the buried blade is developmentally older than the exposed blade, sucrose animals might be expected to show more sprouting in the exposed blade. If ethanol treatment

were to augment the developmental trend toward less sprouting (vide infra), the effect could conceivably be more pronounced on a relatively older region like the buried blade than on the more developmentally recent exposed blade. This could extend the conclusions about the effects of chronic ethanol to encompass effects associated with aging.

Possible Mechanisms of Long-term Ethanol Effects

The results indicating a decreased synaptic reorganization in alcohol animals argue against the idea that alcohol may serve as a "priming" lesion, whereby those metabolic processes required for reactive synaptogenesis are preactivated by small lesions preceding extensive lesions (vide supra). Perhaps this is not surprising, given all the adverse metabolic effects of chronic ethanol consumption, and since even a single dose of ethanol has been shown to potentiate CNS trauma (Flamm et al., '77). However, this conclusion should not imply that synaptic reorganization is not induced by long-term ethanol exposure, that the priming does not occur because no priming lesion occurred. The data on spine density, the unlesioned group Timm's band intensities, and the contralateral side AChE intensities all suggest the opposite.

Several known effects of chronic ethanol consumption could contribute to the diminished synaptic reorganization we describe in our alcohol group. There are several

indications that protein synthetic ability in the CNS is reduced by long-term ethanol consumption (Tewari and Noble, '71; Earvin, '84). Since during the reorganization process there is an apparent increase, in normal animals, of protein precursor incorporation (Fass and Steward, '83), and a mobilization of polyribosomes to intradendritic locations proximal to the formation of new synapses (Steward, '83), impaired protein synthesis in animals exposed to ethanol could explain their failure to complete the same reorganization as controls. Of course, peptides and proteins serve a multitude of functions, and the metabolism of specific proteins following ethanol exposure may vary. One class of particular importance for reactive synaptogenesis is formed specifically in response to CNS injury, and has trophic properties that may facilitate reactive synaptogenesis (Gage et al., '84; Longo et al., '84). The effects of long-term ethanol exposure on the formation of these neuronotrophic peptides is unknown, but whether ethanol decreases protein synthesis selectively or indiscriminately, they may well be decreased.

In many human alcoholics, disordered adrenocorticosteroid regulation is prominent (Abou-Saleh et al., '84; Bertello et al., '82; De La Fuente et al., '83; Kahn et al., '84). The glucocorticoids tend to be more abnormal. While a large degree of variation in individual effects is observed clinically, elevated circulating concentrations, abnormal

rhythmicity of release patterns, and failure to suppress ACTH in response to dexamethasone challenge are commonly reported. The first two have been shown directly to inhibit dentate reactive synaptogenesis (DeKosky et al., '84; Scheff and Cotman, '82; Scheff et al., '80), and the last will most probably lead to either or both of the first. As aged animals exhibit both increased steroid levels and decreased dentate reactive synaptogenesis (Cotman et al., '73), it appears that chronic ethanol exposure may push the animal farther along some developmental continuum of reactive ability in the manner of a premature aging, via disturbances in adrenal steroid systems. Whether this can totally explain the effect of alcohol or not, it is likely that the effects of chronic ethanol exposure on dentate reactive synaptogenesis are related to abnormalities in glucocorticoid metabolism.

Experimental Considerations

The collection of a large number of samples may have actually compromised the statistical resolving power of our experimental design. During the early stages of data collection, we observed an unusual pattern of variation in molecular layer width (King et al., in press). If the molecular layer width does indeed fluctuate about an average width, in both the transverse and longitudinal dimensions, then when two molecular layers are compared at many points a

larger degree of variability is bound to emerge than when the longitudinal variations are eliminated by sampling one of a few closely spaced sections. Consistent with this idea are the dorsal-ventral gradients in the ipsilateral response patterns in the AChE material, significant differences at particular points or D-V levels in our sample, and the larger standard errors of measurement we find compared to West et al., ('82), who used the same image analysis hardware (although a very different approach to band delimitation).

CHAPTER IV GENERAL DISCUSSION

The experiments described above were undertaken to investigate two phenomena important for the clinical treatment of human alcoholics, as well as for understanding the basic neurobiology of alcoholism, brain damage (in general and that specific to alcohol abuse), and brain/behavior relationships. Recovery refers to the capacity of the CNS to revert to, or toward, normal cellular and tissue morphology following the chronic neurotoxic insult engendered by long-term alcohol consumption. Here, recovery specifically refers to the return of altered hippocampal dendritic spine densities toward control animal values during the post-exposure period. Recoverability, in the broad sense, is the ability of CNS tissue to execute restorative mechanisms in response to more acute forms of injury to the brain, as in stroke or head trauma of accidental origin. In the context of the present experiment, it refers to the capacity for reactive synaptogenesis in the dentate gyrus in response to entorhinal deafferentation.

Spine Density Recovery, but Inhibited Reactive
Synaptogenesis?

If alcohol-treated animals can indeed recover the density of dendritic spines, why can they not exhibit normal reactive synaptogenesis within the same neuronal populations? One obvious possibility is the cell loss that occurs with this duration of exposure. Since the hilar neurons are the source of the new axon terminals that expand the C/A band into the deafferented zone, the 15% decrease in the number of hilar neurons in animals treated with ethanol for 20 weeks would require that surviving neurons each produce more than the normal quantity of new terminals if the same amount of C/A expansion is to occur. This may simply be too much to ask of a neuron that has only had 8 weeks to recover from alcohol exposure, since spine density recovery may not be complete even 20 weeks post-exposure.

Another possibility is that, if the entorhinal cortex loses the same proportion of neurons as the hippocampus, after 20 weeks of alcohol treatment, the metabolic signal(s) that initiate reactive synaptogenesis may be correspondingly weaker: fewer afferent fibers are destroyed in alcohol animals. Along these lines, if ethanol treatment, as indicated by electrophysiological experiments from this laboratory (Abraham and Hunter, '82), produces a partial loss of entorhinal input to the dentate, even after 8 weeks or more post-treatment, then reactive synaptogenesis may already in progress when the lesion is made. An additional

initiation signal may not have the same relative metabolic force, in alcohol animals, as the lesion produces in controls. Since granule cells are also reduced in density by about 20%, if the putative sprouting initiation signal requires synaptic relay from granule (deafferented) to hilus (sprouting) neurons, transmission of this signal might be compromised by this loss as well.

Third, the lesion experiment does not reveal anything about the dendritic spine density on the granule cells. Since spine density recovery was only measured at one post-treatment time point, it is possible that this recovery is only transient, or occurs after the 8 week post-diet duration allowed before the entorhinal lesions were performed. Perhaps with a longer pre-lesion interval, the alcohol group would exhibit better sprouting. Furthermore, it is not known, in normal animals, whether spines are extended in search of new afferent terminals, or in response to their proximity. If the critical structure for establishing synaptic contacts in the reorganizing molecular layer is the presynaptic terminal, a normal complement of spines may be irrelevant.

It is recognized in normal animals that deafferenting the OML by entorhinal lesion induces a synaptic turnover in the ipsilateral C/A zone, which is not deafferented by the lesion. In young, but not old animals, a cycle of synaptic turnover is induced in the contralateral C/A zone as well

(Hoff et al., '81). This raises the possibility that the ipsilateral C/A zone of the alcohol animals fails to undergo synaptic turnover for reasons similar to the failure of the contralateral C/A turnover in old animals. While these are only speculative, they include the idea that connection patterns in the CNS become more rigid during aging because of synaptic stabilization, tissue density changes, and metabolic slowdown. This seems like a promising area for future investigation.

It is important to realize that punctate trauma to the CNS often produces different response patterns, and endpoints, compared to equivalent damage that occurs over a long time (Finger and Stein, '82). The meningeal, vascular, and histological insult of an electrolytic lesion, and the immediate and total disruption of electrical circuitry, make the recoverability experiment damage much different than pathology resulting from the long, slow, steady application of a neurotoxic substance. It must be considered likely that spine density recovery proceeds in part because the entire anatomical system, even with some cell loss, is intact, and reorganization of normally occurring pathways is all that is demanded of the system. In contrast, the entorhinal deafferentation must be considered a major insult to the hippocampal system, and requires that new patterns of connectivity be generated. Seen in this light, the impaired recoverability of the dentate in alcohol animals, even when

they can recover from simple alcohol-related alterations, may not be so surprising. Reactive synaptogenesis might simply be a more demanding test of the regenerative ability of neurons exposed to ethanol.

It has been shown here that at least some neurons of the mammalian CNS appear to possess some ability to recover from the neurotoxic effects of chronic alcohol exposure, but that the ability of brain tissue to respond to punctate injury is compromised in alcohol-treated animals. These findings raise new questions about the mechanisms underlying recoverability and recovery in the central nervous system. Are recovery and recoverability really two different properties, or do they each reflect some basic capacity of nervous tissue to respond to physiological demands? How is the failure to complete spine density recovery related to the decreased synaptic reorganization in alcohol-treated animals in response to deafferenting lesions? What role do steroid hormones play in these processes, and should human alcoholic patients be prescribed therapeutic steroids more cautiously than the non-alcoholic population? Might there be ways to modify alcoholic beverages to ameliorate some of the negative effects?

In addition to demonstrating the effects of alcohol exposure on operationally defined paradigms of recovery and recoverability, these experiments have added significantly to the large body of information on the anatomy of the

hippocampal formation, a structure of great interest to many neuroscientists and psychobiologists the world over. The quantitative anatomical descriptions of AChE and Timm's stain patterns, never performed on this scale, will be useful to many researchers in years to come. The techniques for quantifying dentate reactive synaptogenesis will benefit the many investigators who use this phenomenon as a model for recovery from brain injury, and establish the utility of the constellation of measurable dependent variables. The spine count data, molecular layer afferent terminal field morphological descriptions, and molecular layer cell type information that have been collected in the course of these studies will be important to those who are building mathematical models of hippocampal function. Thus, not only have these experiments made important contributions to alcohol research, they have provided knowledge about more basic neuroscience questions as well.

REFERENCES

- Abou-Saleh, M.T., Merry, J., Coppen, A.: Dexamethasone suppression test in alcoholism. *Acta Psychiat. Scand.*, 69: 112-116, 1984.
- Abraham, W.C., Hunter, B.E.: An electrophysiological analysis of chronic ethanol neurotoxicity in the dentate gyrus: Distribution of entorhinal afferents. *Exp. Brain Res.*, 47: 61-68, 1982.
- Abraham, W.C., Hunter, B.E., Zornetzer, S.F., Walker, D.W.: Augmentation of short-term plasticity in CA1 of rat hippocampus after chronic ethanol treatment. *Brain Res.*, 221: 271-287, 1981.
- Abraham, W.C., Manis, P.B., Hunter, B.E., Zornetzer, S.F., Walker, D.W.: Synaptic distribution in stratum radiatum of CA1 after chronic ethanol treatment. *Brain Res.*, 237: 91-105, 1982.
- Abraham, W.C., Rogers, C.J., Hunter, B.E.: Chronic ethanol-induced decreases in the response of dentate granule cells to perforant path input in the rat. *Exp. Brain Res.*, 54: 406-414, 1984.
- Abraham, W.C., McNaughton, N.: Differences in synaptic transmission between medial and lateral components of the perforant path. *Brain Res.*, 303: 251-260, 1984.
- Alling, C., Bostrom, K.: Demyelination of the mammillary bodies in alcoholism. *Acta Neuropath. (Berlin)*, 50: 77-80, 1980.
- Alling, C., Balldin, J., Bostrom, K., Gottfries, C.G., Karlsson, I., Langstrom, G.: Studies on duration of a late recovery period after chronic abuse of ethanol. A cross sectional study of biochemical and psychiatric indicators. *Acta Psychiat. Scand.*, 66: 384-397, 1982.
- Amaral, D.G.: A Golgi study of cell types in the hilar region of the hippocampus in the rat. *J. Comp. Neurol.*, 182: 851-914, 1978.

- Amaral, C.G., Avendano, G., Cowan, W. M.: The effects of neonatal 6-hydroxydopamine treatment on morphological plasticity in the dentate gyrus of the rat following entorhinal lesions. *J. Comp. Neurol.*, 194: 171-191, 1980.
- Avdaloff, W.: Alcohol, seizures, and cerebral atrophy. *Adv. Biol. Psychiat.*, 3: 20-32, 1979.
- Avendano, C.: Suppression of reactive glial proliferation in the denervated dentate gyrus of the rat: Effects on the pattern of acetylcholinesterase staining in the molecular layer. *Brain Res.*, 265: 160-162, 1983.
- Baisden, R.M., Woodruff, M.L., Hoover, D.B.: Cholinergic and non-cholinergic septo-hippocampal projections: A double-label horseradish peroxidase-acetylcholinesterase study in the rabbit. *Brain Res.*, 290: 146-151, 1984.
- Barnes, C.A., McNaughton, B.L.: Physiological compensation for loss of afferent synapses in rat hippocampal granule cells during senescence. *J. Physiol.*, 309: 473-485, 1980.
- Baudry, M., Lynch, G.: Hypothesis regarding the cellular mechanisms responsible for long-term synaptic potentiation in the hippocampus. *Exp. Neurol.*, 68: 202-204, 1980.
- Bayer, S.: Development of the hippocampal region in the rat--I. Neurogenesis examined with 3H-thymidine autoradiography. *J. Comp. Neurol.*, 190: 87-114, 1980.
- Begleiter, H., Porjesz, B., Tenner, M.C.: Neuroradiological and neuropsychological evidence of brain deficits in chronic alcoholics. *Acta Psychiat. Scand.*, suppl. 286: 3-13, 1980.
- Berglund, M., Risberg, J.: Reversibility in alcohol dementia. *Adv. Exp. Med. Biol.*, 126: 787-796, 1980.
- Bertello, P., Agrimonti, F., Gurioli, L., Frairia, R., Fornaro, D., Angeli, A.: Circadian patterns of plasma cortisol and testosterone in chronic male alcoholics. *Alc. Clin. Exp. Res.*, 6: 475-481, 1982.
- Blackstad, T.W., Kjaerheim, A.: Special axodendritic synapses in the hippocampal cortex: Electron and light microscopic studies on the layer of the mossy fibers. *J. Comp. Neurol.*, 117: 133-159, 1961.
- Blackstad, T.W., Brink, J.H., Jeune, B.: Distribution of hippocampal mossy fibers in the rat. An experimental study with silver impregnation methods. *J. Comp. Neurol.*, 138: 433-450, 1970.

Bond, N.W., DiGuisto, E.L.: Impairment of Hebb-Williams maze performance following prolonged alcohol consumption in rats. *Pharm. Biochem. Behav.*, 5: 85-86, 1976.

Bondareff, W., Genisman, Y.: Loss of synapses in the dentate of the senescent rat. *Am. J. Anat.*, 145: 129, 1976.

Bondareff, W., Genisman, Y., Dodge, J.T.: Dendritic atrophy in the dentate gyrus of the senescent rat. *Am. J. Anat.*, 152: 321-330, 1978.

Brewer, C., Perrett, L.: Brain damage due to alcohol consumption: An air encephalographic, psychometric, and electroencephalographic study. *Br. J. Addict.*, 66: 170-182, 1971.

Bridges, J.W., Benford, D.J., Hubbard, S.A.: Mechanisms of toxic injury. *Ann. N. Y. Acad. Sci.*, 407: 42-63, 1983.

Brion, S.: Korsakoff's syndrome: Clinico-anatomic and pathophysiological considerations. In G.A. Talland, N.C. Waugh (eds.), *The Pathology of Memory*. New York: Academic Press, pp. 29-39, 1969.

Brizzee, K., Ord, J.M.: Age pigments, cell loss, and hippocampal function. *Mech. Ageing Dev.* 9: 143-162, 1979.

Buell, S., Coleman, P.: Dendritic growth in the aged human brain and failure of growth in senile dementia. *Science*, 206: 854-856, 1979.

Butters, N., Cermak, L.: Some analyses of amnesic syndromes in brain damaged patients. In R.L. Isaacson, K.H. Pribram (eds.), *The Hippocampus*, v. 2. New York: Plenum Press, 1975.

Butters, N., Cermak, L.S., Montgomery, K., Adinolfi, A.: Some comparisons of the memory and visuoperceptive deficits of chronic alcoholics, and patients with Korsakoff's disease. *Alcoholism: Clin. Exp. Res.*, 1: 73-80, 1977.

Caceres, A., Payne, M.R., Binder, L.I., Steward, O.: Immunocytochemical localization of actin and microtubule-associated protein MAP2 in dendritic spines. *Proc. Nat. Acad. Sci. USA.*, 80: 1738-1742, 1983.

Cajal, S. Ramon y: *The Structure of Ammon's Horn*. Springfield, IL: Charles Thomas, 1968.

Cala, L.A., Mastaglia, F.L.: Computerized tomography in chronic alcoholics. *Alcoholism: Clin. Exp. Res.*, 3: 283-294, 1981.

Carlen, P.L., Wilkinson, D.A.: Alcoholic brain damage and reversible deficits. *Acta Psychiat. Scand.*, suppl. 286: 103-118, 1980.

Carlen, P.L., Wortzman, G., Holgate, R.C., Wilkinson, D.A., Rankin, J.G.: Reversible cerebral atrophy in recently abstinent alcoholics measured by computed tomography scans. *Science*, 200: 1076-1078, 1978.

Cermak, L.S., Ryback, R.S.: Recovery of verbal short-term memory in alcoholics. *J. Stud. Alc.*, 37: 46-52, 1976.

Chen, L.L., VanHoesen, G.W., Barnes, C.L., West, J.R.: Enhanced acetylcholinesterase staining in the hippocampal perforant pathway zone after combined lesions of the septum and entorhinal cortex. *Brain Res.*, 272: 354-359, 1983.

Chen, S., Hillman, D.E.: Marked reorganization of Purkinje cell dendrites and spines in adult rat following vacating of synapses due to deafferentation. *Brain Res.*, 245: 131-135, 1982.

Clark, J., Houghton, E.: A study of intellectual impairment and recovery in heavy drinkers in Ireland. *Brit. J. Psychiat.*, 126: 178-184, 1975.

Clark, W., Midanik, L.: Alcohol use and alcohol problems among U.S. adults: Results of the 1979 national survey. *Alcohol and Health Monograph No. 1*, U.S. Dept. Health and Human Services, 1982.

Coger, R.W., Dymond, Am. M., Serafetinides, E.A., Lowenstam, I., Pearson, D.: EEG signs of brain impairment in alcoholism. *Biol. Psychiat.*, 13: 729-739, 1979.

Cohen, R.S., Wolosewick, J.J., Becker, R.P., Pappas, G.D.: Fine structure of synapses of the central nervous system in resinless sections. *J. Submicrosc. Cytol.*, 15: 849-863, 1983.

Cohen, S., Gallant, D.M.: Diagnosis of Drug and Alcohol Abuse. *Med. Monograph Series v. 1(6)*. Career Teacher Center, SUNY Downstate Med. Ctr., Brooklyn, 1981.

Collins, M.A., Nijm, W.P., Borge, G., Teas, G., Goldfarb, C.: Dopamine-related tetrahydroisoquinolines: Significant urinary excretion by alcoholics after alcohol consumption. *Science*, 206: 1184-1186, 1979.

Connor, J.R., Diamond, M.C., Johnson, R.E.: Aging and environmental influences on two types of dendritic spine in the rat occipital cortex. *Exp. Neurol.*, 70: 371-379, 1980a.

- Connor, J.R., Diamond, M.C., Johnson, R.E.: Occipital cortical morphology of the rat: Alterations with and environment. *Exp. Neurol.*, 68: 158-170, 1980b.
- Cotman, W.W., Gentry, C., Steward, O.: Synaptic replacement in the dentate gyrus after unilateral entorhinal lesion: Electron microscopic analysis of the extent of replacement of synapses by the remaining entorhinal cortex. *J. Neurocytol.*, 6: 455-565, 1977.
- Cotman, C.W., Matthews, D.A., Taylor, D., Lynch, G.: Synaptic rearrangement in the dentate gyrus: Histochemical evidence of adjustments after lesions in immature and adult rats. *Proc. Nat. Acad. Sci.*, 70: 3473-3477, 1973.
- Cotman, C.W., Nadler, J.V.: Reactive synaptogenesis in the hippocampus. In Cotman, C.W. (ed.), *Neuronal Plasticity*, pp. 227-271. New York: Raven Press, 1978.
- Cotman, W.W., Nieto-Sampedro, M., Harris, E.W.: Synapse replacement in the nervous system of adult vertebrates. *Physiol. Rev.*, 61: 684-784, 1981.
- Cotman, C.W., Scheff, S.W.: Compensatory synapse growth in aged animals after neuronal death. *Mech. Ageing Dev.*, 9: 103-117, 1979.
- Courville, C.B.: *Effects of Alcohol on the Nervous System of Man*. Los Angeles: San Lucas Press, 1966.
- Coyle, P.: Spatial features of the rat hippocampal vascular system. *Exp. Neurol.*, 58: 549-561, 1978.
- Crawford, I.L., Connor, J.D.: Zinc in maturing rat brain: Hippocampal concentrations and localization. *J. Neurochem.*, 19: 1451-1458, 1972.
- Crews, F.T., Majchrowicz, E., Meeks, R.: Changes in cortical synaptosomal plasma membrane fluidity and composition in ethanol-dependent rats. *Psychopharm.*, 81: 208-213, 1983.
- Cupp, C.J., Uemura, E.: Age related changes in prefrontal cortex of *Macacca mulatta*: Quantitative analysis of dendritic branching patterns. *Exp. Neurol.*, 69: 143-163, 1980.
- Danscher, G.: Histochemical demonstration of heavy metals: A revised version of the sulfide silver method suitable for both light and electronmicroscopy. *Histochemistry*, 71: 1-16, 1981.

DeKosky, S.T., Scheff, S.W., Cotman, C.W.: Elevated corticosterone levels: A possible cause of reduced axon sprouting in aged animals. *Neuroendocrinology*, 38: 33-38, 1984.

De La Fuente, J.R., Rosenbaum, A.H., Morse, R.M., Niven, R.N., Abboud, C.F., Jiang, N-S., Schatzberg, A.F.: The hypothalamic-pituitary-adrenal axis in alcoholics. *Alcoholism: Clin. Exp. Res.*, 7: 35-37, 1983.

Denoble, V.J., Begleiter, H.: Impairment of acquisition of a DRL schedule following prolonged ethanol consumption. *Pharm. Biochem. Behav.*, 10: 393-396, 1979.

Dent, J.A., Galvin, N.J., Stanfield, B.B., Cowan, W.M.: The mode of termination on the hypothalamic projection to the dentate gyrus: An EM autoradiographic study. *Brain Res.*, 258: 1-10, 1983.

Desmond, N.L., Levy, W.B.: Ultrastructural and numerical alterations in dendritic spines as a consequence of long-term potentiation. *Anat. Rec.*, 199: 68A, 1981.

Desmond, N.L., Levy, W.B.: A quantitative anatomical study of the granule cell dendritic fields of the rat dentate gyrus using a novel probabilistic model. *J. Comp. Neurol.*, 212: 131-145, 1982.

Douglas, R.M., McNaughton, B.L., Goddard, G.V.: Commissural inhibition and facilitation of granule cell discharge in fascia dentata. *J. Comp. Neurol.*, 219: 285-294, 1983.

Duffy, C.J., Rakic, P.: Differentiation of granule cell dendrites in the dentate gyrus of the rhesus monkey: A quantitative Golgi study. *J. Comp. Neurol.*, 214: 224-237, 1983.

Dunmire, C.R., LaVelle, F.W.: Effect of ethanol on nucleolar structure: A cytological indication of change in RNA/protein synthesis. *Anat. Rec.*, 206: 363-371, 1983.

Durand, D., Carlen, P.L.: Impairment of long-term potentiation in rat hippocampus following chronic ethanol treatment. *Brain Res.*, 308: 325-332, 1984.

Durand, D., Carlen, P.L., McMullen, P.: Impairment of long-term potentiation following chronic ethanol consumption in rats. *Neurosci. Abstr.*, 6: 89, 1980.

Earvin, V.G., McClearn, G.E., Kuse, A.R.: Interrelationships of alcohol consumption, actions of alcohol, and biochemical traits. *Pharmacol. Biochem. Behav.*, 13: 297-302, 1980.

- Eisenhofer, G., Lambie, D.G., Johnson, R.H.: Effect of ethanol on plasma catecholamines and norepinephrine clearance. *Clin. Pharm. Ther.*, 34: 143-147, 1983.
- Ellenberg, L., Rosenbaum, G., Goldman, M.S., Whitman, R.D.: Recoverability of psychological functioning following alcohol abuse: Lateralization effects. *J. Consult. Clin. Psychol.*, 48: 503-510, 1980.
- Fabian, M.S., Parsons, O.A., Sheldon, M.D.: Effects of gender and alcoholism on verbal and visual-spatial learning. *J. Nerv. Ment. Dis.*, 172: 16-20, 1984.
- Farmer, R.H.: Functional changes during early weeks of abstinence, measured by BenderGestalt. *Quart. J. Stud. Alc.*, 34: 786-796, 1973.
- Fass, B., Steward, O.: Increases in protein-precursor incorporation in the denervated neuropil of the rat dentate gyrus during reinnervation. *Neuroscience*, 9: 653-664, 1983.
- Feldman, M.L., Peters, A.: A technique for estimating total spine numbers on Golgi-impregnated dendrites. *J. Comp. Neurol.*, 188: 527-542, 1979.
- Flamm, E.S., Demopoulos, H.B., Seligman, M.L., Tomasula, J.J., DeCrescito, V., Ransohoff, J.: Ethanol potentiation of central nervous system trauma. *J. Neurosurg.*, 46: 328, 1977.
- Fifkova, E., Anderson, C.L.: Stimulation-induced changes in dimensions of stalks of dendritic spines in the dentate molecular layer. *Soc. Neurosci. Abstr.*, 11: 288.15, 1982.
- Fifkova, E., Delay, R.J.: Cytoplasmic actin in neuronal processes as a possible mediator of synaptic plasticity. *J. Cell Biol.*, 95: 345-350, 1982.
- Fifkova, E., Van Harreveld, A.: Long-lasting morphological changes in dendritic spines of dentate granule cells following stimulation of entorhinal area. *J. Neurocytol.*, 6: 211-230, 1977.
- Finger, S., Stein, D.G.: *Brain Damage and Recovery*. New York: Academic Press, 1982.
- Fjordingstad, E., Danscher, G., Fjordingstad, E.J.: Zinc content in hippocampus and whole brain of normal rats. *Brain Res.*, 79: 338-342, 1974a.
- Fjordingstad, E.J., Danscher, G., Fjordingstad, E.: Hippocampus: Selective concentration of lead in the normal rat brain. *Brain Res.*, 80: 350-354, 1974b.

Freund, G.: The interaction of chronic alcohol consumption and aging on brain structure and function. *Alcoholism: Clin. Exp. Res.*, 6: 13-21, 1982.

Freund, G., Walker, D.W.: Impairment of avoidance learning by prolonged ethanol consumption in mice. *J. Pharm. Exp. Ther.*, 179: 284-292, 1971.

Fricke, R., Cowan, W.M.: An autoradiographic study of the commissural and ipsilateral hippocampo-dentate connections in the adult rat. *J. Comp. Neurol.*, 181: 253-270, 1978.

Frotscher, M.: Dendritic plasticity in response to partial deafferentation. In W. Seifert (ed.), *Neurobiology of the Hippocampus*. New York: Academic Press, 1983.

Frotscher, M., Hamori, J., Wenzel, J.: Transneuronal effects of entorhinal lesions in the early postnatal period on synaptogenesis in the hippocampus of the rat. *Exp. Brain Res.*, 30: 549-560, 1977.

Frotscher, M., Zimmer, J.: Lesion-induced mossy fibers to the molecular layer of the rat fascia dentata: Identification of postsynaptic granule cells by the Golgi-EM technique. *J. Comp. Neurol.*, 215: 299-311, 1983.

Gage, F.H., Bjorklund, A., Stenevi, U.: Denervation releases a neuronal survival factor in adult rat hippocampus. *Nature*, 308: 637-639, 1984.

Gall, C., Brecha, N., Chang, K.-J., Kartens, H.J.: Ontogeny of enkephalin-like immunoreactivity in the rat hippocampus. *Neuroscience*, 11: 359-380, 1984.

Gall, C., Rose, G., Lynch, G.: Proliferative and migratory activity of glial cells in the partially deafferented hippocampus. *J. Comp. Neurol.*, 183: 539-550, 1979.

Geneser-Jensen, F.A., Blackstad, T.W.: Distribution of acetyl cholinesterase in the hippocampal region of the guinea pig. I. Entorhinal area, parasubiculum, and presubiculum. *Z. Zellforsch.*, 114: 460-481, 1971.

Globus, A., Rosenzweig, M., Bennett, E., Diamond, M.C.: Effects of differential experience on dendritic spine counts in rat cerebral cortex. *J. Comp. Physiol. Psychol.*, 82: 175-181, 1973.

Goldman, H., Sapirstein, L.A., Murphy, S., Moore, J.C.: Alcohol and regional blood flow in brains of rats. *Proc. Soc. Exp. Biol. Med.*, 144: 983-988, 1973.

Goldowitz, D., Scheff, S.W., Cotman, C.W.: The specificity of reactive synaptogenesis: A comparative study in the adult rat hippocampal formation. *Brain Res.*, 170: 427-441, 1979.

Goldstein, B., Maxwell, B.D.S., Ellison, G., Hammer, E.P.: Dendritic vacuolization in the central nervous system of rats after long-term voluntary consumption of ethanol. *J. Neuropath. Exp. Neurol.*, 42: 579-589, 1983.

Goodwin, D.W., Hill, S.Y.: Chronic effects of alcohol and other psychoactive drugs. In J.G. Rankin (ed.), *Alcohol, Drugs, and Brain Damage*, pp. 55-70. Toronto: Addiction Research Foundation, 1975.

Gottlieb, D.I., Cowan, W.M.: Evidence for a temporal factor in the occupation of available synaptic sites during the development of the dentate gyrus. *Brain Res.*, 41: 452-456, 1972.

Gottlieb, D.I., Cowan, W.M.: Autoradiographic studies of the commissural and ipsilateral association connections of the hippocampus and dentate gyrus of the rat. I. The commissural connections. *J. Comp. Neurol.*, 149: 392-422, 1973.

Guthrie, A.: The first year after treatment: Factors affecting time course of reversibility of memory and learning deficits in alcoholism. *Adv. Exp. Med. Biol.*, v. 26, pp. 757-770. New York: Plenum Press, 1980.

Guthrie, A., Elliot, W.A.: The nature and reversibility of cerebral impairment in alcoholism. *J. Stud. Alc.*, 41: 363-367, 1980.

Hamlyn, L.H.: Electron microscopy of mossy fibers in Ammon's horn. *Nature*, 190: 645-646, 1961.

Hamori, J.: The inductive role of presynaptic axons in the development of postsynaptic spines. *Brain Res.*, 62: 337-344, 1973.

Harris, E.W., Lasher, S.S., Steward, O.: Habituation-like decrements in transmission along the normal and lesion-induced temporo-dentate pathways in the rat. *Brain Res.*, 151: 623-631, 1978.

Harris, R.A.: Defining the membrane pathology produced by chronic alcohol consumption. *Lab. Invest.*, 50: 113-114, 1984.

- Haug, F-M. S.: Light microscopical mapping of the hippocampal region, the pyriform cortex and the corticomedial amygdaloid nuclei of the rat with Timm's sulphide silver method. I. Area dentata, hippocampus, and subiculum. *Z. Anat. Entwickl.-Gesch.*, 145: 1-27, 1974.
- Haug, J.O.: Pneumoencephalographic evidence of brain damage in chronic alcoholics. *Acta Psychiat. Scand. (suppl.)*, 203: 135-143, 1968.
- Henke, H., Lang, W.: Cholinergic enzymes in neocortex, hippocampus, and basal forebrain of non-neurological and senile dementia of Alzheimer-type patients. *Brain Res.*, 267: 281-291, 1983.
- Herkenham, M.: The connections of the nucleus reuniens thalami: Evidence for a direct thalamo-hippocampal pathway in the rat. *J. Comp. Neurol.*, 177: 589-610, 1978.
- Hester, R.K., Smith, J.W., Jackson, T.R.: Recovery of cognitive skills in alcoholics. *J. Stud. Alc.*, 41: 363-367, 1980.
- Hill, S.Y., Mikhael, M.: Computed tomography scans of alcoholics: Cerebral atrophy? *Science*, 204: 1237-1238, 1979.
- Hirano, A.: The normal and aberrant development of synaptic structures between parallel fibers and Purkinje cell dendritic spines. *J. Neural Trans.*, suppl. 18: 1-18, 1983.
- Hjorth-Simonsen, A.: Some intrinsic connections of the hippocampus in the rat: An experimental analysis. *J. Comp. Neurol.*, 147: 145-162, 1973.
- Hjorth-Simonsen, A., Laurberg, S.: Commissural afferents to the hippocampus of the rabbit. *J. Comp. Neurol.*, 176: 495-513, 1977.
- Hoff, S.F., Scheff, S.W., Kwan, A.Y., Cotman, C.W.: A new type of lesion-induced synaptogenesis: II. The effect of aging on synaptic turnover in non-denervated zones. *Brain Res.*, 222: 15-27, 1981.
- Honkanen, R., Ertama, L., Kuosmanen, P., Linnoila, M., Alha, A., Visuri, T.: The role of alcohol in accidental falls. *J. Stud. Alc.* 44: 231-245, 1983.
- Irle, E., Markowitsch, H.J.: Widespread neuroanatomical damage and learning deficits following chronic alcohol consumption or vitamin-B1 (thiamin) deficiency in rats. *Behav. Brain Res.*, 9: 277-294, 1983.

- Ishii, T.: A comparison of cerebral atrophy in CT scan findings among alcoholic groups. *Acta Psyciat. Scand.*, 69 (suppl. 309): 7-30, 1983.
- Johansen, F.P., Jorgensen, M.B., Ekstrom Von Lubitz, D.K.J., Diemer, N.H.: Selective dendrite damage in hippocampal CA1 stratum radiatum with unchanged axon ultrastructure and glutamate uptake after transient cerebral ischemia in the rat. *Brain Res.*, 291: 373-377, 1984.
- Jones, W.H., Thomas, D.B.: Changes in the dendritic organization of neurons in the cerebral cortex following deafferentation. *J. Anat. (Lond.)*, 96: 375-381, 1962.
- Juraska, J.M.: Sex differences in dendritic response to differential experience in the rat visual cortex. *Brain Res.*, 295: 27-34, 1984.
- Kahn, A., Ciraulo, D.A., Nelson, W.H., Becker, J.T., Nies, A., Jaffe, J.H.: Dexamethasone suppression test in recently detoxified alcoholics: Clinical implications. *J. Clin. Psychopharm.*, 4: 94-97, 1984.
- Kalant, H.: Direct effects of alcohol on the nervous system. *Fed. Proc.*, 34: 1930-1941, 1975.
- Kiishi, K., Stanfield, B.B., Cowan, W.M.: A quantitative EM autoradiographic study of the commissural and associational connections of the dentate gyrus in the rat. *Anat. Embryol.*, 160: 173-186, 1980.
- King, M.: A Golgi study of non-granule neurons in the dentate gyrus of the rat. *Neurosci. Abstr.*, 1984.
- King, M.A., Reep, R.L., Walker, D.W., Hunter, B.E.: The three dimensional morphology of afferent terminal fields in the rat dentate gyrus: Periodic variation. *J. Comp. Neurol.*, in press.
- Kirino, T., Sano, K.: Selective vulnerability in the gerbil hippocampus following transient ischemia. *Acta Neuropathol. (Berl.)*, 62: 201-208, 1984a.
- Kirino, T., Sano, K.: Fine structural nature of delayed neuronal death following ischemia in the gerbil hippocampus. *Acta Neuropathol. (Berl.)*, 62: 209-218, 1984b.
- Kissin, B.: Biological investigations in alcohol research. *J. Stud. Alc.*, suppl. 8: 146-180, 1979.
- Koda, L.Y., Bloom, F.E.: A light and electron microscopic study of noradrenergic terminals in the rat dentate gyrus. *Brain Res.*, 120: 327-335, 1977.

Kohler, C., Haglund, L., Swanson, L.W.: A diffuse α -MSH-immunoreactive projection to the hippocampus and spinal cord from individual neurons in the lateral hypothalamic area and zona incerta. *J. Comp. Neurol.*, 223: 501-514, 1984.

Koval', A.Z.: Clinical characteristics in the course of cerebral infarct in alcohol intoxication patients. *Vrachebnoye Delo*, 5: 145-147, 1978.

Kristensson-Aas, A., Sandstrom, J., Starmark, J-E., Wallerstedt, S., Westin, J.: The emergency department--the alcoholic's encounter with acute care. *Lakartidningen*, 78: 437-440, 1981.

Kunz, G., Englisch, H-J., Wenzel, J.: Untersuchungen zur spines-verteilung an pyramedenneuronen der CA1-Region des hippocampus der ratte nach langzeiger oraler alkoholapplikation. *J. Hirnforsch.*, 17: 351-363, 1976.

Laatch, R.H., Cowan, W.M.: Electron microscopic studies of the dentate gyrus of the rat. I. Normal structure with special reference to synaptic organization. *J. Comp. Neurol.*, 128: 359-396, 1966.

Laatch, R.H., Cowan, W.M.: Electron microscopic studies of the dentate gyrus of the rat. II. Degeneration of the commissural afferents. *J. Comp. Neurol.*, 130: 241-262, 1967.

Landis, D.M.D., Reese, T.S.: Cytoplasmic organization in cerebellar dendritic spines. *J. Cell Biol.*, 97: 1169-1178, 1983.

Larkin, E.C., Watson-Williams, E.J.: Alcohol and the blood. *Med. Clin. N. Am.*, 68: 105-120, 1984.

Laurberg, S.: Commissural and intrinsic connections of the rat hippocampus. *J. Comp. Neurol.*, 184: 685-708, 1979.

Laurberg, S., Sorensen, K.E.: Associational and commissural collaterals of neurons in the hippocampal formation (hilus fasciae dentatae and subfield CA3). *Brain Res.*, 212: 287-300, 1981.

Lee, K., Dunwiddie, T., Deitrich, R., Lynch, G., Hoffer, B.: Chronic ethanol consumption and hippocampal neuron dendritic spines: A morphometric and physiological analysis. *Exp. Neurol.*, 71: 541-549, 1981.

Lee, K.S., Stanford, E.J., Cotman, C.W., Lynch, G.S.: Ultrastructural evidence for bouton sprouting in the adult mammalian brain. *Exp. Brain Res.*, 29: 475-485, 1977.

Lieber, C.S.: Metabolism and metabolic effects of alcohol. Med. Clin. N. Am., 68: 3-31, 1984.

Loesche, J., Steward, G.: Behavioral correlates of denervation and reinnervation of the hippocampal formation in the rat: Recovery of alternation performance following unilateral entorhinal cortex lesions. Brain Res. Bull., 2: 31-39, 1977.

Long, J.A., McLachlan, J.F.C.: Abstract reasoning and perceptual-motor efficiency in alcoholics: Impairment and reversibility. Quart. J. Stud. Alc., 35: 1220-1229, 1974.

Longo, F.M., Selak, I., Zovickian, J., Manthorpe, M., Varon, S., U, H.S.: Neuronotrophic activities in cerebrospinal fluid of head trauma patients. Exp. Neurol., 84: 207-218, 1984.

Lorente de No, R.: Studies on the structure of the cerebral cortex. II. Continuation of the study of the ammonic system. J. Psychol. Neurol., 46: 113-177, 1934.

Loy, R., Koziell, D.A., Lindsey, J.D., Moore, R.Y.: Noradrenergic innervation of the adult rat hippocampal formation. J. Comp. Neurol., 189: 699-710, 1980.

Luthin, G.R., Tabakoff, B.: Effects of ethanol on calmodulin levels in mouse striatum and cerebral cortex. Alcoholism: Clin. Exp. Res., 8: 68-72, 1984.

Lynch, G., Gall, C., Rose, G., Cotman, C.: Changes in the distribution of the dentate gyrus associational system following unilateral or bilateral entorhinal lesions in the adult rat. Brain Res., 110: 57-71, 1976.

Lynch, G., Matthews, D.A., Mosko, S., Parks, T., Cotman, C.W.: Induced acetylcholine-rich layer in rat dentate gyrus following entorhinal lesions. Brain Res., 42: 311-318, 1972.

Lynch, M.J.G.: Brain lesions in chronic alcoholism. Arch. Pathol., 69: 342-353, 1960.

MacDonnall, J.W., Marcucella, H.: Short-term memory deficits following prolonged ethanol consumption by rats. In F.A. Sexias (ed.), Currents in Alcoholism, v. 3, p. 245. New York: Grune and Stratton, 1978.

Machado-Salas, J.P., Scheibel, A.B.: Limbic system of the aged mice. Exp. Neurol., 63: 347-355, 1979.

Malin, H., Coakley, J., Kaelber, C.: An epidemiologic perspective on alcohol use and abuse in the United States.

Alcohol and Health Monograph No. 1, U.S. Dept. of Health and Human Services, 1982.

Matthews, D.A., Cotman, C., Lynch, G.: An electron microscopic study of lesion-induced synaptogenesis in the dentate gyrus of the adult rat. I. Magnitude and time course of degeneration. *Brain Res.*, 115: 1-21, 1976a.

Matthews, D.A., Cotman, C.W., Lynch, G.: An electron microscopic study of lesion-induced synaptogenesis in the dentate gyrus of the adult rat. II. Reappearance of morphologically normal contacts. *Brain Res.*, 115: 23-41, 1976b.

McLardy, T.: Gyrus dentatus granule cell pathology in chronic alcoholism. *Int. Res. Comm. Syst. Med. Sci.*, 73: 16-8-2, 1973a.

McLardy, T.: Dentate granule cell sensitivity to proximity of blood vessels in chronic alcoholism. *Int. Res. Comm. Syst. Med. Sci.*, 73: 16-8-6, 1973b.

McMullen, P.A., Saint-Cyr, J.A., Carlen, P.L.: Morphological alterations in rat CA1 hippocampal pyramidal cell dendrites resulting from chronic ethanol consumption and withdrawal. *J. Comp. Neurol.*, 225: 111-118, 1984.

McNaughton, B.L.: Evidence for two physiologically distinct perforant pathways to the fascia dentata. *Brain Res.*, 199: 1-19, 1980.

McNaughton, N., Miller, J.J.: Medial septal projections to the dentate gyrus of the rat: Electrophysiological analysis of distribution and plasticity. *Exp. Brain Res.*, 56: 243-256, 1984.

McWilliams, R., Lynch, G.: Terminal proliferation and synaptogenesis following partial deafferentation: The reinnervation of the inner molecular layer of the dentate gyrus following removal of its commissural afferents. *J. Comp. Neurol.*, 180: 581-616, 1978.

McWilliams, J.R., Lynch, G.: Rate of synaptic replacement in denervated rat hippocampus declines precipitously from the juvenile period to early adulthood. *Science* 217: 572-574, 1983.

Mehraein, P., Yamanda, M., Tarnowska-Dziduszko, E.: Quantitative study on dendrites and dendritic spines in Alzheimer's disease and senile dementia. In G.W. Kreutzberg (ed.), *Adv. in Neurol.*, v. 12, pp. 453-458, 1975.

Meibach, R.C., Siegel, A.: Efferent connections of the hippocampal formation in the rat. *Brain Res.*, 124: 197-224, 1977.

Mervis, R.: Cytomorphological alterations in the aging animal brain with emphasis on Golgi studies. In J.E. Johnson (ed.), *Aging and Cell Structure*, v. 1, pp. 143-185. New York: Plenum Press, 1981.

Milner, B., Corkin, S., Teuber, H.L.: Further analysis of the hippocampal amnesic syndrome. *Neuropsychologia*, 6: 267-282, 1968.

Milner, T.A., Loy, R., Amaral, D.G.: An anatomical study of the development of the septo-hippocampal projection in the rat. *Dev. Brain Res.*, 8: 343-371, 1983.

Miyakawa, T., Hattori, E., Shikai, I., Shimoji, A., Nagatoshi, K., Suzuiki, T.: Histopathological changes of chronic alcoholism. *Folia Psychiat. Neurol. Jap.*, 31: 253-261, 1977.

Moore, R.Y., Halaris, A.E.: Hippocampal innervation by serotonin neurons of the midbrain raphe in the rat. *J. Comp. Neurol.*, 164: 171-185, 1975.

Montgomery, R.L., Pick, J.R., Ellis, F.W., Christian, E.L.: Microscopic studies of hippocampal and cortical areas of rhesus monkeys physically dependent on ethanol. *Anat. Rec.*, 193: 627, 1979.

Morest, D.K.: The growth of dendrites in the mammalian brain. *Z. Anat. Entwickl.-Gesch.*, 128: 290-317, 1969.

Moss, M., Mahut, H., Zola-Morgan, S.: Concurrent discrimination learning of monkeys after hippocampal, entorhinal, or fornix lesions. *J. Neurosci.*, 1: 227-240, 1981.

Nadler, J.V., Paoletti, C., Cotman, C.W., Lynch, G.: Histochemical evidence of altered development of cholinergic fibers in the rat dentate gyrus following lesions. II. Effects of partial entorhinal and simultaneous multiple lesions. *J. Comp. Neurol.*, 171: 589-604, 1977.

Nadler, J.V., Perry, B.W., Gentry, C., Cotman, C.W.: Loss and reacquisition of hippocampal synapses after selective destruction of CA3-CA4 afferents with kainic acid. *Brain Res.*, 191: 387-404, 1980.

Nafstad, P.H.J.: An electron microscope study of the termination of the perforant path fibers in the hippocampus and fascia dentata. *Z. Zellforsch.*, 76: 532-542, 1967.

- Nakada, T., Knight, R.T.: Alcohol and the central nervous system. *Med. Clin. N. Am.*, 68: 121-131, 1984.
- Nirenberg, M., Wilson, S., Higashida, H., Rotter, A., Krueger, K., Busis, N., Ray, R., Kenimer, J.G., Adler, M.: Modulation of synapse formation by cyclic adenosine monophosphate. *Science*, 222: 794-799, 1983.
- Noble, E.P., Tewari, S.: Protein and nucleic acid metabolism in brains of mice following chronic alcohol consumption. *Ann. NY Acad. Sci.* 215: 333-345, 1974.
- Nordberg, A., Larsson, C., Perdahl, E., Winblad, B.: Cholinergic activity in hippocampus in chronic alcoholism. *Drug and Alcohol Dependence*, 10: 333-344, 1982.
- O'Keefe, J., Nadel, L.: *The Hippocampus as a Cognitive Map*. New York: Oxford University Press, 1978.
- Page, R.D., Linden, J.D.: "Reversible" organic brain syndrome in alcoholics: A psychometric evaluation. *Quart. J. Stud. Alc.*, 35: 98-107, 1974.
- Parnavelas, J.G., Lynch, G., Brecha, N., Cotman, C.W., Globus, A.: Spine loss and regrowth in the hippocampus following deafferentation. *Nature*, 248: 71-73, 1974.
- Parsons, O.A.: Neuropsychological deficits in alcoholics: Facts and fancies. *Alcoholism: Clin. Exp. Res.*, 1: 51-56, 1977.
- Paxinos, G., Watson, D.R.R.: *The Rat Brain in Stereotaxic Coordinates*. New York: Academic Press, 1982.
- Pentney, R.J.: Quantitative analysis of ethanol effects on Purkinje cells after long-term alcohol consumption. *Brain Res.*, 249: 397-401, 1982.
- Phillips, S.C., Cragg, B.G.: Chronic consumption of alcohol by adult mice: Effect on hippocampal cells and synapses. *Exp. Neurol.*, 80: 216-226, 1983.
- Pickel, V.M., Segal, M., Bloom, F.E.: Axonal proliferation following lesions of cerebellar peduncles: A combined fluorescence microscopic and radioautographic study. *J. Comp. Neurol.*, 155: 43-50, 1974.
- Pokorny, J., Yamamoto, T.: Postnatal ontogenesis of hippocampal CA1 area. I. Development of dendritic arborization in pyramidal neurons. *Brain Res. Bull.*, 7: 113-120, 1981.

Popova, E.N.: Reversibility of changes in cortical neurons in experimental alcohol intoxication. (translation) *Byulleten' Eksperimental'noi Biologii i Meditsiny*, 96: 101-104, 1983.

Powell, T.P.S.: Transneuronal cell degeneration in the olfactory bulb shown by the Golgi method. *Nature (Lond.)*, 215: 425-426, 1967.

Puro, D.G.: Glucocorticoid regulation of synaptic development. *Dev. Brain Res.*, 8: 283-290, 1983.

Purpura, D.P.: Dendritic spine "dysgenesis" and mental retardation. *Science*, 186: 1126-1128, 1974.

Raisman, G.: The connexions of the septum. *Brain*, 89: 317-348, 1966a.

Raisman, G.: An experimental analysis of the efferent projections of the hippocampus. *Brain*, 89: 83-108, 1966b.

Reymann, K., Pohle, W., Muller-Welde, P., Ott, T.: Dopaminergic innervation of the hippocampus: Evidence for midbrain raphe neurons as the site of origin. *Biomed. Biochim. Acta*, 42: 1247-1253, 1983.

Riley, J.N., Moore, R.Y.: Diencephalic and brainstem afferents to the hippocampal formation of the rat. *Brain Res. Bull.*, 6: 437-444, 1981.

Riley, J.N., Walker, D.W.: Morphological alterations in hippocampus after long-term alcohol consumption in mice. *Science*, 210: 646-648, 1978.

Ron, M.A.: Brain damage in chronic alcoholism: A neuropathological, neuroradiological, and psychological review. *Psychol. Med.*, 7: 103-112, 1977.

Rose, A.M., Hattori, T., Fibiger, H.C.: Analysis of the septo-hippocampal pathway by light and electron microscopic autoradiography. *Brain Res.*, 108: 170-174, 1976.

Rose, G., Lynch, G., Cotman, C.W.: Hypertrophy and redistribution of astrocytes in the deafferented dentate gyrus. *Brain Res. Bull.*, 1: 87-92, 1976.

Ryan, C.: Learning and memory deficits in alcoholics. *J. Stud. Alc.*, 41: 437-447, 1980.

Salamy, J.G., Wright, J.R., Faillace, L.A.: Changes in average evoked responses during abstinence in chronic alcoholics. *J. Nerv. Ment. Dis.*, 168: 19-25, 1980.

Saletu, B., Saletu, M., Grunberger, J., Mader, R.: Spontaneous and drug-induced remission of alcoholic organic brain syndrome: Clinical, psychometric, and neurophysiological studies. *Psychiat. Res.*, 10: 59-75, 1983.

Schau, E.J., O'Leary, M.R., Chaney, E.F.: Reversibility of cognitive deficits in alcoholics. *J. Stud. Alc.*, 41: 733-740, 1980.

Scheff, S.W., Bernardo, L.S., Cotman, C.W.: Effect of serial lesions on sprouting in the dentate gyrus: Onset and decline of the catalytic effect. *Brain Res.*, 150: 45-53, 1978a.

Scheff, S.W., Bernardo, L.S., Cotman, C.W.: Lesion-induced vascular changes in the dentate gyrus following removal of the entorhinal cortex in adult rats. *Exp. Neurol.*, 62: 815-820, 1978b.

Scheff, S.C., Bernardo, L.S., Cotman, C.W.: Hydrocortisone administration retards axon sprouting in the rat dentate gyrus. *Exp. Neurol.*, 68: 195-201, 1980a.

Scheff, S.C., Bernardo, L.S., Cotman, C.W.: Decline in reactive fiber growth in the dentate gyrus of aged rats compared to the young adult rat following entorhinal cortex removal. *Brain Res.*, 199: 21-38, 1980b.

Scheff, S.C., Cotman, C.W.: Chronic glucocorticoid therapy alters axon sprouting in the hippocampal dentate gyrus. *Exp. Neurol.*, 76: 644-654, 1982.

Scheibel, M.E., Lindsay, R.D., Tomiyasu, Y., Scheibel, A.B.: Progressive dendritic changes in aging human limbic system. *Exp. Neurol.*, 53: 420-430, 1976.

Scheibel, M.E., Scheibel, A.B.: The methods of Golgi. In R.T. Robertson (ed.), *Neuroanatomical Research Techniques*, pp. 89-114. New York: Academic Press, 1978.

Schwegler, H., Lipp, H.P.: Hereditary covariations of neuronal circuitry and behavior: Correlations between the proportions of hippocampal synaptic fields in the regio inferior and two-way avoidance in mice and rats. *Behav. Brain Res.*, 7: 1-38, 1983.

Segal, M.: A potent inhibitory monosynaptic hypothalamo-hippocampal connection. *Brain Res.*, 162: 137-141, 1979.

Sharp, J.R., Rosenbaum, G., Goldman, M.S., Whitman, R.D.: Recoverability of psychological functioning following alcohol abuse: Acquisition of meaningful synonyms. *J. Consult. Clin. Psychol.*, 45: 1023-1028, 1977.

Sherlock, S.: Nutrition and the alcoholic. *Lancet*, 8374: 436-439, 1984.

Sidman, M., Stoddard, L.T., Mohr, J.F.: Some additional quantitative observations of immediate memory in a patient with bilateral hippocampal lesions. *Neuropsychologia*, 6: 245-254, 1968.

Smith, G.J., Meyer, J.S., Hull, J.H., Thomas, D.A.: Behavioral effects of prolonged ethanol consumption on temporal shock discrimination. *Physiol. Behav.*, 22: 609-612, 1979.

Stanfield, B.B., Cowan, M.W.: The sprouting of septal afferents to the dentate gyrus after lesions of the entorhinal cortex in adult rats. *Brain Res.*, 232: 162-170, 1982.

Stengaard-Pedersen, K., Fredens, K., Larsson, L-I.: Comparative localization of enkephalin and cholecystekinin immunoreactivities and heavy metals in the hippocampus. *Brain Res.*, 273: 81-96, 1983.

Steward, O., Cotman, C., Lynch, G.: Quantitative autoradiographic and electrophysiological study of reinnervation of dentate gyrus by contralateral entorhinal cortex following ipsilateral entorhinal lesions. *Brain Res.*, 114: 181-200, 1976b.

Steward, O., Smith, L.K.: Metabolic changes accompanying denervation and reinnervation of the dentate gyrus of the rat measured by [³H]2-deoxyglucose autoradiography. *Exp. Neurol.*, 69: 513-527, 1980.

Steward, O.: Topographic organization of the projections from the entorhinal area to the hippocampal formation of area to the hippocampal formation of the rat. *J. Comp. Neurol.*, 167: 285-314, 1976.

Steward, O.: Alterations in polyribosomes associated with dendritic spines during the reinnervation of the dentate gyrus of the adult rat. *J. Neurosci.*, 3: 177-188, 1983.

Steward, O., Caceres, A.: Dendritic reorganization in the denervated dentate gyrus of the rat following entorhinal cortical lesions: A Golgi and electron microscopic analysis. *J. Comp. Neurol.*, 214: 387-403, 1983.

Steward, O., Cotman, C.W., Lynch, G.: Re-establishment of electrophysiologically functional entorhinal cortical input to the dentate gyrus deafferented by ipsilateral entorhinal lesions. *Exp. Brain Res.*, 18: 396-414, 1973.

Steward, O., Cotman, C.W., Lynch, G.S.: Growth of a new fiber projection in the brain of adult rats: Reinnervation of the dentate gyrus by the contralateral entorhinal cortex following ipsilateral entorhinal lesions. *Exp. Brain Res.*, 20: 45-66, 1974.

Steward, O., Cotman, C.W., Lynch, G.: A quantitative autoradiographic and electrophysiological study of the reinnervation of the dentate gyrus by the contralateral entorhinal cortex following ipsilateral entorhinal lesions. *Brain Res.*, 115: 181-200, 1976.

Steward, O., Levy, W.B.: Preferential localization of polyribosomes under the base of dendritic spines in granule cells of the dentate gyrus. *J. Neurosci.*, 2: 284-291, 1982.

Steward, O., Scoville, S.A.: Cells of origin of entorhinal cortical afferents to the hippocampus and fascia dentata of the rat. *J. Comp. Neurol.*, 169: 347-370, 1976.

Steward, O., Vinsant, S.L.: Collateral projection of cells in the surviving entorhinal area which reinnervate the dentate gyrus of the rat following unilateral entorhinal lesions. *Brain Res.*, 149: 216-222, 1978.

Steward, O., Vinsant, S.: The process of reinnervation in the dentate gyrus of the adult rat: A quantitative electron microscopic analysis of terminal proliferation and reactive synaptogenesis. *J. Comp. Neurol.*, 214: 370-386, 1983.

Steward, O., White, W.F., Cotman, C.W., Lynch, G.: Potentiation of excitatory synaptic transmission in the normal and reinnervated dentate gyrus of the rat. *Exp. Brain Res.*, 26: 423-441, 1976.

Stoltenburg-Didinger, G., Spohr, H.L.: Fetal alcohol syndrome and mental retardation: Spine distribution of pyramidal cells in prenatal alcohol-exposed rat cerebral cortex; a Golgi study. *Dev. Brain Res.*, 11: 119-123, 1983.

Storm-Mathisen, J.: Choline acetyltransferase and acetylcholinesterase in fascia dentata following lesions of the entorhinal afferents. *Brain Res.*, 80: 181-197, 1974.

Storm-Mathisen, J.: Quantitative histochemistry of acetylcholinesterase in the rat hippocampal region correlated to histochemical staining. *J. Neurochem.*, 17: 739-754, 1970.

Swanson, L.W., Cowan, W.M.: An autoradiographic study of the organization of the efferent connections of the hippocampal formation in the rat. *J. Comp. Neurol.*, 172: 749-784, 1977.

- Swanson, L.W., Cowan, W.M.: The connections of the septal region in the rat. *J. Comp. Neurol.*, 186: 621-656, 1979.
- Swanson, L.W., Hartman, B.K.: The central adrenergic system, immunofluorescence study of the location of cell bodies and their efferent connections in the rat utilizing dopamine- β -hydroxylase as a marker. *J. Comp. Neurol.*, 163: 467-506, 1975.
- Swanson, L.W., Sawchenko, P., Cowan, W.M.: Evidence that the commissural, associational, and septal projections of the regio inferior of the hippocampus arise from the same neurons. *Brain Res.*, 197: 207-212, 1980.
- Swanson, L.W., Sawchenko, P., Cowan, W.M.: Evidence for collateral projections by neurons in Ammon's horn, the dentate gyrus, and the subiculum: A multiple retrograde labelling study in the rat. *J. Neurosci.*, 1: 548-559, 1981.
- Swanson, L.W., Teyler, T.J., Thompson, R.F.: Hippocampal long-term potentiation: Mechanisms and implications for memory. *Neurosci. Res. Prog. Bull.*, 20: 613-767, 1982.
- Swanson, L.W., Wyss, J.M., Cowan, W.M.: An autoradiographic study of the organization of intrahippocampal association pathways in the rat. *J. Comp. Neurol.*, 181: 681-715, 1978.
- Tabakoff, B., Hoffman, P.L.: Development of functional dependence on ethanol in dopaminergic systems. *J. Pharmacol. Exp. Ther.*, 208: 216-222, 1979.
- Tarter, R.E.: Psychological deficits in chronic alcoholics: A review. *Int. J. Addict.*, 10: 327-368, 1975.
- Tavares, M.A., Paula-Barbosa, M.M.: Alcohol-induced granule cell loss in the cerebellar cortex of the adult rat. *Exp. Neurol.*, 78: 574-582, 1982.
- Tavares, M.A., Paula-Barbosa, M.M., Gray, E.G.: A morphometric Golgi analysis of the Purkinje cell dendritic tree after long-term alcohol consumption in the adult rat. *J. Neurocytol.*, 12: 939-948, 1983a.
- Tavares, M.A., Paula-Barbosa, M.M., Gray, E.G.: Dendritic spine plasticity and chronic alcoholism in rats. *Neurosci. Lett.*, 42: 235-238, 1983b.
- Templer, D.E., Ruff, C.F., Simpson, K.: Trail making test performance of alcoholics abstinent at least a year. *Int. J. Addict.*, 10: 609-612, 1975.

- Towle, A.C., Sze, P.Y.: Chronic ethanol reduces brain calmodulin levels. *Trans. Am. Soc. Neurochem.*, 12: 88, 1981.
- Tumarkin, B., Wilson, J.D., Snyder, G.: Cerebral atrophy due to alcoholism in young adults. *US Armed Forces Med. J.*, 6: 64-74, 1955.
- Turner, D.A., Schwartzkroin, P.A.: Electrical characteristics of dendrites and dendritic spines in intracellularly stained CA3 and dentate hippocampal neurons. *J. Neurosci.*, 3: 2381-2394, 1983.
- Uemura, E.: Age-related changes in prefrontal cortex of Macacca mulatta: Synaptic density. *Exp. Neurol.*, 69: 164-172, 1981.
- Victor, M., Adams, R.D., Collins, G.H.: The Wernicke-Korsakoff Syndrome. Philadelphia: P.A. Davis, 1971.
- Wagman, A.M.I., Allen, R.F.: Effects of alcohol ingestion and abstinence on slow wave sleep in alcoholics. In M.M. Gross (ed.), *Alcohol Intoxication and Withdrawal; Experimental Studies. II.* (*Adv. Exp. Med. Biol.*, v. 59), pp. 453-466. New York: Plenum Press, 1977.
- Walker, D.W., Barnes, D.E., Zornetzer, S.F., Hunter, B.E., Kubanis, P.: Neuronal loss in hippocampus induced by prolonged ethanol consumption in rats. *Science*, 209: 711-713, 1980.
- Walker, D.W., Freund, G.: Impairment of shuttlebox avoidance learning following prolonged alcohol consumption in rats. *Physiol. Behav.*, 7: 773-778, 1971.
- Walker, D.W., Hunter, B.E.: Short-term memory impairment following chronic alcohol consumption in rats. *Neuropsychologia*, 16: 545-553, 1978.
- Walker, D.W., Hunter, B.E.: Prolonged alcohol consumption in the rat: Absence of retrograde amnesia for an avoidance response. *Pharm. Biochem. Behav.*, 2: 63-66, 1974.
- Walker, D.W., Hunter, B.E., Abraham, W.C.: Neuroanatomical and functional deficits subsequent to chronic ethanol administration in animals. *Alcoholism: Clin. Exp. Res.*, 1981.
- Walker, D.W., King, M.A., Reep, R.L., Hunter, B.E.: Chronic ethanol exposure alters synaptic reorganization following partial deafferentation of rat dentate gyrus. *Neurosci. Abstr.*, 1984.

- Walker, D.W., Means, L.W.: Single-alternation performance in rats with hippocampal lesions: Disruption by an irrelevant task interposed during the intertrial interval. *Behav. Biol.*, 9: 93-104, 1973.
- Wallgren, H.: Absorption, diffusion, distribution and elimination of ethanol: Effect on biological membranes. In J. Tremolieres (ed.), *International Encyclopedia of Pharmacology and Therapeutics*, sec. 20, v. 1, pp. 161-188. New York: Pergamon Press, 1970.
- West, J.R., Deadwyler, S.A., Cotman, C.W., Lynch, G.: Time dependent changes in commissural field potentials in the dentate gyrus following lesions of the entorhinal cortex in adult rats. *Brain Res.*, 97: 215-233, 1975.
- West, J.R., Lind, M.D., Demuth, R.M., Parker, E.S., Alkana, R.L., Cassell, M., Black, A.C.: Lesion-induced sprouting in the rat dentate gyrus is inhibited by repeated ethanol administration. *Science*, 218: 808-810, 1982.
- West, J.R., Nornes, H.O., Barnes, C.L., Brofenfrenner, M.: The cells of origin of the commissural afferents to the area dentata in the mouse. *Brain Res.*, 160: 203-215, 1979.
- West, J.R., Lind, M.D., Demut, R.M., Parker, E.S., Alkana, R.L., Cassell, M., Black, A.C.: Lesion-induced sprouting in the rat dentate gyrus is inhibited by repeated ethanol administration. *Science*, 218: 808-810, 1982.
- West, M.J., Anderson, A.H.: An allometric study of the area dentata in the rat and mouse. *Brain Res. Rev.*, 2: 317-348, 1980.
- White, L.E., Westrum, L.E.: Dendritic spine changes in prepyriform cortex following olfactory bulb lesions. *Anat. Rec.*, 149: 410-411, 1964.
- Wilkinson, D.A.: Examination of alcoholics by computed tomography (CT) scans: A critical review. *Alcoholism: Clin. Exp. Res.*, 6: 31-45, 1982.
- Williams, R.S., Matthysse, S.: Morphometric analysis of granule cell dendrites in the mouse dentate gyrus. *J. Comp. Neurol.*, 215: 154-164, 1983.
- Wilson, R.C., Levy, W.B., Steward, O.: Functional effects of lesion-induced plasticity: Long term potentiation in normal and lesion-induced temporodentate connections. *Brain Res.*, 176: 65-78, 1979.
- Winocur, G.: Effects of interference on discrimination learning and recall by rats with hippocampal lesions. *Physiol. Behav.*, 22: 339-345, 1979.

Wyss, J.M.: An autoradiographic study of the efferent connections of the entorhinal cortex in the rat. J. Comp. Neurol., 199: 495-512, 1981.

Wyss, J.M., Swanson, L.J., Cowan, W.M.: A study of the subcortical afferents to the hippocampal formation in the rat. Neurosci., 4: 463-476, 1979.

Wyss, J.M., Swanson, L.H., Cowan, W.M.: Evidence for an input to the molecular layer and the stratum granulosum of the dentate gyrus from the supramammillary region of the hypothalamus. Anat. Embryol., 156: 165-176, 1979.

Zimmer, J.: Ipsilateral afferents to the commissural zone of the fascia dentata, demonstrated in decommissurated rats by silver impregnation. J. Comp. Neurol., 142: 393-416, 1971.

Zimmer, J.: Extended commissural and ipsilateral projections in postnatally deentorhinated hippocampus and fascia dentata demonstrated by silver impregnation. Brain Res., 64: 293-311, 1973.

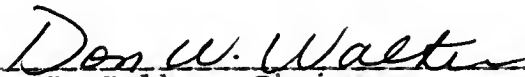
Zimmer, J.: Long term synaptic reorganization in the rat fascia dentata deafferented at adolescent and adult stages: Observations with the Timm's method. Brain Res., 76: 336-342, 1974.

Zimmer, J., Hjorth-Simonsen, A.: Crossed pathways from the entorhinal area to the fascia dentata. Provokable in rats. J. Comp. Neurol., 161: 71-102, 1975.

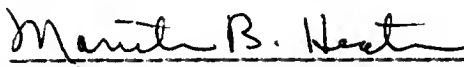
BIOGRAPHICAL SKETCH

Michael King is the eldest of five children of a high school science teacher, who he credits for his interest in a career in science. Mike came to the Department of Neuroscience at the University of Florida after obtaining his B.S. in Psychology from the University of Massachusetts in 1979. He is married and has one daughter. He leaves Florida to become a postdoctoral fellow in the Neuroplasticity and Regeneration Training Program in the Department of Neurological Surgery at the University of Virginia School of Medicine.

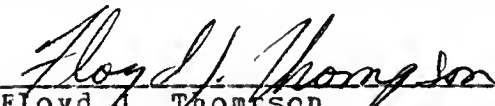
I certify that I have read this study and that in my opinion it conforms to acceptable standards of scholarly presentation and is fully adequate, in scope and quality, as a dissertation for the degree of Doctor of Philosophy.


Don W. Walker, Chairman
Professor of Neuroscience


I certify that I have read this study and that in my opinion it conforms to acceptable standards of scholarly presentation and is fully adequate, in scope and quality, as a dissertation for the degree of Doctor of Philosophy.


Marieta B. Heaton
Associate Professor of Neuroscience

I certify that I have read this study and that in my opinion it conforms to acceptable standards of scholarly presentation and is fully adequate, in scope and quality, as a dissertation for the degree of Doctor of Philosophy.


Floyd J. Thompson
Associate Professor of Neuroscience

I certify that I have read this study and that in my opinion it conforms to acceptable standards of scholarly presentation and is fully adequate, in scope and quality, as a dissertation for the degree of Doctor of Philosophy.


Christopher M. West
Assistant Professor of Anatomy

This dissertation was submitted to the Graduate Faculty of the College of Medicine and to the Graduate School, and was accepted as partial fulfillment of the requirements for the degree of Doctor of Philosophy.

May 1985

John Dickey Jr 1/07/85
Dean, College of Medicine

Madelyn Lockhart
Dean for Graduate Studies and
Research

UNIVERSITY OF FLORIDA



3 1262 08554 5027